

General Disclaimer

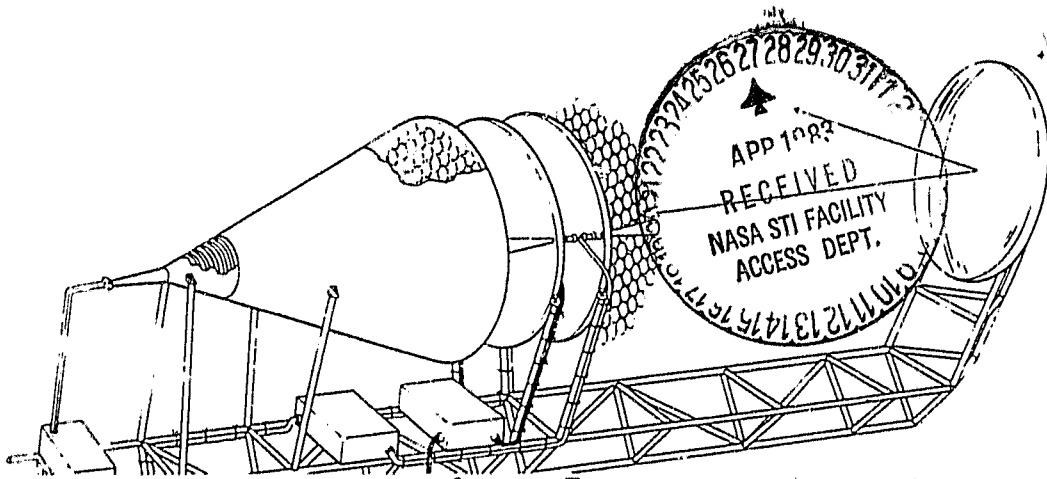
One or more of the Following Statements may affect this Document

- This document has been reproduced from the best copy furnished by the organizational source. It is being released in the interest of making available as much information as possible.
- This document may contain data, which exceeds the sheet parameters. It was furnished in this condition by the organizational source and is the best copy available.
- This document may contain tone-on-tone or color graphs, charts and/or pictures, which have been reproduced in black and white.
- This document is paginated as submitted by the original source.
- Portions of this document are not fully legible due to the historical nature of some of the material. However, it is the best reproduction available from the original submission.

NASA-CR-168078

APRIL 1983

TECHNOLOGY ASSESSMENT
 FOR
**PHASED ARRAY-FED
 ANTENNA
 CONFIGURATION STUDY**
NAS 3-23252



(NASA-CR-168078) PHASED ARRAY-FED ANTENNA
 CONFIGURATION STUDY: TECHNOLOGY ASSESSMENT
 (Harris Corp., Melbourne, Fla.) 141 p
 HC A07/MF A01

N83-22495

CSSL 20N

Unclass

G3/32 03437

PREPARED FOR
 NASA LEWIS RESEARCH CENTER



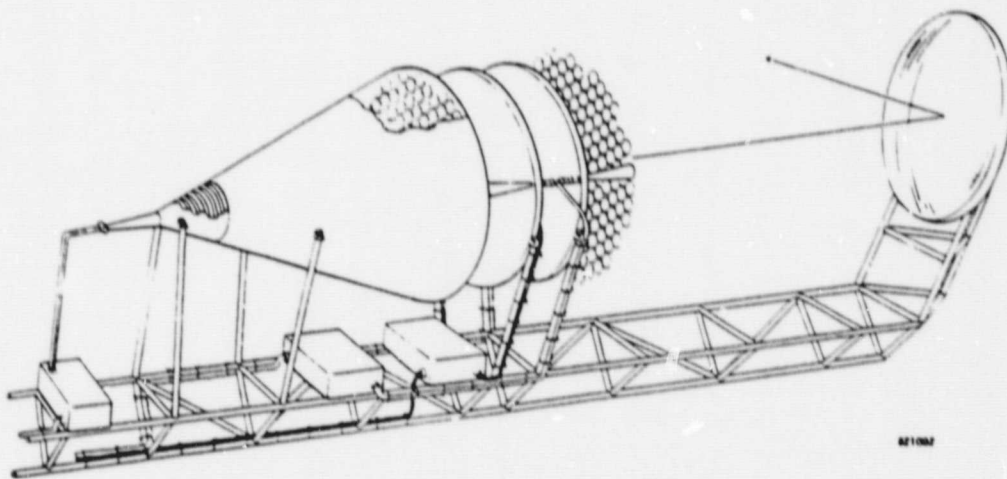
HARRIS CORPORATION GOVERNMENT ELECTRONIC SYSTEMS DIVISION
 P.O. BOX 96000, MELBOURNE, FLORIDA 32901, (305) 727-4000

ORIGINAL PAGE IS
OF POOR QUALITY

Nasa-CR-168078

APRIL 1983

TECHNOLOGY ASSESSMENT
FOR
**PHASED ARRAY-FED
ANTENNA
CONFIGURATION STUDY**
NAS 3-23252



PREPARED FOR
NASA LEWIS RESEARCH CENTER

ORIGINAL PAGE 13
OF POOR QUALITY

1. Report No. CR 168078	2. Government Accession No.	3. Recipient's Catalog No.	
4. Title and Subtitle Phased Array-Fed Antenna Configuration Study-Technology Assessment		5. Report Date April 1983	6. Performing Organization Code
		8. Performing Organization Report No.	
7. Author(s) W.F. Croswell, D.E. Ball, R.C. Taylor		10. Work Unit No.	
		11. Contract or Grant No. NAS 3-23252	
9. Performing Organization Name and Address Harris Corporation Government Electronic Systems Division P.O. Box 37 Melbourne, FL 32901		13. Type of Report and Period Covered	
		14. Sponsoring Agency Code	
12. Sponsoring Agency Name and Address NASA Lewis Research Center Cleveland, Ohio 44135			
15. Supplementary Notes			
16. Abstract This report addresses the technologies available for spacecraft array-fed reflector antenna systems for particular application to a Multiple Fixed Spot Beam/Multiple Scanning Spot Beam System. Reflector optics systems are reviewed in addition to an investigation of the feasibility of the use of monolithic microwave integrated circuit (MMIC) power amplifiers and phase shifters in each element of the array feed. This assessment includes results of the work performed under the Phased Array-Fed Antenna Configuration Study.			
17. Key Words (Suggested by Author(s)) Multiple Beam Antenna Scanning Beam Antenna Phased Array Feed Monolithic Microwave Integrated Circuits		18. Distribution Statement Distribution Unlimited	
19. Security Classif. (of this report) Unclassified	20. Security Classif. (of this page) Unclassified	21. No. of pages 135	22. Price*

* For sale by the National Technical Information Service, Springfield, Virginia 22161

ORIGINAL PAGE IS
OF POOR QUALITY

PHASED ARRAY-FED ANTENNA
CONFIGURATION STUDY

Task I Report
TECHNOLOGY ASSESSMENT

April 1983

NAS 3-23252

By

W. F. Crosswell
D. E. Ball
R. C. Taylor

HARRIS Corp./Government Electronics Systems Division
Melbourne, Florida

Prepared for:
NASA Lewis Research Center
Cleveland, Ohio

TABLE OF CONTENTS

	<u>Page(s)</u>
SECTION 1. INTRODUCTION	2 - 5
SECTION 2. LIMITED FIELD OF VIEW ANTENNAS PARABOLIC REFLECTORS	6 - 8
Optics Configuration	9 - 12
Offset vs. Symmetric Configurations	13
Single Reflector vs. Dual Reflector Configurations	14
Focused vs. Near-Field Scanning Methods	15 - 16
Transforming Property of Reflectors	17 - 19
1. <u>Front Fed Symmetric Parabola</u>	20
Topics of Authors, Summary	21
Examples from Ruze's Paper	22 - 23
Example of Array Compensation	24
2. <u>Cassegrain Fed Symmetric Parabola</u>	25 - 26
Front-Fed Offset Paraboloid	27 - 30
Focused Offset Cassegrain Calculated Results	31 - 32
Focused Offset Cassegrain Measured Results	33 - 34
Focused Offset Cassegrain	35 - 40
Scan Properties vs. f/D Ratio for the Offset Cassegrain	41 - 42
Optimum Focal Surface	43 - 44
Feed System Design	45
5. <u>Focused Offset Gregorian</u>	46
6. <u>Near-Field Symmetric Parabola</u>	47 - 49
7. <u>Symmetric Near-Field Cassegrain</u>	50 - 52
Symmetric Near-Field Cassegrain Secondary Aperture Distribution	53 - 54
8. <u>Near-Field Symmetric Gregorian</u>	55

TABLE OF CONTENTS

ORIGINAL PAGE IS
OF POOR QUALITY

pg. -1b-

	<u>Page(s)</u>
9. <u>Offset Near-Field Parabola</u>	56
10. <u>Offset Near-Field Cassegrain</u>	57
Offset Near-Field Cassegrain Design Procedure	58 - 59
Performance of Near-Field Cassegrain	60
Offset Near-Field Cassegrain Configuration	61 - 62
Typical Array Chosen for Near-Field Cassegrain Feed	63 - 64
Performance of Near-Field Cassegrain as a Function of Magnification R _A Ratio	65 - 68
Multiple Beam Near-Field System	69 - 70
Feed System Design	71 - 73
Recommended SSPA Element Designs	74 - 76
Waveguide to Microstrip Transition	77 - 81
Array Heat Removal	82
11. <u>Offset Near-Field Gregorian</u>	83 - 85
Polarization	86 - 87
SECTION 3. ARRAY FEEDS	88
Array Properties	89
Equation of a 2-Dimensional Array	90 - 91
General Properties of Array Element Weights	92
Grating Lobe Controls and Minimum Controls	93 - 94
Near-Field of an Array	95 - 96
Oversized Radiating Elements, Widely Spaced Array Elements	97 - 98
Active Element Reflection Coefficient	99 - 100
Scan Limits of a Near-Field Array	101 - 102
SECTION 4. EHF SOLID STATE AND PASSIVE COMPONENTS	103
Technology of RF Amps and Phase Shifters	104
RF Linear Amplifier Considerations	105 - 106
Array Phase Calibration	107 - 108

TABLE OF CONTENTS

ORIGINAL PAGE IS
OF POOR QUALITY

pg. -1c-

	<u>Page(s)</u>
GaAs FETS, UNIT-TO-UNIT VARIATIONS	109 - 110
SSPA/Radiating Element Design	111 - 114
Array Elements	115 - 116
SSPA to Waveguide Radiator Transitions	117 - 120
SSPA ELEMENTS/CIRCULAR RADIATOR INTERFACE	121 - 124
Scanning Beam EIRP DC Power Requirements	125
Power Comparison TWT/BFN vs. Monolithic Module Array	126
Active Array Heat Dissipation	127
EHF Components	128 - 129
SECTION 5. SUMMARY	130 - 131
BIBLIOGRAPHY	132 - 135

1. INTRODUCTION

~~PRECEDING PAGE BLANK NOT FILMED~~

MAJOR GOALS OF THE TECHNOLOGY ASSESSMENT

- Investigate technologies available for Multiple Fixed Spot Beam/ Multiple Scanning Spot Beam systems where reflector optics systems are used in conjunction with array feeds.
- Investigate the feasibility of the use of monolithic microwave integrated circuit (MMIC) power amplifiers and phase shifters to combine and control array feeds.
- Study technologies for EHF operation: 20 GHz transmit, 30 GHz receive.

APPLICATION

- Typical system deployment: space shuttle launched geostationary satellite, early 1990's technology.
- Multiple Fixed Spot Beam System: major U.S. cities are simultaneously connected with multiple independent beams (up to 18).
- Multiple Scanning Spbt Beam System: six sectors of the continental U.S. are simultaneously scanned with high power beams to reach outlying areas.

MOTIVATION FOR USE OF ARRAY FEEDS
IN REFLECTOR ANTENNAS

- Array feeds provide an effective means to combine RF power generated by many individual solid state power amplifiers (SSPA's).
- Emerging EHF GaAs technology indicates space qualified SSPA's using MMIC's will be available in the latter part of this decade.
- Beam shape compensation for undesirable reflector effects and for improving carrier-to-interference (C/I) performance can be accomplished with array feeds.
- Rapid scanning from city to city can be implemented (~10-100 nanoseconds).
- Sophisticated systems of the 1990's will permit dynamic control of Effective Isotropic Radiated Power (EIRP) and C/I performance based on measured performance indicies.

LIMITATIONS

- High EIRP requirements are difficult to meet with existing and planned SSPA's for scanning beam systems.
- MMIC amplifier and phase shifter units have not yet been developed for antenna use at EHF frequencies.
- Thermal dissipation from SSPA's (15% maximum efficiency typical) needs technology development.

ADVANTAGES OF SOLID STATE POWER
USING GaAs TECHNOLOGY

- Increased reliability on a per device basis.
- Eliminates the single point failure mode encountered with TWT designs.
- Failure mode results in a graceful degradation for scanning beams.
- Modules allow dynamic beam control for multibeams.
- Fast switching times (10-100 nanoseconds) are feasible.
- Low power, lightweight array control elements (amplifiers, phase shifters) can be used.
- Space fed lenses rather than corporate BFN's are feasible, thus lower losses.

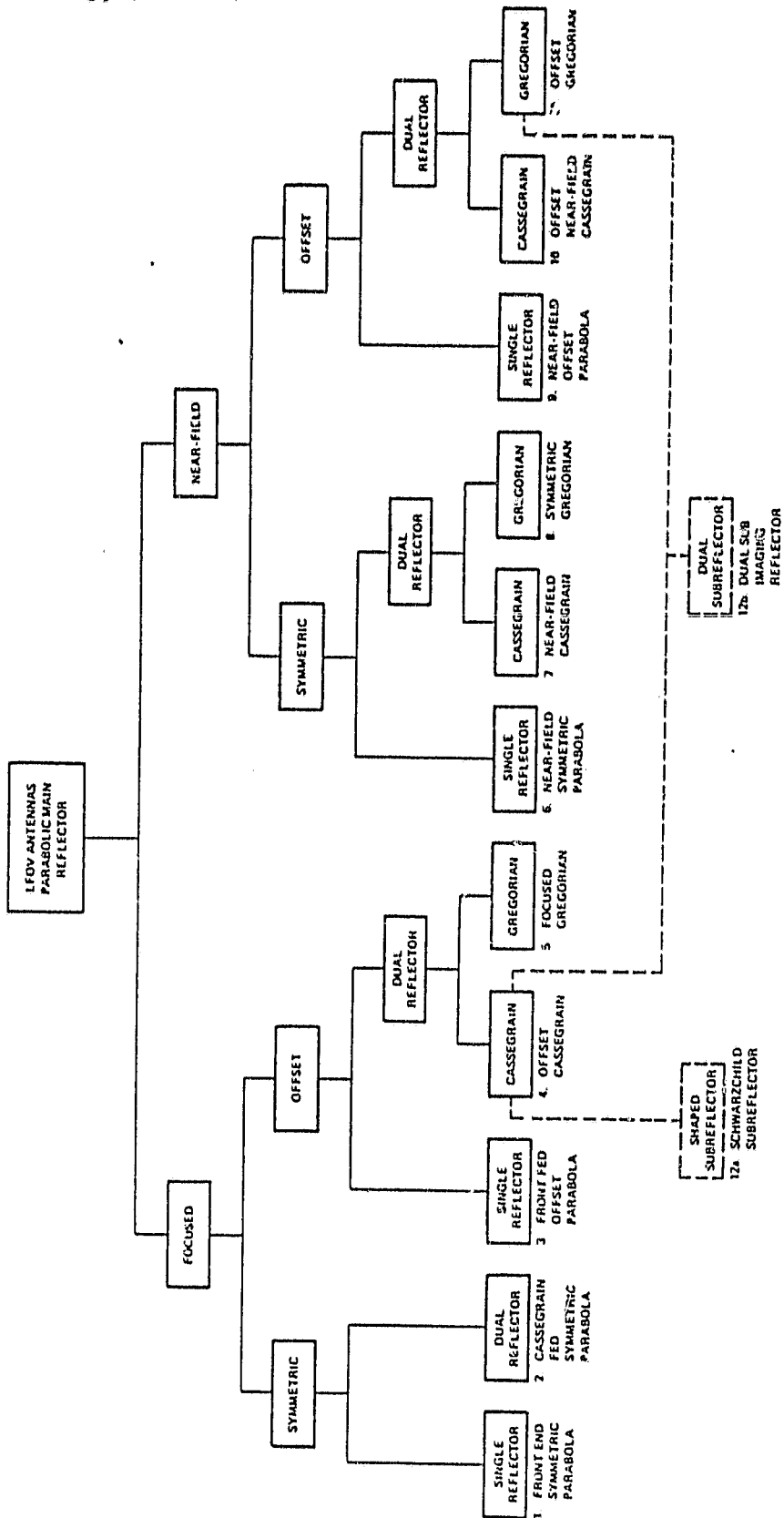
2. LIMITED FIELD OF VIEW ANTENNAS
PARABOLIC REFLECTORS

LIMITED FIELD OF VIEW ANTENNAS

The antenna systems considered in this assessment are known as limited field of view (LFOV) antennas. LFOV antenna designs in some way take advantage of the fact that limited scan requirements are imposed on the satellite system. These antennas can be scanned rapidly over a small angular region of space without mechanical repositioning of the reflector system. Typically, a feed array of limited size (compared to the main reflector) is electronically adjusted in order to produce beam scanning or beam shaping. All reflector systems used for off-axis beams, i.e., scanned beams or multiple beams, are LFOV systems. The discussions in this report are generally limited to reflector systems that use a parabolic main reflector.

The diagram on the next page illustrates a method by which LFOV antennas can be classified. Although not all of these configurations would be successful in meeting the requirements of the Advanced Communications Technology Satellite (ACTS) program, they are useful for describing the techniques available for off-axis beams. The major attributes and drawbacks of each category will be discussed. Examples of off-axis properties are given for most of the configurations. In this report, specific examples are not always compared to one another due to the vastly different design parameters (such as aperture size and f/D ratios) chosen by various authors of the reference material.

CLASSIFICATION OF LIMITED FIELD OF VIEW (LFOV) ANTENNA SYSTEMS
UTILIZING A PARABOLIC MAIN REFLECTOR

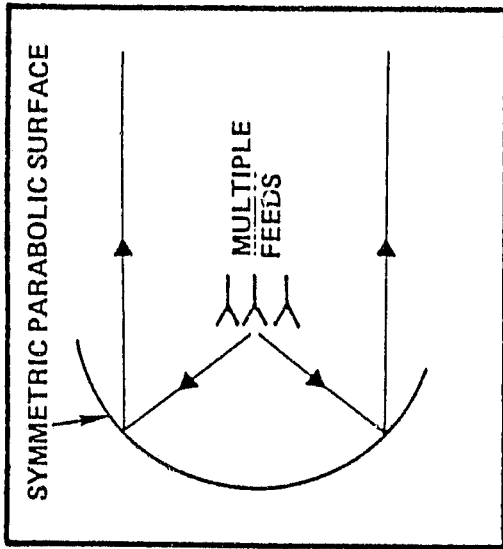


ORIGINAL PAGE IS
OF POOR QUALITY

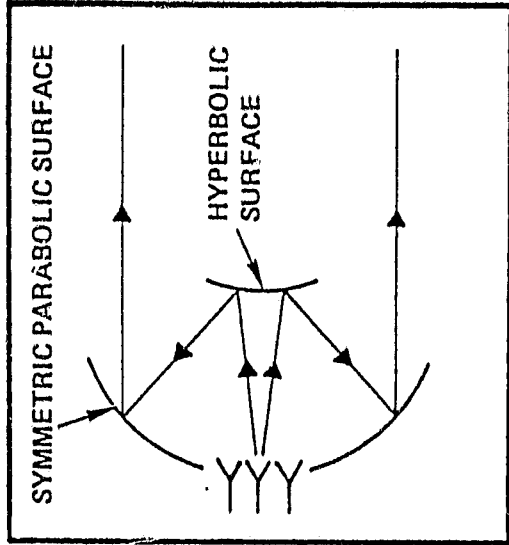
OPTICS CONFIGURATIONS

The following three pages present a sketch of each of the optics configurations of the previous table. It is important to note the type of subreflector surface, e.g., hyperbolic, parabolic, or elliptical. The Schwarzschild (12A) configuration is not shown since it follows very closely the offset Cassegrain configuration, but with the reflectors' shape defined by the Abbe' sine condition. Another feature to observe is the schematic of the feed. Three individual feeds represent individual horns or small clusters (typically ≤ 25 elements) of array elements grouped with individual amplitude and phase shift control. A block of many feeds represents an array of many elements (typically ≥ 100 to 200) with dynamic phase and amplitude control.

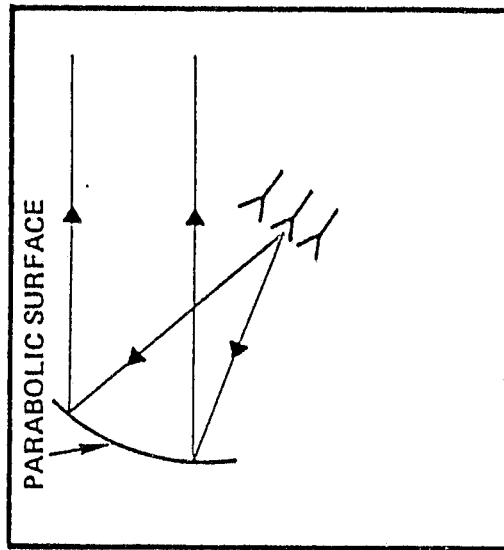
LFOV CONFIGURATIONS



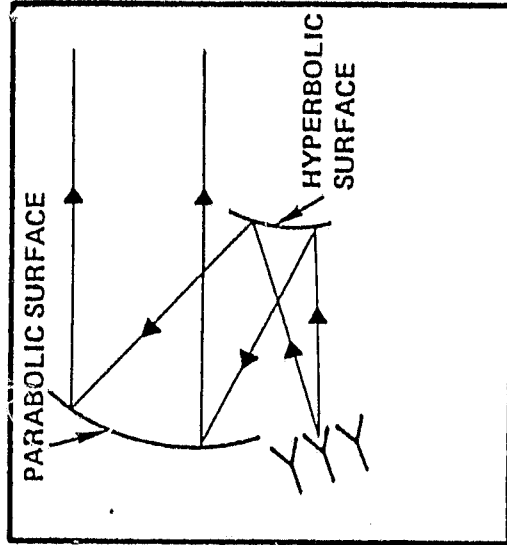
1. FRONT FED SYMMETRIC PARABOLA



2. CASSEGRAIN FED SYMMETRIC PARABOLA



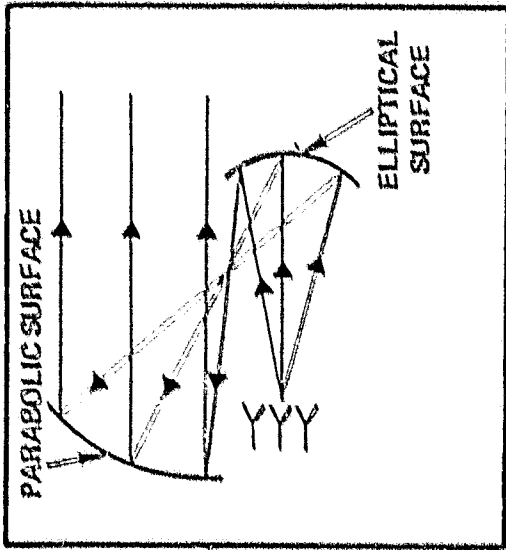
3. FRONT-FED OFFSET PARABOLA



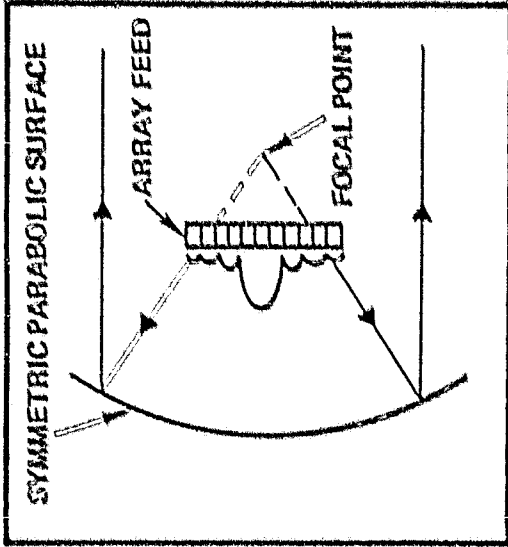
4. OFFSET CASSEGRAIN

820455

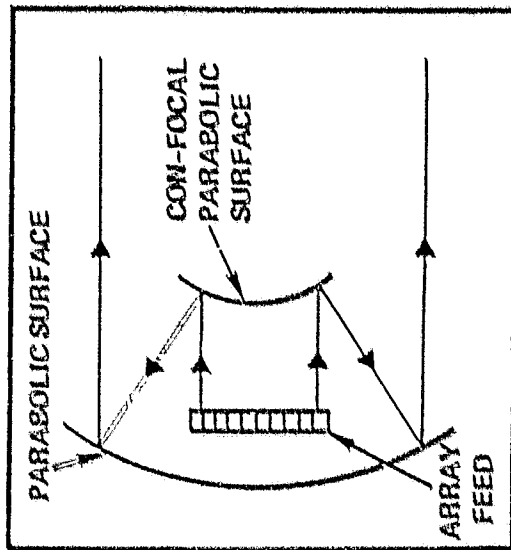
LFOV CONFIGURATIONS



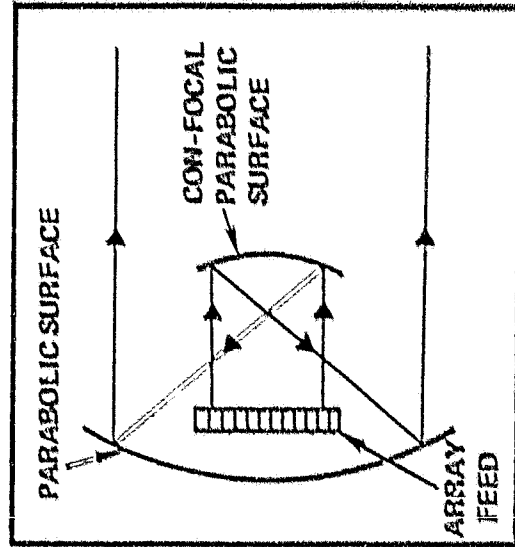
5. FOCUSED GREGORIAN



6. NEAR FIELD SYMMETRIC PARABOLA



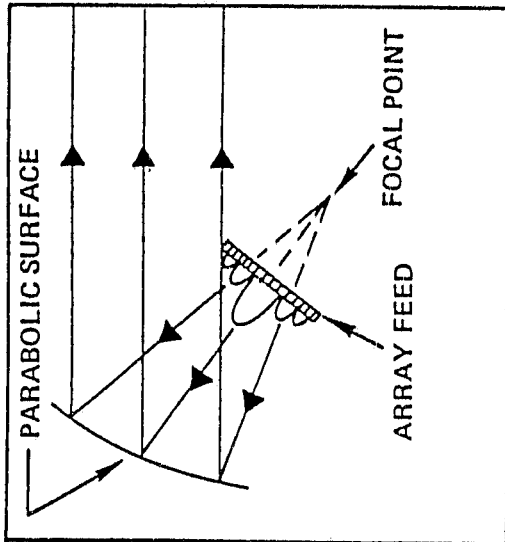
7. NEAR FIELD CASSEGRAIN



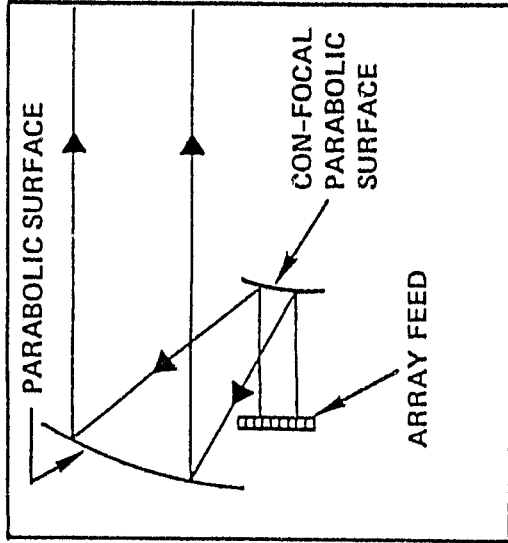
8. SYMMETRIC NEAR FIELD GREGORIAN

LFOV CONFIGURATIONS

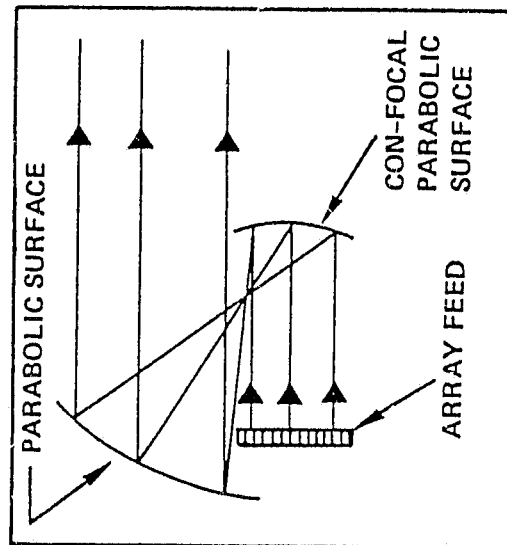
ORIGINAL PAGE 13
OF POOR QUALITY



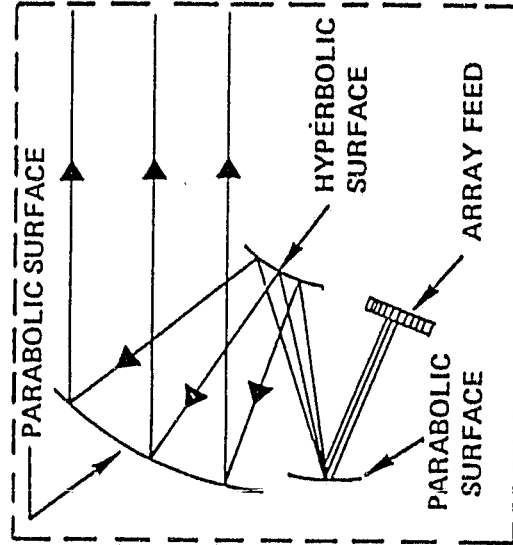
9. NEAR FIELD OFFSET PARABOLA



10. OFFSET NEAR FIELD CASSEGRAIN



11. OFFSET GREGORIAN



12b. IMAGING REFLECTOR

820467

OFFSET VS. SYMMETRIC CONFIGURATIONS

Offset configurations are generally favored in order to meet stringent C/I requirements. Some of the disadvantages of the symmetric configuration, and the relative advantages of the offset geometry, are:

- Aperture blockage caused by feeds, subreflector and/or support structures in the symmetric configuration.
- Aperture blockage results in higher sidelobes, higher cross-polarization levels, and lost aperture efficiency.
- Sidelobe levels below 25 dB are more difficult to obtain in symmetric systems.
- Mutual coupling among multiple feeds in the offset configuration is reduced because of the use of larger high gain feeds.
- Mutual coupling between the feeds (via the reflector) is reduced to an insignificant level in the offset geometry; this is important for broadband feed matching.

SINGLE REFLECTOR VS. DUAL REFLECTOR CONFIGURATIONS

There are several major trade-offs to consider when selecting a single reflector design versus a dual reflector design. Some advantages of dual reflector designs are:

- Focused dual reflector systems can implement larger equivalent f/D ratios than front fed configurations in the same volume constraint. Large equivalent f/D's generally lead to better off-axis performance.
- Array feeds can be kept closer to the satellite body; long RF transmission path lengths are avoided; feed support structures are replaced by simpler subreflector supports.
- Effective near-field designs require subreflectors to collimate primary and secondary aperture beams, i.e., the secondary aperture is a magnified image of the feed aperture.

But, dual reflector designs have some drawbacks.

- Dual reflector systems require precise alignment of subreflector surfaces.
- The forward pointing feeds encountered in dual reflecting systems contribute to lower C/I ratios. The amount of forward scatter field is dependent upon the feed horn illumination taper at the feed horn. For small edge tapers Rusch (10.4) reports the forward lobe peak to be about equal to the feed horn peak amplitude.

FOCUSED VS. NEAR-FIELD SCANNING METHODS

The figure on the following page depicts the implementation of a scanning beam feed in both a focused system, shown on the left, and a near-field system, shown on the right.

Focused Scanning

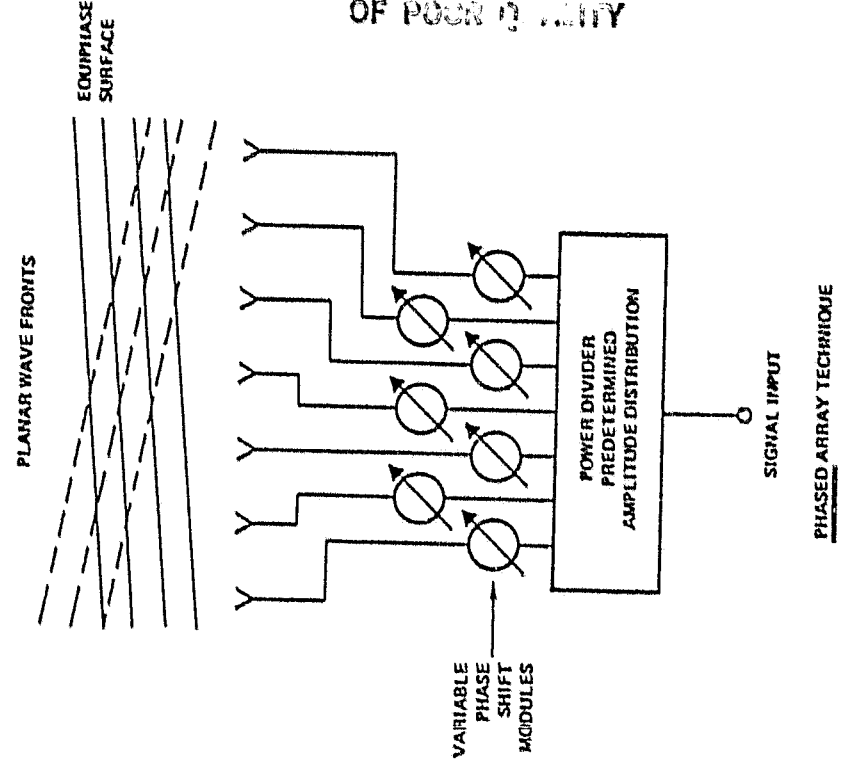
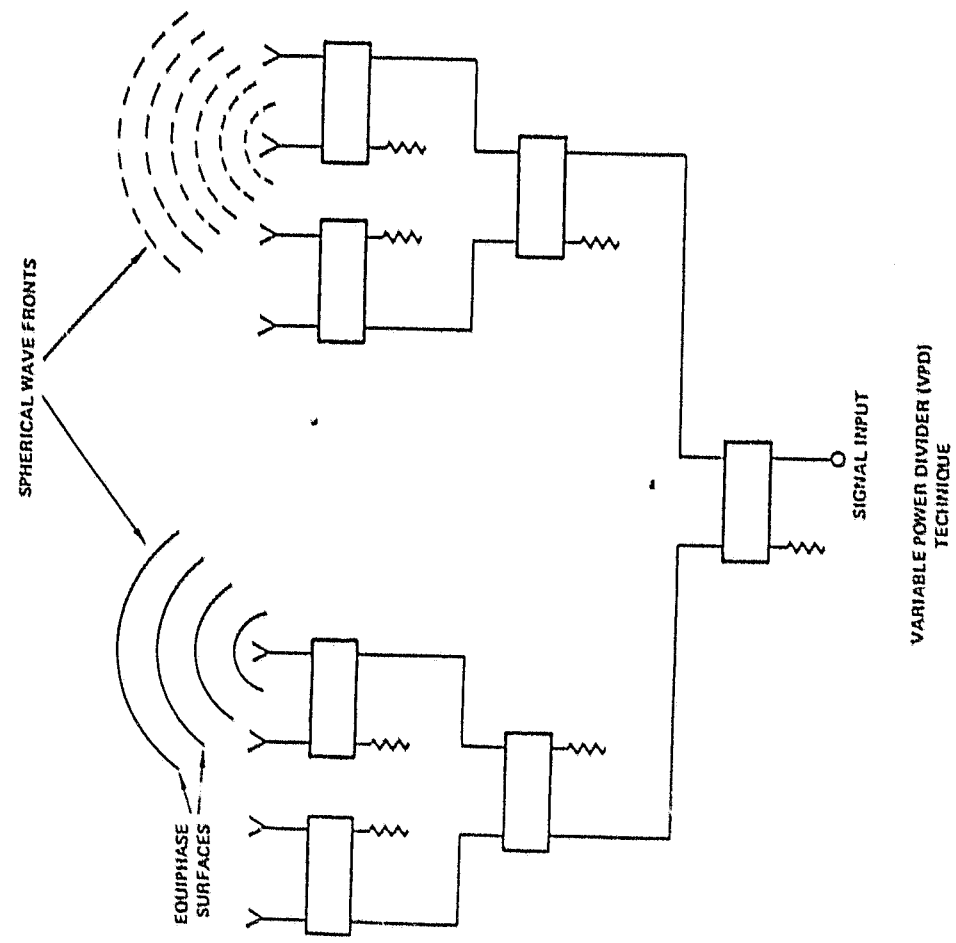
- Focused scanning uses an RF switching matrix or variable power divider (VPD) network.
- Signals from each feed are spherical wavefronts.
- Scanning is achieved by physically changing the location of the phase centers, either mechanically or electrically.
- A large number of feeds are required; at least one feed is required for each scanning beam position. Many more elements are required when free space combining of RF power is implemented.
- Only a small portion of elements are used at any given time. If SSPA's with on/off switching are used to simplify the power divider network, even amplifiers in the off state will absorb signal power.
- However, multiple scanning beams are easier to implement in focused systems.

Near Field Scanning

- Phase shifters can be used to control a linear phase taper across the array. Each element is fed by a power divider either of the fixed type or from a space fed lens.
- The image distorts as a function of f/D and scan angle. Correction methods require both amplitude and phase control of each feed element.
- The number of elements required relates to the subreflector size and magnification ratio.
- Multiple beam antennas require multiple near field feeds physically tilted to achieve isolation.

ORIGINAL DRAWING
OF POOR QUALITY

PHASE CENTER SWITCHING COMPARED TO PLANE WAVE STEERING



328478

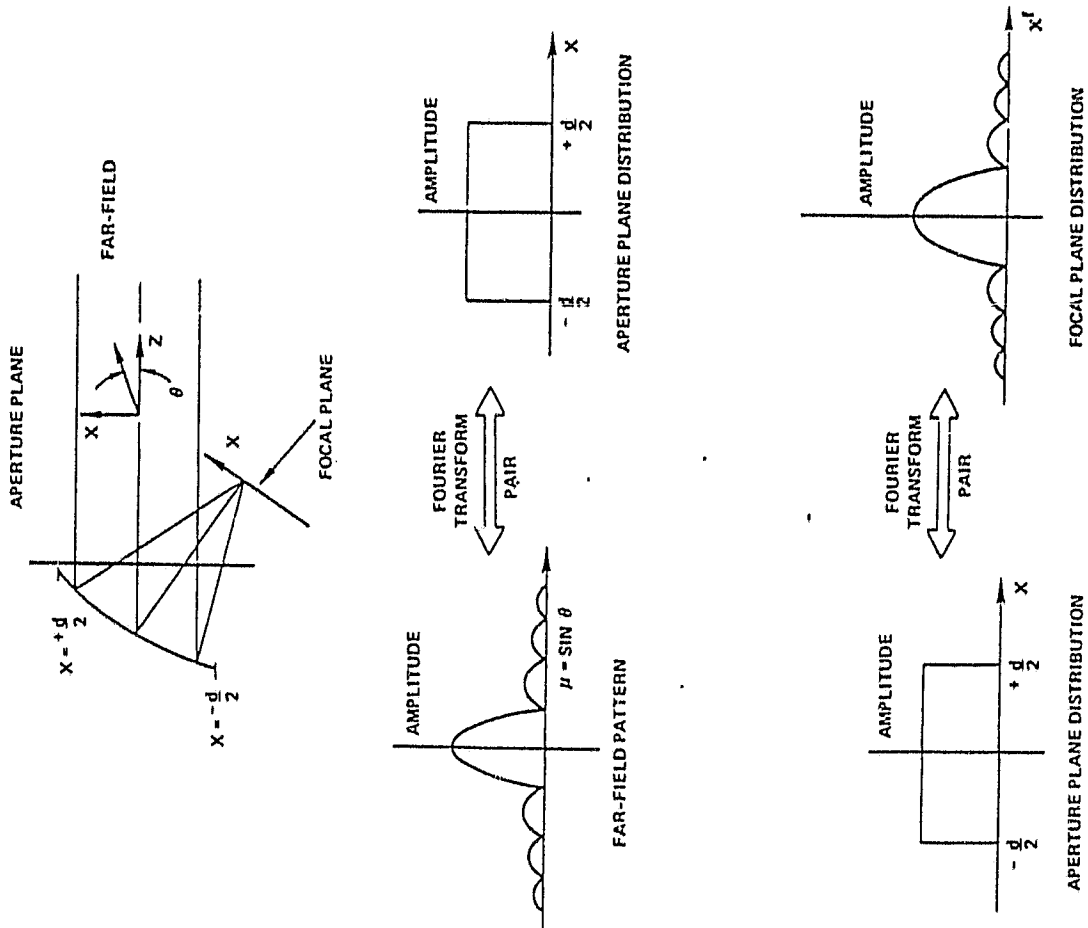
ORIGINAL VALUE IS
OF POOR QUALITY

TRANSFORMING PROPERTY OF REFLECTORS

The fundamental difference between near-field optic systems and focused optic systems is illustrated on the pages following by spatial Fourier transform relationships. From antenna theory, we know that the far field pattern (in sine space) of an aperture antenna is the spatial Fourier transform of the aperture distribution. Additionally, by selecting the proper focal plane in a parabolic reflector, the principal component of the electric field in the focal plane can be related to the aperture field distribution by a spatial two-dimensional Fourier transform pair (7.4). Thus, in the appropriate transform plane, the field distribution has the form of the far-field radiation pattern.

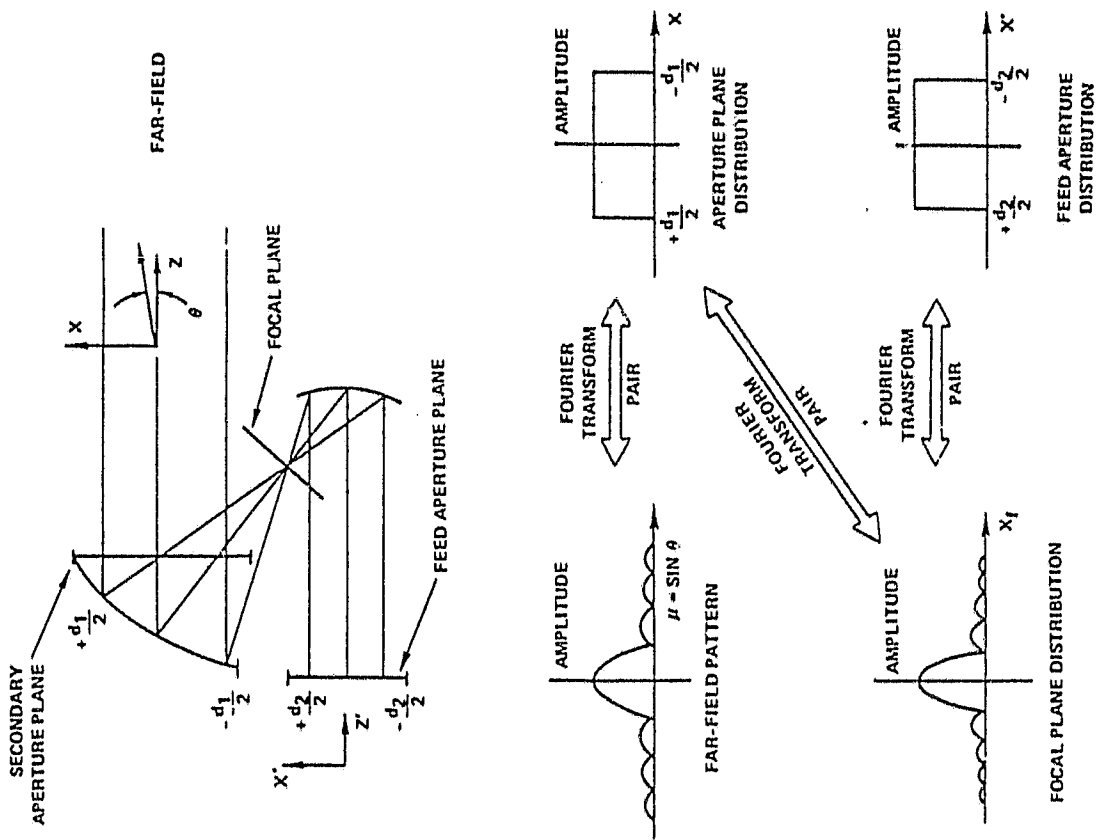
ORIGINAL PAGE IS
OF POOR QUALITY

FOURIER TRANSFORM RELATIONSHIPS IN A FOCUSED SYSTEM



ORIGINAL PAGE IS
OF POOR QUALITY

FOURIER TRANSFORM RELATIONSHIPS IN A NEAR-FIELD SYSTEM



120444

ORIGINAL PAGE IS
OF POOR QUALITY

1. Front Fed Symmetric Parabola

- Many references are available that have studied this configuration.
- Multiple beams and/or scanning beams (i.e. off axis beams) are formed by lateral feed displacement in the focal region.
- Feed and Support structures create blockage; hence, sidelobes and lost aperture efficiency. Therefore this configuration could not be considered viable for the 30/20 GHz application.
- Off-axis scans suffer from comatic aberrations.

TOPICS OF AUTHORS, SUMMARY

1. Y.T. Lo; beam deviation factor
 - a. analysis and measurement
 - b. parameter: f/D ratio
 - c. The beam deviation factor becomes closer to unity as f/D is increased
2. Ruze;
 - a. beam broadening
 - b. loss in gain
 - c. coma lobes
 - d. scans limited to a very few beamwidths
 - e. primary coma; beam degradation, beam shift opposite direction, first sidelobe away from the axis changes sign and merges with main beam
3. Rudge & Withers;
 - a. experimentally shown ± 15 beamwidth scans
 - b. little pattern degradation, minimal gain loss
 - c. arrayed feeds in scan plane
 - d. feed implements a spacial Fourier transform of the distorted focal region
4. Rusch & Ludwig;
 - a. locus and orientation of feed for optimum scanning
 - b. related to the Petzval surface (optics)
 - c. Higher scan gain obtained when feed remains parallel to reflector axis for moderate to low f/D ratios
5. Imbriale, Ingerson, and Wong;
 - a. vector formulation for accuracy
 - b. agreement with experimental results
 - c. beam scans to 29 beamwidths with 14 dB gain loss, poor patterns.

EXAMPLES FROM RUZE'S PAPER

● Example:

$f/D = .33$ 5 beamwidths scanned 10 dB edge taper

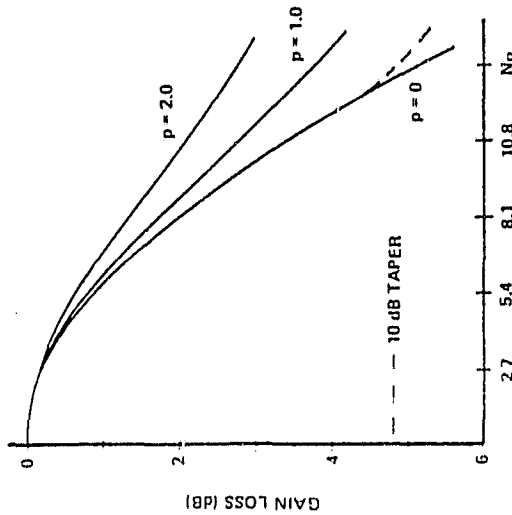
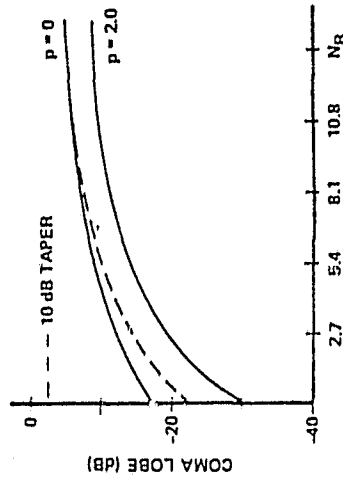
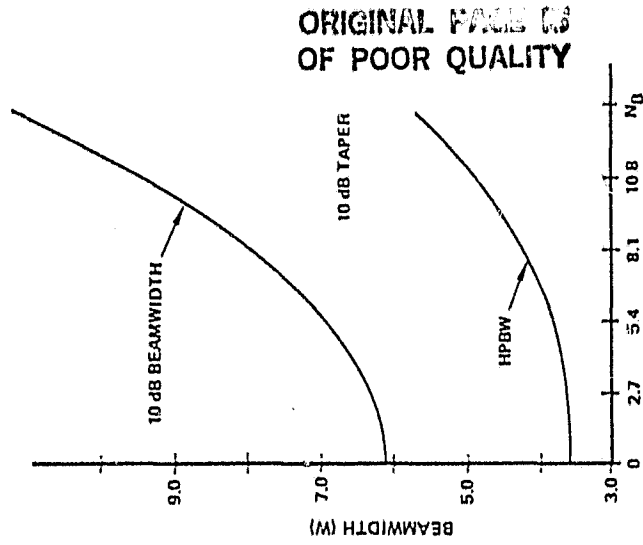
1. Beamwidth increases 1.3:1 over on-axis case
2. Sidelobe level increases from -22 dB on-axis to -8 dB (coma lobe)
3. The gain loss at 5 beamwidths is 2.8 dB

● Example;

$f/D = 1.0$ 5 beamwidths scanned 10 dB edge taper

1. Minimal increase in HPBW
2. Sidelobe level increases from -22 dB on-axis to -18 dB (coma lobe)
3. Gain loss of <.2 dB

FRONT FED SYMMETRIC PARABOLA
OFF-AXIS PROPERTIES, RUZE [1]



N_B = NUMBER OF HALF POWER BEAMWIDTHS SCANNED

ILLUMINATION FUNCTION $(1 - r^2)^p$, r = RADIUS FROM APERTURE CENTER
 $f/D = 0.5$ p = PARAMETER

820473

EXAMPLE OF ARRAY COMPENSATION
A. W. Rudge, M. J. Withers (7.4)

- This technique is similar to the focal-plane-array technique of Loux and Martin, and Assaly and Ricardi.
- Here the feed is not restricted to the focal plane.
- This is an example of a front-fed circularly symmetric parabola; the intent is to illustrate how the spacial Fourier transform was applied.
- This approach requires no amplitude weighting.
- A sampled spatial Fourier transform is physically implemented with a hybrid matrix. The sampled transform is then phase weighted to correct for the phase errors introduced in the optics and then summed in a beam forming network.
- A ± 15 beamwidth scan was achieved with a scan loss of 0.5 dB.

Other studies that have addressed methods leading to the reduction of distortion for moderate scan angles.

1. Takeshima; defocusing, balancing of 2 or more aberrations.
2. Hannan; compensatory phase-error technique, tilting of the subreflector in Cassegrainian systems.
3. Loux & Martin; focal-plane-array technique, amplitude weighting, phasing, and summing.
4. Assaly & Ricardi; focal-plane-array technique.

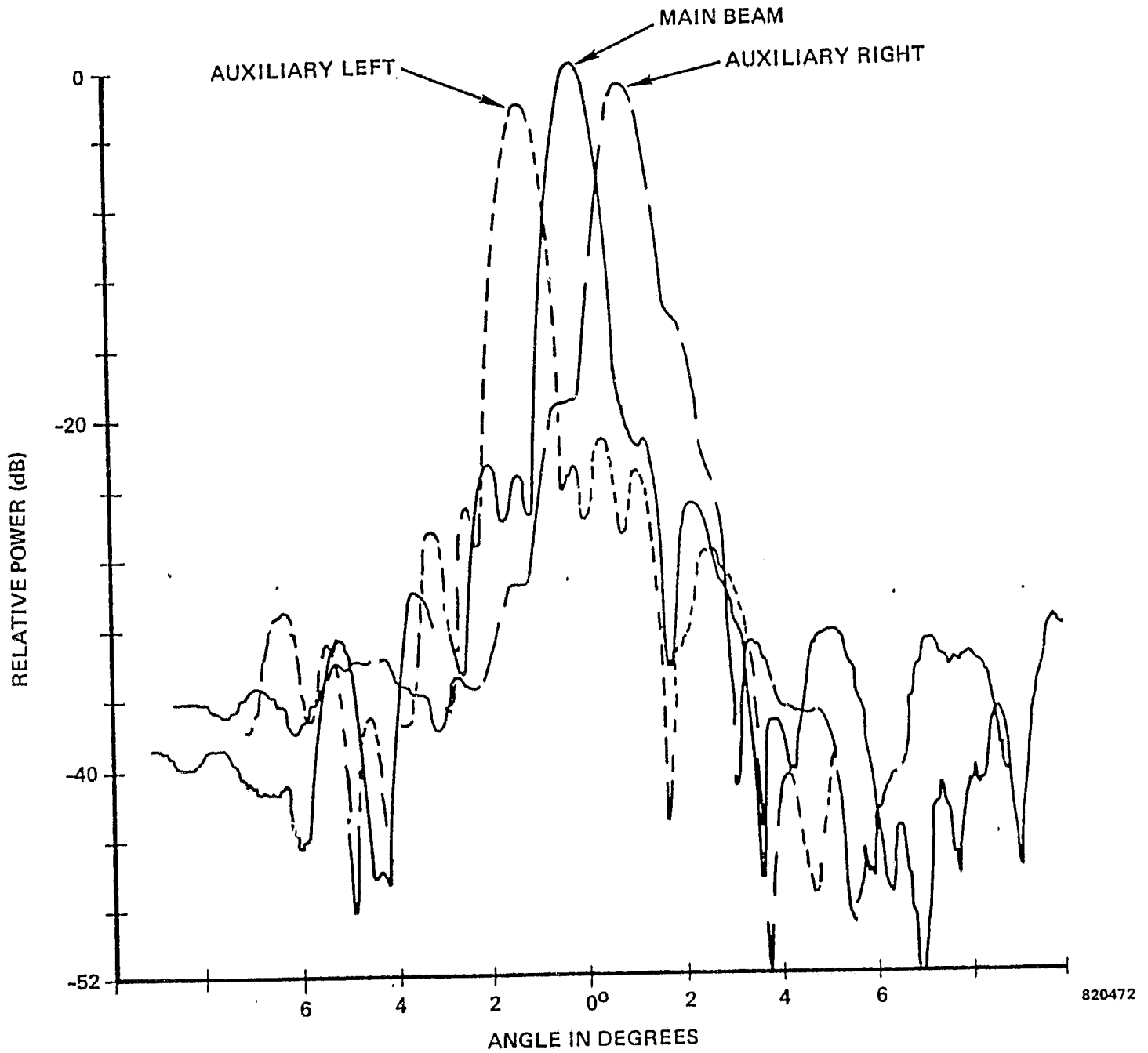
2. Cassegrain Fed Symmetric Parabola

Discussed here is an example of off-axis feeds in a symmetric Cassegrain configuration. These results are taken from breadboard measurements of a Harris sidelobe canceller system consisting of 1 on-axis feed (the main beam) and 4 off-axis feeds (auxiliary channels). Only 2 auxiliary beams are shown; the remaining 2 are situated in the orthogonal plane. Each element of the five element feed is a small pyramidal horn with element-to-element spacing of 2.5λ . The element spacing was chosen such that the beams formed an approximate set of orthogonal secondary beams.

The main parabolic reflector was 95λ and the auxiliary beams were scanned off 2 beamwidths. Even at these small scan angles the sidelobe performance and the scan loss of the auxiliary patterns was poor. The 20 to 25 dB sidelobes are typical of sidelobe levels encountered in symmetric configurations.

However, as an adaptive sidelobe canceller the system worked well. Using complex weights on the 4 auxiliary channels the system could effectively null two jammers in all regions outside of the main beam peak. Conversely, the conjugate weights can be used in the transmit case to improve sidelobe levels in specific directions of the secondary pattern even when relatively poor off-axis auxiliary beams are used.

SYMMETRIC CASSEGRAIN WITH OFF-AXIS FEEDS
(HARRIS CORPORATION)



3. Front-Fed Offset Paraboloid

This configuration is a viable candidate for use on the 30/20 GHz program since the lack of aperture blockage permits designs with 30 dB sidelobes or better.

Several off-axis examples from a paper by Rudge (8.1) are given here:

● Left Hand Figure

- a) $f/D = .392$ (of parent parabola)
- b) off-set feeds at $0, 1.4\lambda,$ and 2.8λ in the focal plane
- c) measured sidelobes increased from -25 dB to -22.5 dB at 2 beamwidths scan
- d) slight beamwidth increase at 2 BW scan
- e) cross-polarization increased from -25 dB to -22.5 dB
- f) scan loss was approximately .5 dB at 2 BW scan
- g) cross-over levels were at -5 to -6 dB

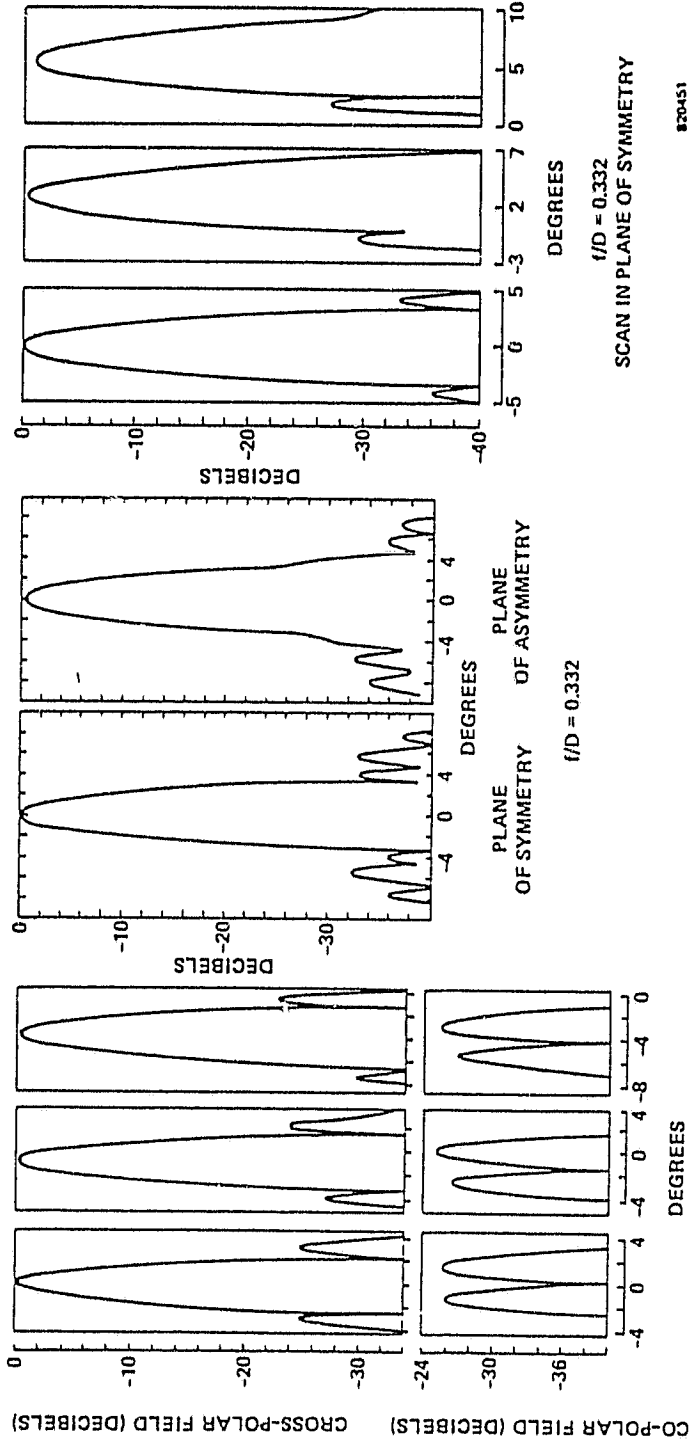
● Center Figure

- a) change edge illumination to -17 dB and f/D to .332
- b) The boresight patterns are shown for the two principal planes
- c) sidelobe levels at -32 dB, note shoulders in the plane-of-symmetry pattern at -28 dB

● Right Hand Figure

- a) measured scan properties with -17 dB edge illumination and $f/D = .332$
- b) sidelobe levels increase from -33 dB to -27 dB at 2 beamwidths scan
- c) The high sidelobe occurred on the boresight axis side of the main beam; at the same time the sidelobe away from the axis merged with the main beam; this is the same type of comatic aberrations observed in the symmetric paraboloid.

OFFSET PARABOLIC REFLECTOR RUDGE



FRONT-FED OFFSET PARABOLOID

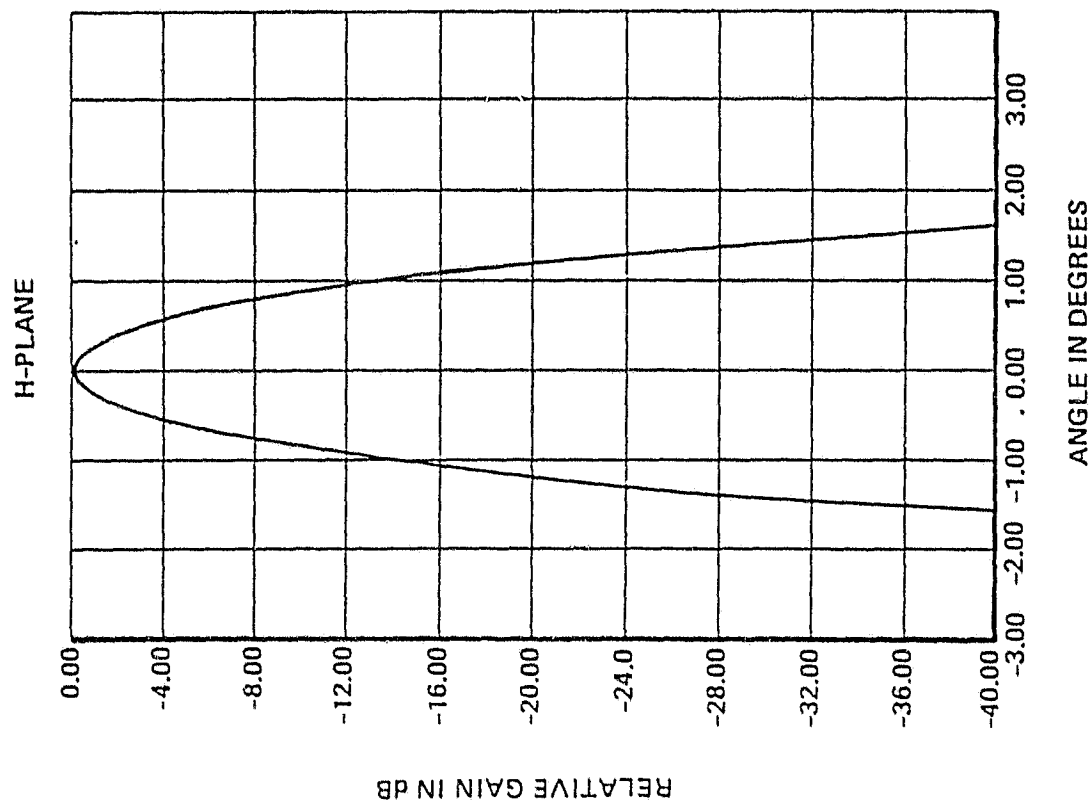
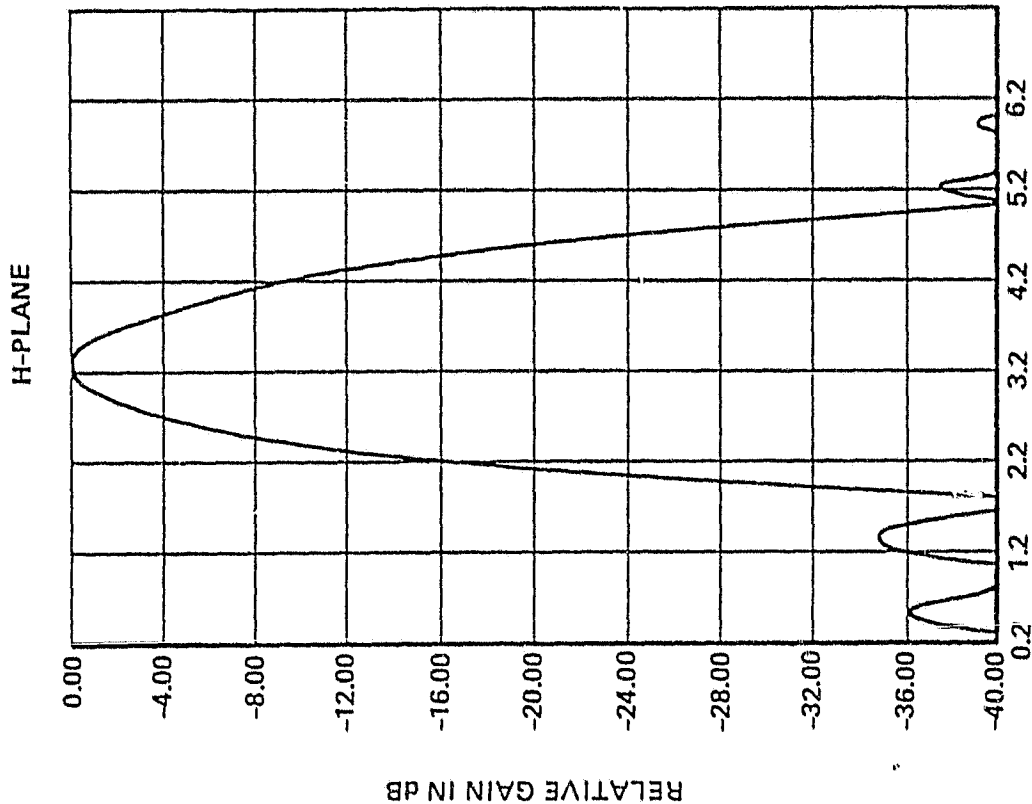
Shown on the following page is another example of off-axis beams in an offset paraboloid. This example uses a 9 element array feed.

- Ku-Band feed of small pyramidal horns grouped in a cluster.
- The patterns shown are calculated secondary patterns based on measured near-field patterns made of the feed.
- The cluster was used to form the high taper needed to achieve 35 dB sidelobes.
- The on-axis pattern is compared with a pattern scanned off 2.5 beamwidths.
- Scan was accomplished by lateral displacement of the feed cluster.
- Main reflector diameter 78.9λ
- 3 dB beamwidth $.95^\circ$
- Increase in sidelobe >40.0 dB to 34.6 dB, 3.5 BW scan
- Beam broadening $<.05^\circ$
- The beam forming network used to feed the 9 element array was fabricated in waveguide. H-Plane septum power dividers were used.

OFFSET PARABOLIC REFLECTOR
 COMPUTED SECONDARY PATTERNS USING
 MEASURED NEAR-FIELD FEED DATA, TRW

ORIGINAL PAGE IS
 OF POOR QUALITY.

820453



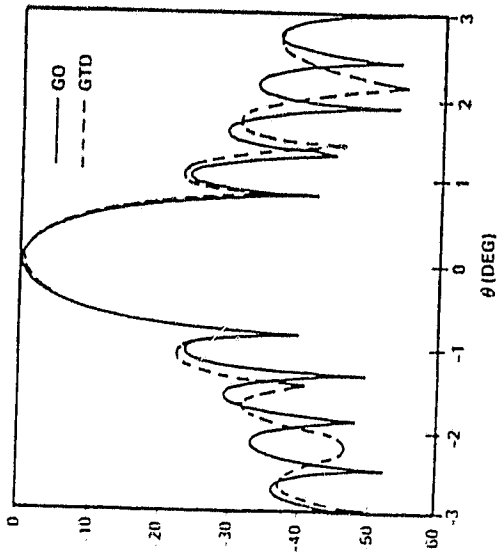
78.9 λ APERTURE DIAMETER
 $f/D = 0.43$

4. Focused Offset Cassegrain Calculated Results

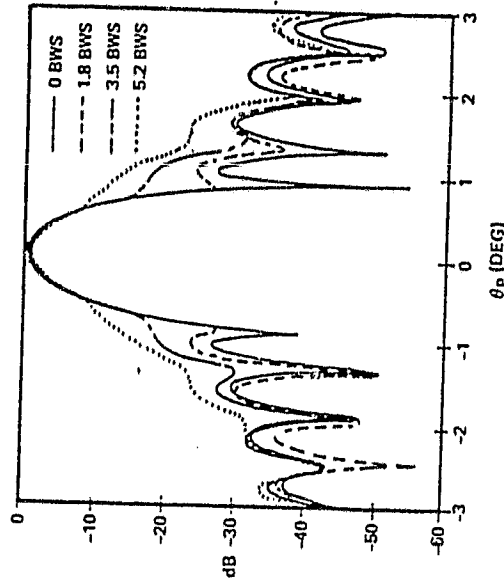
- Results calculated by Rahmat-Samii and Galindo (1.1). They use what they claimed was an efficient combination of methods to formulate accurate results:
 1. Scattering from the subreflector was computed using the Geometrical Theory of Diffraction (GTD),
 2. The fields reflected to the secondary aperture were computed by Geometrical Optics (GO), and
 3. The far fields were computed from the secondary aperture fields using a Jacobi-Bessel series expansion.
- The figure on the left compares the solution using GTD from the subreflector to the results using only GO from the subreflector. The main beam compares well, but the first few sidelobes are in slight disagreement.
- Note that the first few sidelobes are predicted to be higher using GTD. This is to be expected since the edge scattered fields act as additional interference in the secondary aperture. This is analogous to the aperture interference generated by feed or subreflector support blockage in symmetric antennas.
- This configuration, with an equivalent f/D of 0.6, has limited off-axis performance with conventional feeds. If 20 dB sidelobes were the goal, then the off-axis scan must be less than 3.5 beamwidths. Array compensation techniques similar to (Rudge) might improve the scan performance.
- This configuration (equiv. $f/D = 0.6$) has better scan loss characteristics than an offset paraboloid with a $f/D = 0.4$.

FOCUSED OFFSET CASSEGRAIN
RAHMAT-SAMI

CALCULATED RESULTS



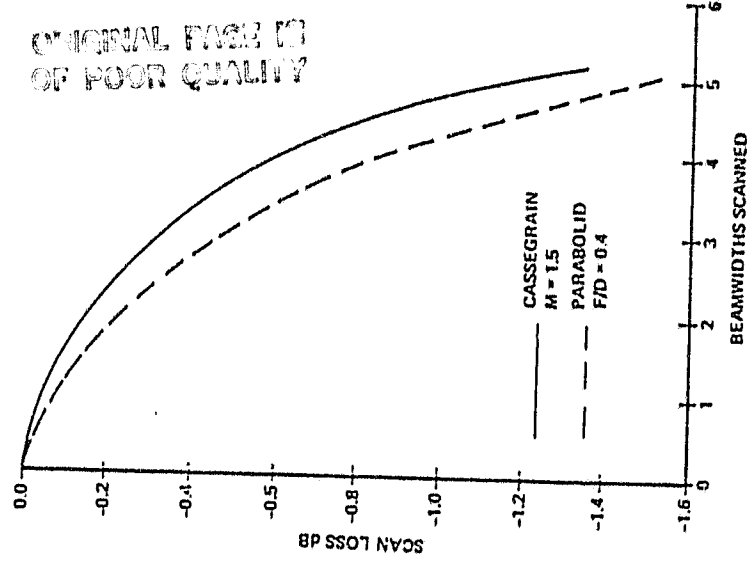
ON-AXIS SECONDARY PATTERN
GEOMETRIC OPTICS COMPARED
TO GEOMETRIC THEORY OF
DIFFRACTION SOLUTION



SCANNED SECONDARY PATTERNS
BWS = BEAMWIDTHS SCANNED ELEVATION SCAN

APERTURE = 100λ M = 1.5 EQUIV F/D = 0.6
F/D = 0.96

F/D = PRIME FOCAL LENGTH TO MAIN APERTURE DIAMETER RATIO



SCAN PERFORMANCE
CASSEGRAIN COMPARED TO A PARABOLID

2-2471

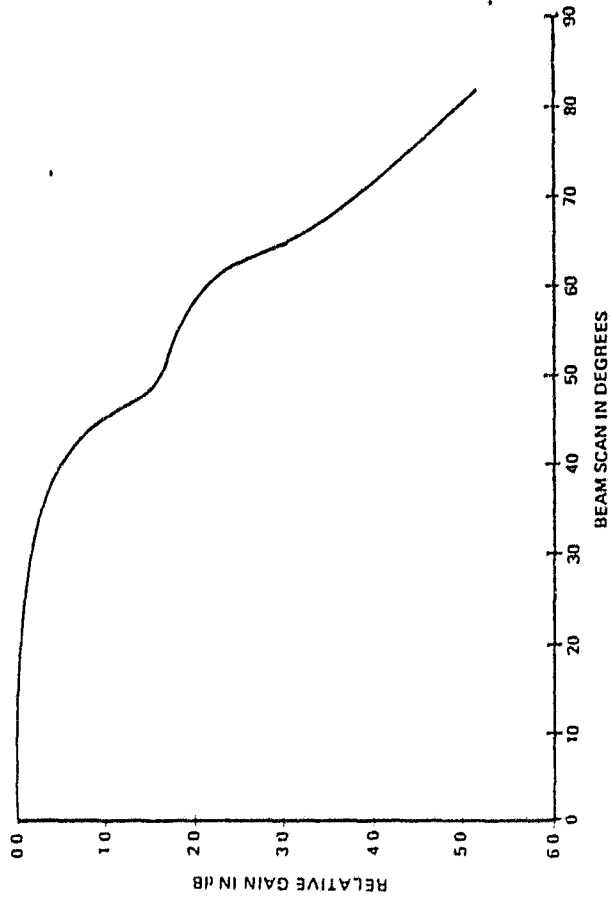
ORIGINAL PAGE IS
OF POOR QUALITY

Focused Offset Cassegrain Measured Results

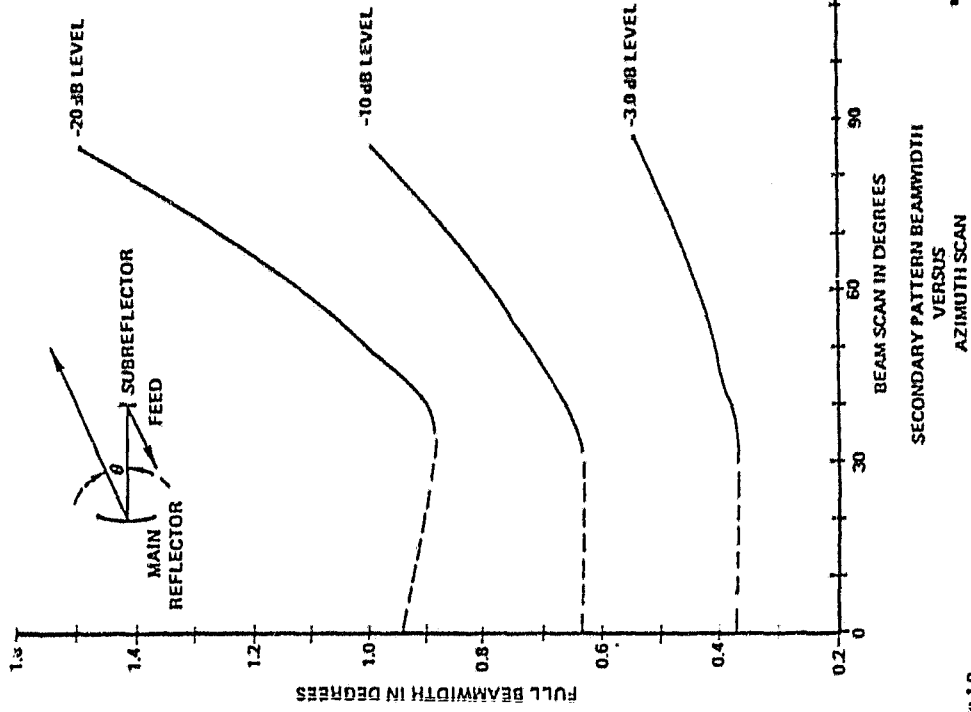
- These results were measured by Semplak (9.2) at 100 GHz.
- Main reflector diameter = 203λ
 Large f/D ratio; i.e. 1.9
 HPBW of $.39^\circ$
 On-axis sidelobes of -25 dB
 Illumination taper of 18 dB
- Unexpected results were observed; the sidelobes decreased as the beam was scanned. For example, at 4.3° scan (11 beamwidths) the sidelobes had decreased to -30.5 dB with a well shaped pattern. Scan loss at that point was only .4 dB.
- At a 5° scan angle the sidelobe away from the axis merges with the main beam. This broadens the coverage at the -30 dB level from 1.1° at a 4.3° scan to 1.35° at the 5° scan.
- A plot of Gain vs Scan angle indicates a maximum of .25 dB loss at a scan angle of 9 beamwidths; it also indicates a shoulder in the curve where the scan loss does not fall off as rapidly as predicted by calculation on similar configurations.
- A plot of beamwidth vs. scan angle is given at the -3.0, -10, and -20 dB levels; note that after scanning past 4° the -20 dB beamwidth increases very rapidly, this is the result of the sidelobe merging with the main beam (comatic aberation).

FOCUSED OFFSET CASSEGRAIN
SEMPLAK

MEASURED RESULTS



GAIN VERSUS AZIMUTH SCAN ANGLE



SECONDARY PATTERN BEAMWIDTH
VERSUS
AZIMUTH SCAN

APERTURE = 203λ F/D = 1.9

F/D = PRIME FOCAL LENGTH TO MAIN APERTURE DIAMETER RATIO

ORIGINAL PAGE IS
OF POOR QUALITY

4. FOCUSED OFFSET CASSEGRAIN

CALCULATED RESULTS

- 12' diameter main reflector with fixed f/D ratio, 45" subreflector.
- Frequency of operation is 20 GHz.

INITIAL POINT DESIGN GEOMETRIC PARAMETERS
HYPERBOLOIDAL SUBREFLECTOR

<u>EQUIVALENT f/D</u>	<u>MAGNIFICATION FACTOR</u>	<u>APPROX. SUBDISH DIAMETER</u>	<u>SUBTENDED ANGLE OF SUB</u>	<u>DISTANCE BETWEEN SUB FOCI</u>
0.65	1.61	45 inches	26.9°	80 inches
1.00	2.48	45 inches	18.2°	110 inches
1.35	3.35	45 inches	13.6°	140 inches
1.71	4.22	45 inches	10.9°	170 inches

COMPUTER CODE DESCRIPTION/VERIFICATION

- Utilizes geometrical optic raytracing techniques with far field radiation pattern determined by an aperture integration or surface current integration

- Checked against two independent reflector codes
 - Numerical Electromagnetic Code (NEC), Ohio State University, Equivalent Parabola Geometry, Aperture Integration Method

 - Raj Mittra, University of Illinois, Dual Reflector Code, Surface Current Integration Method

	Gain		Maximum Sidelobe		Maximum X-Pol	
	OCR	MITRA	OCR	MITRA	OCR	MITRA
ON f/D = 0.652	55.66 dB	56.66 dB	27.51 dB @ 0.46° 27.61 dB @ 0.45°	27.49 dB @ 0.46°	21.14 dB @ 0.20° 21.18 dB @ 0.19°	21.17 dB @ 0.20°
FOCUS f/D = 1.710	56.67 dB	56.66 dB	27.98 dB @ 0.46° 28.13 dB @ 0.45°	27.66 dB @ 0.46°	4.89 dB @ 0.18° 4.91 dB @ 0.19°	5.17 dB @ 0.18°
6 BW f/D = 0.652	55.60 dB @ -1.86°	55.88 dB @ -1.86°	28.90 dB @ -1.42°	29.20 dB @ -1.42°	25.00 dB @ -1.82°	21.22 dB @ -1.68°
SCAN f/D = 1.710	55.09 dB @ -1.80°	55.34 dB @ -1.80°	29.15 dB @ -1.36°	28.80 dB @ -1.36°	29.03 dB @ -1.80°	23.49 dB @ -1.80°

Gain	Δ Sidelobe	X-Pol
0.00 dB	0.02 dB	0.03 dB
0.01 dB	0.32 dB	0.28 dB
0.28 dB	0.30 dB	3.78 dB
0.25 dB	0.35 dB	5.54 dB

Offset Cassegrain Code Comparison Aperture Integration Technique

	Gain		Maximum Side-lobe		Maximum X-Pol	
	OCR	MITRA	OCR	MITRA	OCR	MITRA
ON f/D = 0.652	56.65 dB	56.66 dB	27.61 dB @ 0.450	27.49 dB @ 0.460	21.29 dB @ 0.190	21.17 dB @ 0.200
FOCUS f/D = 1.710	56.67 dB	56.66 dB	28.15 dB @ 0.450	27.66 dB @ 0.460	5.37 dB @ 0.190	5.17 dB @ 0.180
6 BW f/D = 0.652	55.89 dB @ -1.860	55.88 dB @ -1.860	28.92 dB @ -1.420	29.20 dB @ -1.420	27 dB @ -1.680	21.22 dB @ -1.680
SCAN f/D = 0.652	55.37 dB @ -1.800	55.34 dB @ -1.800	28.85 dB @ -1.370	28.80 dB @ -1.360	23.53 dB @ -1.790	23.49 dB @ -1.800

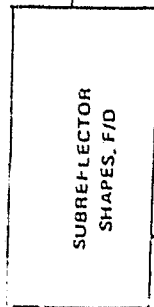
Gain	Side-lobe	X-Pol
0.01 dB	0.12 dB	0.12 dB
0.01 dB	0.49 dB	0.20 dB
0.01 dB	0.28 dB	0.05 dB
0.03 dB	0.05 dB	0.04 dB

Offset Cassegrain Code Comparison Surface Current Integration

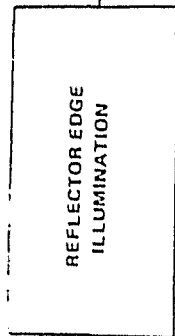
ORIGINAL FILED
OF POOR QUALITY

1508 82

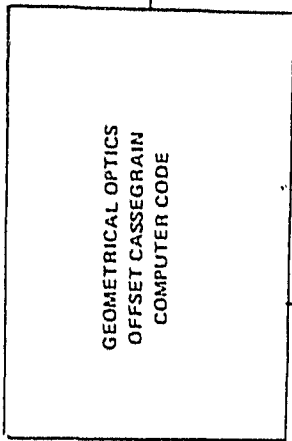
INPUTS



- 0.65
- 1.00
- 1.35
- 1.71



- 7 dB
- 14 dB
- 21 dB



- ON-FOCUS
- 8 BW SCAN ON FOCAL PLANE
- 8 BW SCAN ON FOCAL SURFACE

OUTPUTS

- MINIMUM GAIN LOSS
- FAR FIELD PATTERNS
- APERTURE FIELDS
- SELECTION OF EDGE TAPER
- SIDELobe LEVEL
- BEAM BROADENING
- CROSS POLARIZATION

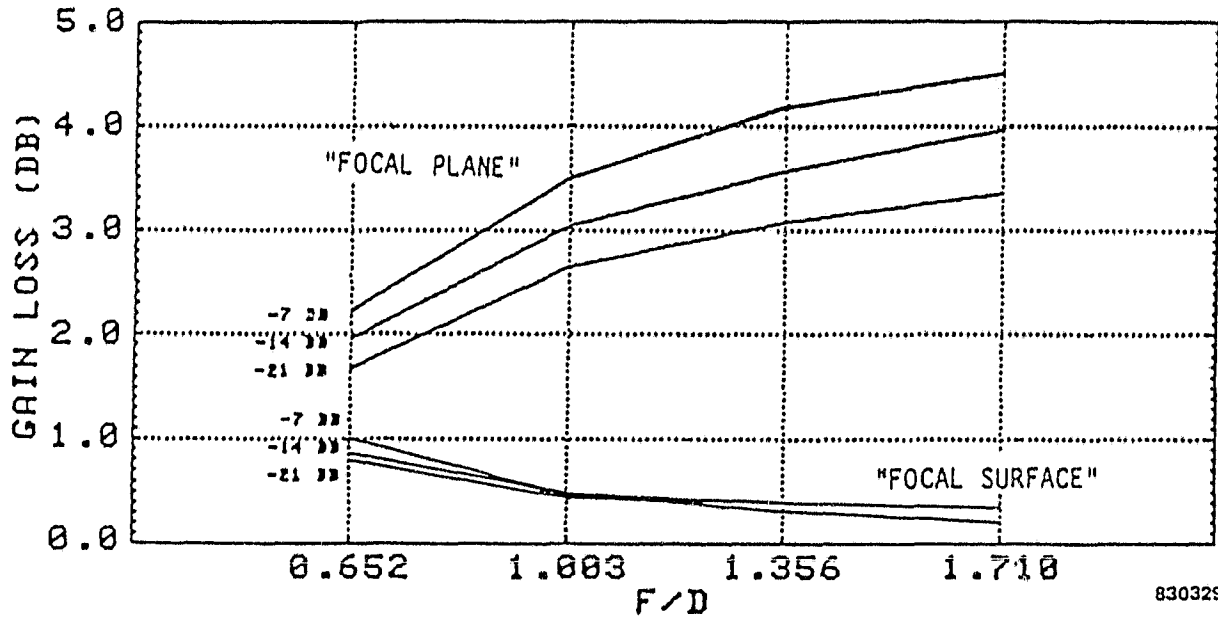
Multi-Beam Parametric Analysis Flow

ORIGINAL PAGE IS
OF POOR QUALITY

SCAN PROPERTIES VS F/D RATIO FOR THE OFFSET CASSEGRAIN

- Gain loss for feeds in focal plane are excessive
- Gain loss for feeds located on the focal surface is less than 1.0 dB for eight beamwidths off axis
- Low secondary pattern sidelobes requires low edge illumination of subreflector. (approximately -17 dB for 30 dB C/I ratio)

ORIGINAL PAGE IS
OF POOR QUALITY

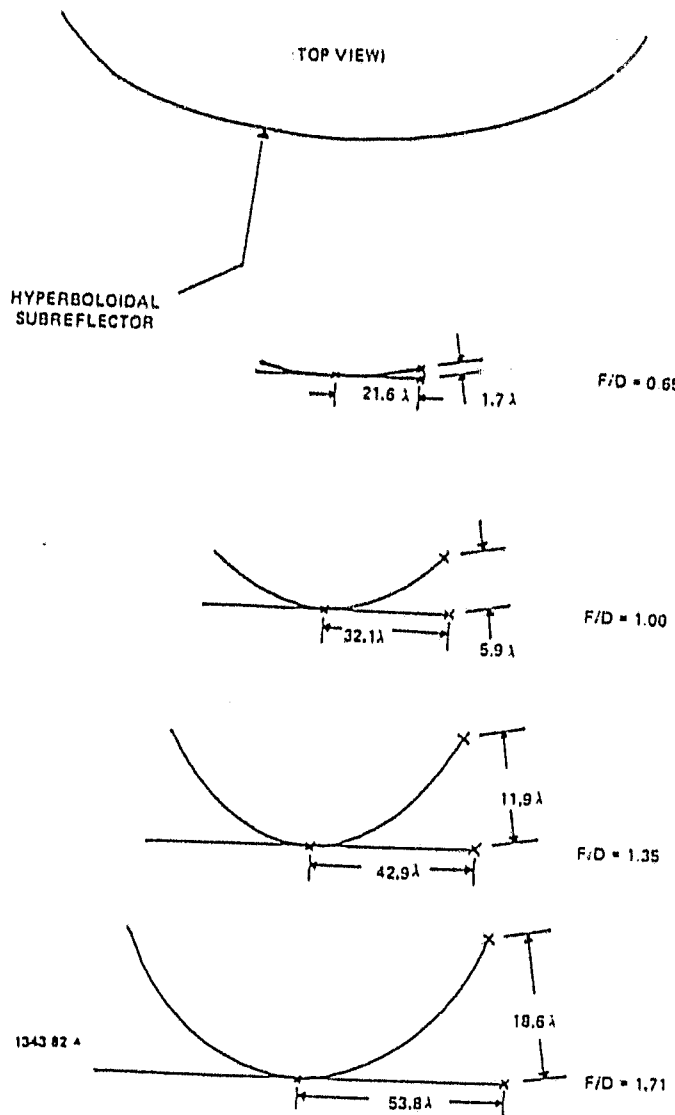


830329

Gain Loss vs F/D Ratio in an Offset Cassegrain Antenna for Feeds Offset Along both the "Focal Plane" and Optimum "Focal Surface" Corresponding to Eight Beamwidths Scan.

OPTIMUM FOCAL SURFACE

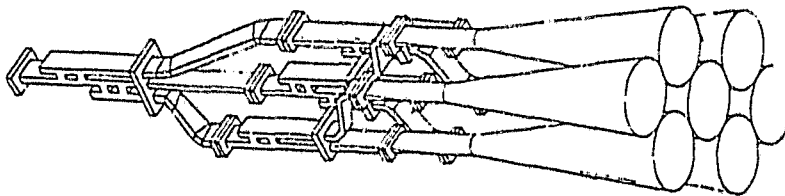
- There is an optimum focal surface for feed placement for the offset Cassegrain
- Approximate focal surface location can be found using geometrical optics. More accurate location requires physical optics and/or experimental verification
- The curvature of the optimum surface increases with f/D ratio



Feed Plane Versus Optimum Focal Surface

FEED SYSTEM DESIGN

- CLOSE PROXIMITY OF CLUSTERS AND NECESSITY OF SHARING SOME ELEMENTS MAKES SPACE FEEDING DIFFICULT
- CORPORATE FEED HAS CAPABILITY FOR EXACT POWER DIVISION BETWEEN ELEMENTS
- TYPICAL SEVEN ELEMENT CORPORATE FED CLUSTER (NO SHARED ELEMENT)



5. FOCUSED OFFSET GREGORIAN

- This approach was studied as an alternative configuration to provide large f/D ratios in a compact geometry. No distinct advantage is known that favors this configuration over an offset Cassegrain configuration.
- The subreflector surface is a portion of an ellipsoid. One focus is placed coincident with the main parabolic reflector focus and the other focus is the location of the feed.
- Scanning is accomplished by displacing the feed on the focal surface for off-axis beams.
- The off-axis scan properties in the symmetric plane were reported in Ref. [9.3]. It was shown that the scan loss at 3 beamwidths off-axis was -3 dB. Good cross-polarization performance was predicted, i.e., less than -31 dB at 1 beamwidth scan and less than -26 dB at 3 beamwidths scan.

6. NEAR-FIELD SYMMETRIC PARABOLA

A multi-element array compensation technique for off-axis beams was studied by Assaly and Ricardi (8.3).

- In this optics configuration, the array feed is placed in front of the focal point.
- Assaly & Ricardi's analysis was based on scalar wave theory, a simple approximation for the EM fields, and used only a 2-dimensional geometry.
- The synthesis of the transmit array distribution is simple (conjugate matching technique):
 1. Assume a plane wave incident from free space for several off-axis angles.
 2. Compute the complex weight of the received signal at each array element.
 3. Set the transmit element weight equal to the complex conjugate of the received signal.
 4. Compute the far-field secondary pattern from the sum of the individual elements.
- Element Spacing Effects - It was found that the secondary patterns exhibited a grating lobe like phenomenon when the elements were spaced at 1.0λ in the feed aperture. Even at $.8\lambda$ spacing relatively high sidelobes were observed at 12 beamwidths from the main beam (see Figure).
- Array Position - As the array was moved closer to the focal point the amplitude and phase weights on the elements became very critical. As the array was moved away from the focal point, more elements were required.
- This configuration was also studied by Mistik and Smith (3.2), and C. Winter (11.1), among others.

Results observed in Ref. (8.3).

- The array gain was higher than the gain of a single feed element located at the on-axis focus.

6. NEAR-FIELD SYMMETRIC PARABOLA - contd.ORIGINAL PAGE IS
OF POOR QUALITY

- The array pattern beamwidths were always larger than the single element case for scans as high as 4 beamwidths.

focal length = 30λ distance from vertex to array = 26λ

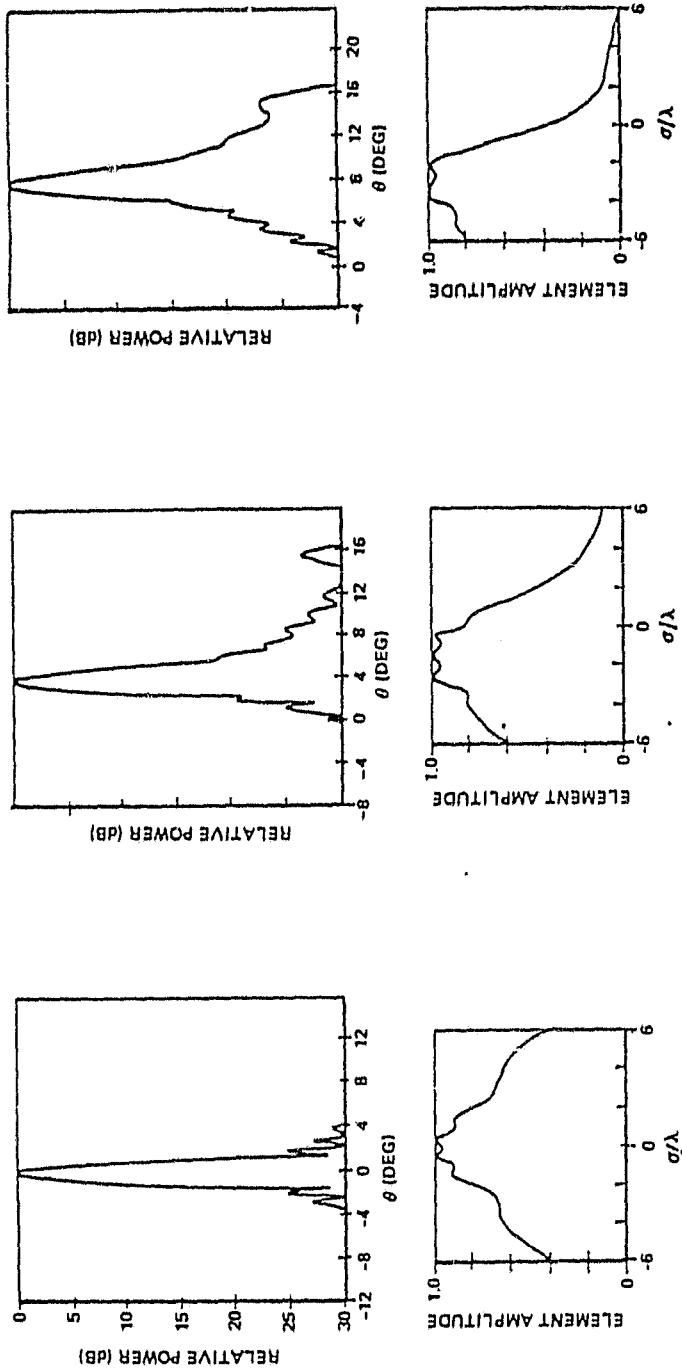
FEED CONFIGURATION	GAIN (dB)	HPBW (deg)	10 dB BEAMWIDTH (deg)	SIDELobe LEVEL* (dB)
Single Element Feed	25	1.0	1.75	-23.5
21 Element Feed 0° Scan	25.3	1.1	1.80	-29.5
21 Element Feed 4° Scan	25.1	1.2	2.00	-22.5

* Blockage neglected

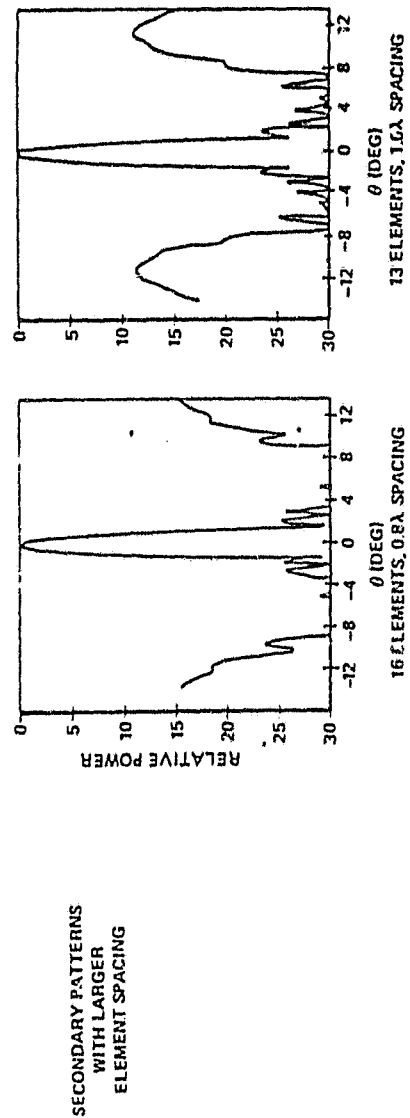
ORIGINAL PAGE IS
OF POOR QUALITY

NEAR-FIELD SYMMETRIC PARABOLA, REF [B.3]

SCANNED SECONDARY PATTERNS, ARRAY FEED
21 ELEMENTS, 0.6 SPACING



σ/λ ELEMENT LOCATION FROM AXIS



220187

7. SYMMETRIC NEAR-FIELD CASSEGRAIN

One of the major investigators of the NFC system was Fitzgerald [1.2]. He presents both analytical results based on ray tracing and measured results.

A small planar phased array is placed such that it is in the near field of the parabolic subreflector.

This is a circularly symmetric antenna; hence, there is a considerable amount of blockage resulting from the presence of the subreflector.

In his investigation, Fitzgerald studied the 5 different parameters:

- 1). the ratio of subreflector diameter to main reflector diameter,
- 2). the focal length to main diameter ratio,
- 3). the main reflector diameter in wavelengths,
- 4). the distance of the feed array aperture from the subreflector, and
- 5). the electric field distribution on the feed aperture.

Two aperture distributions were studied: a $1-p^2$ distribution and a uniform distribution.

Scan loss is caused by phase aberrations and to a lesser extent, amplitude dispersion.

Computed patterns showing scan loss are shown. It is seen that the beam can be scanned to 3 degrees before the scan loss reaches 3 dB, this is equivalent to a scan of 15 half-power beamwidths from boresight. The sidelobe levels did not increase when the beam was scanned to 3 degrees, although the boresight beam levels were excessively high due to the uniform feed distribution.

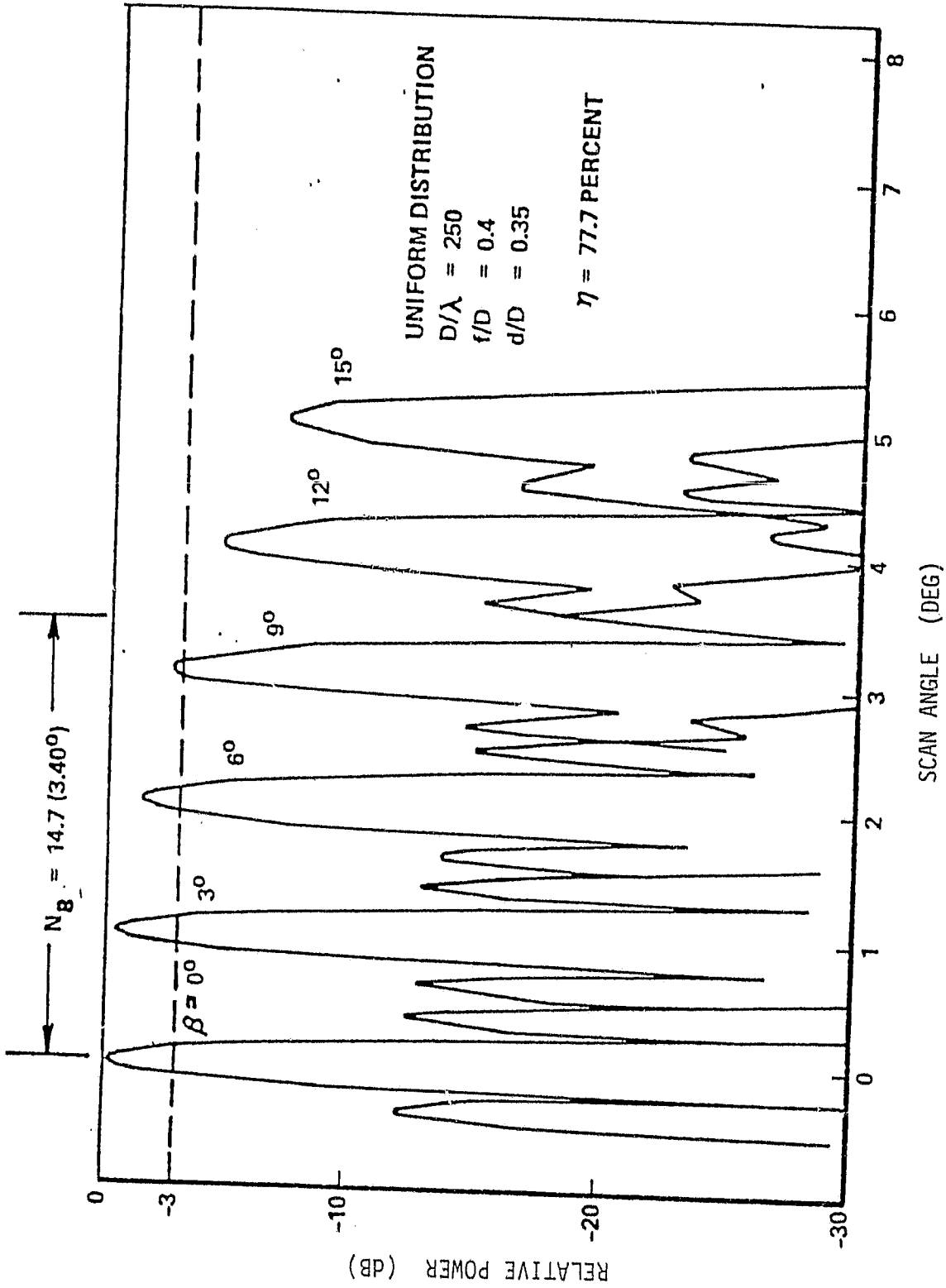
7. SYMMETRIC NEAR-FIELD CASSEGRAIN - contd.

The principal conclusions from Fitzgerald's investigation of the NFC antenna are that:

- The feed array demonstrates linear phase scanning property (linear phase taper, although the primary to secondary transfer is not linear).
- The feed array element spacing can be made large due to the limited-field-of-view requirement, thus reducing cost and complexity.
- The "coma" lobes associated with an off-axis focused paraboloid are avoided.
- The system can scan up to 15 beamwidths from boresight with only 3 dB scan loss and 7 beamwidths with 1 dB scan loss.

The disadvantage of the symmetric near field Cassegrain system is the large amount of blockage resulting from the subreflector. This blockage is greater than a similar off-axis Cassegrain antenna configuration using a hyperbolic subreflector.

ORIGINAL PAGE IS
OF POOR QUALITY



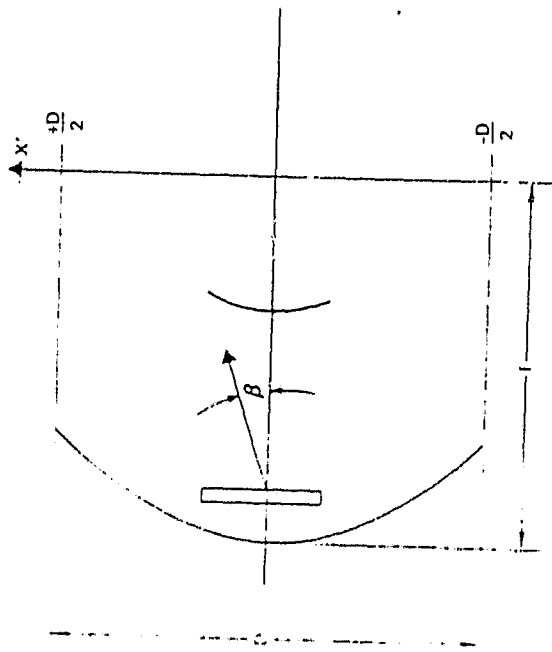
Symmetric Near-Field Cassegrain
Secondary Scanned Patterns, Fitzgerald [1.2]

ORIGINAL PAGE IS
OF POOR QUALITY

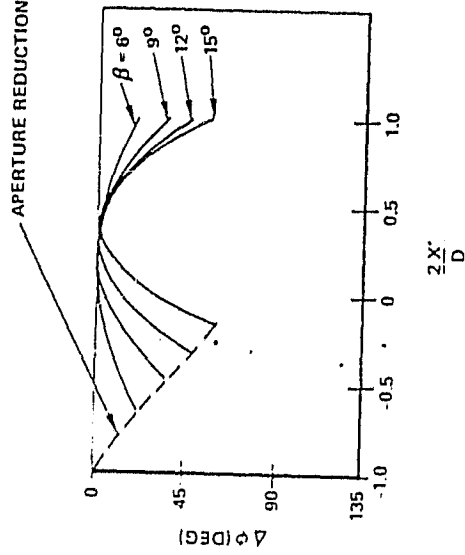
SYMMETRIC NEAR-FIELD CASSEGRAIN
SECONDARY APERTURE DISTRIBUTION

The figure on the following page shows the path length errors determined by Fitzgerald (1.2) across the central strip of the secondary aperture. The linear phase distribution that represents the beam steering component has been subtracted out; hence, only phase errors are shown. Amplitude variations resulting from space attenuation on the central strip were small. The amplitude distribution was found to be approximately linear with variations of less than 2 dB when the primary aperture scan angle, β , equaled 15° .

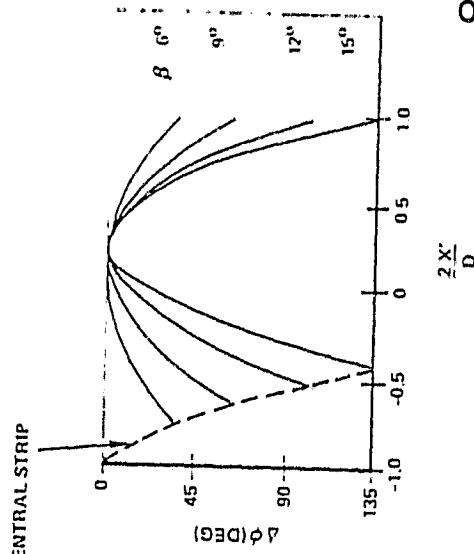
The effects of f/D ratio on aperture reduction and path length errors are seen. Smaller f/D ratios have less aperture reduction but greater path length errors.



SYMMETRIC NEAR-FIELD CASSEGRAIN



PATH LENGTH PHASE ERROR
f/D = 0.4, D = 250 lambda
MAGNIFICATION = 4



PATH LENGTH PHASE ERROR
f/D = 0.3, D = 250 lambda
MAGNIFICATION = 3.3

SECONDARY APERTURE DISTRIBUTIONS, NEAR-FIELD CASSEGRAIN

87147D

ORIGINAL PAGE IS
OF POOR QUALITY

8. NEAR-FIELD SYMMETRIC GREGORIAN

Little information has been published about the off-axis properties of this configuration. Dragone and Hogg (11.2) implicitly talked about its radiation patterns and the reflection coefficient seen at the feed. Morgan (11.3) discussed the possibility of using the concave subreflector to minimize spillover and wide angle sidelobes. He found that antennas of practical proportions were difficult to design.

9. OFFSET NEAR-FIELD PARABOLA

This particular configuration has received little attention in the literature. The theory of operation, in principle, is very similar to its symmetric counterpart discussed earlier. The obvious advantage of the offset configuration is the elimination of feed blockage, resulting in a significant improvement in far field beam performance.

ORIGINAL PAGE IS
OF POOR QUALITY

10. Offset Near-Field Cassegrain

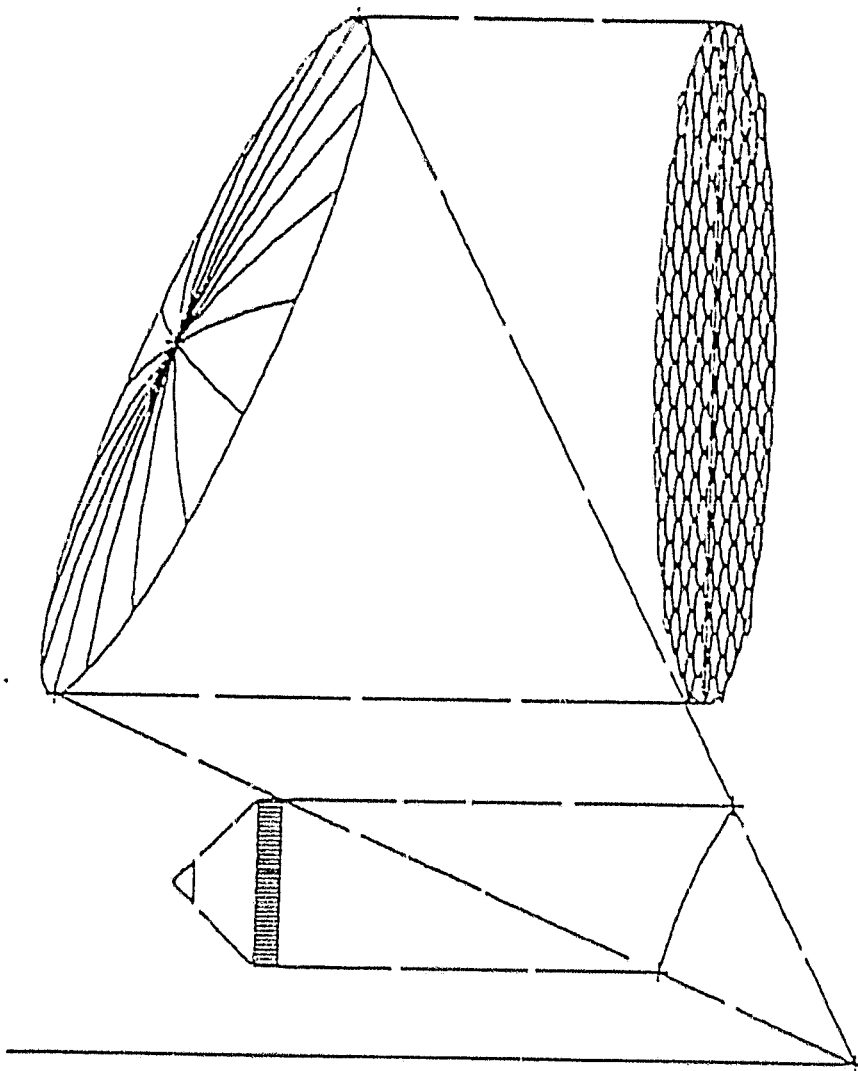
- This is one approach that Harris is studying for the scanning beam case.
- A phased array generates a plane wave that is incident on the parabolic subreflector.
- Beam steering results from applying varying phase tilts to the feed array.
- The input and output signals (array feed and secondary beam, respectively) are collimated beams.
- This configuration follows that of the symmetric near field Cassegrain presented by Fitzgerald (1.2).

ORIGINAL PAGE IS
OF POOR QUALITY

OFFSET NEAR-FIELD CASSEGRAIN DESIGN PROCEDURE

- 0 Relate the far field beam requirements of the antenna system to physical dimensions of the feed array and subreflector.
- 0 Assume a perfect imaging reflector system.
- 0 Apply a 3 dB sector edge illumination criterion to aperture array elements.
- 0 Note that this implies a 3 dB gain loss at sector edge. (Other edge criteria could be applied, resulting in more feed array elements.)
- 0 Determine actual feed array size and element spacing through magnification factor.

ORIGINAL PAGE IS
OF POOR QUALITY



1453 82

Offset Near-Field Cassegrain Geometry Showing Aperture Array

ORIGINAL PAGE IS
OF POOR QUALITY

PERFORMANCE OF NEAR-FIELD CASSEGRAIN

- Chosen to minimize physical size for spacecraft applications.
- Disadvantage is the amount of spillover. For limited scan applications the amount of spillover may be acceptable.
- Offset Gregorian may be used where the confocal parabola has excessive spillover. However image distortion increases with scan angle.

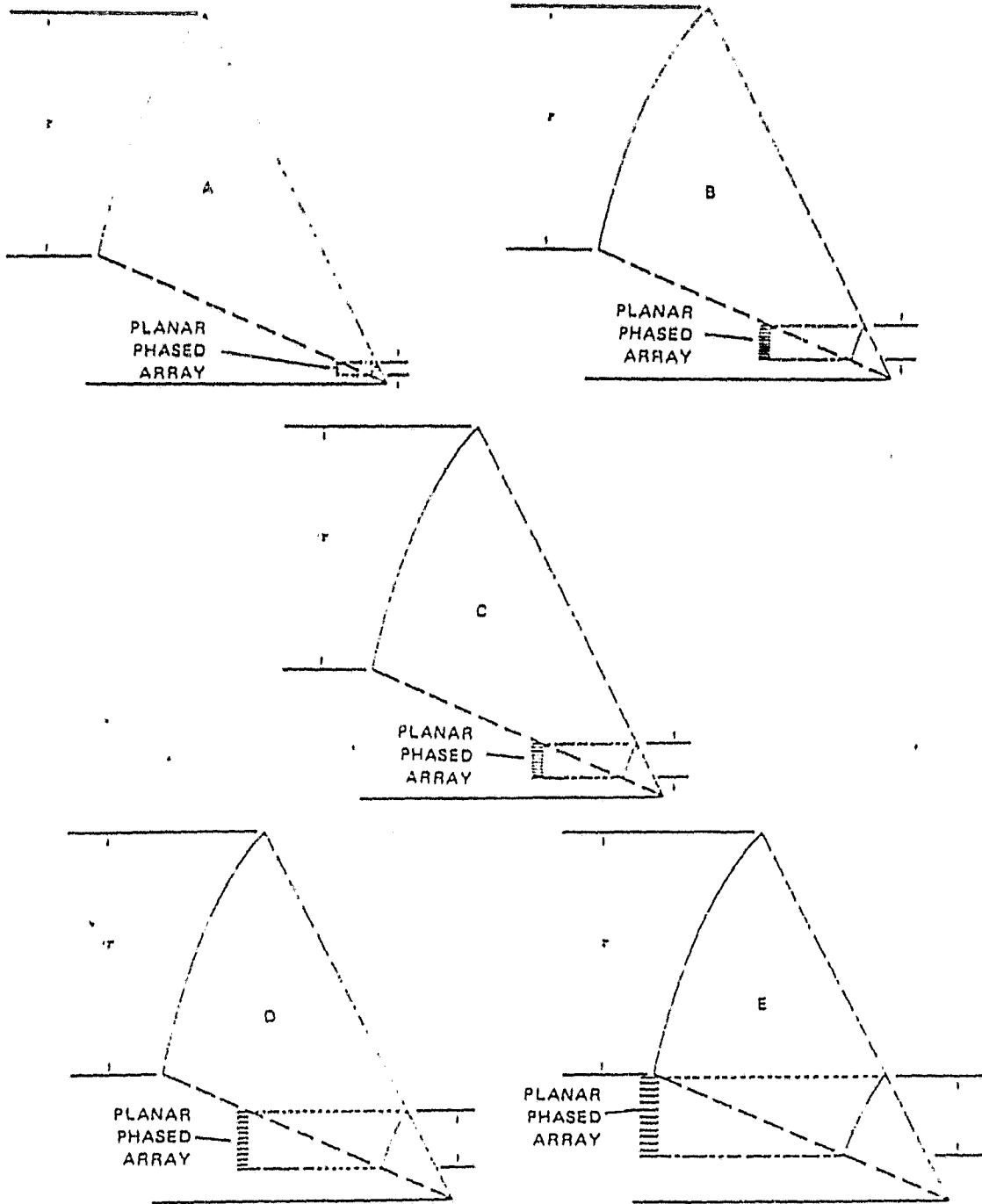
ORIGINAL PAGE IS
OF POOR QUALITY

OFFSET NEAR-FIELD CASSEGRAIN CONFIGURATION

- 12' main reflector with fixed f/D ratio and offset angle
- Operating frequency 20 GHz
- Largest subreflector chosen to prevent blockage

Table Of The Offset Near Field Cassegrains Studied

	<u>SUBREFLECTOR DIAMETER (INCHES)</u>	<u>MAG FACTOR</u>	<u>SUBREFLECTOR F/D</u>	<u>SUBREFLECTOR FOCAL LENGTH (INCHES)</u>
A	9	16	0.405	11.1
B	18	8	0.405	22.2
C	27	5.3	0.405	33.4
D	36	4	0.405	44.5
E	45	3.2	0.405	55.6



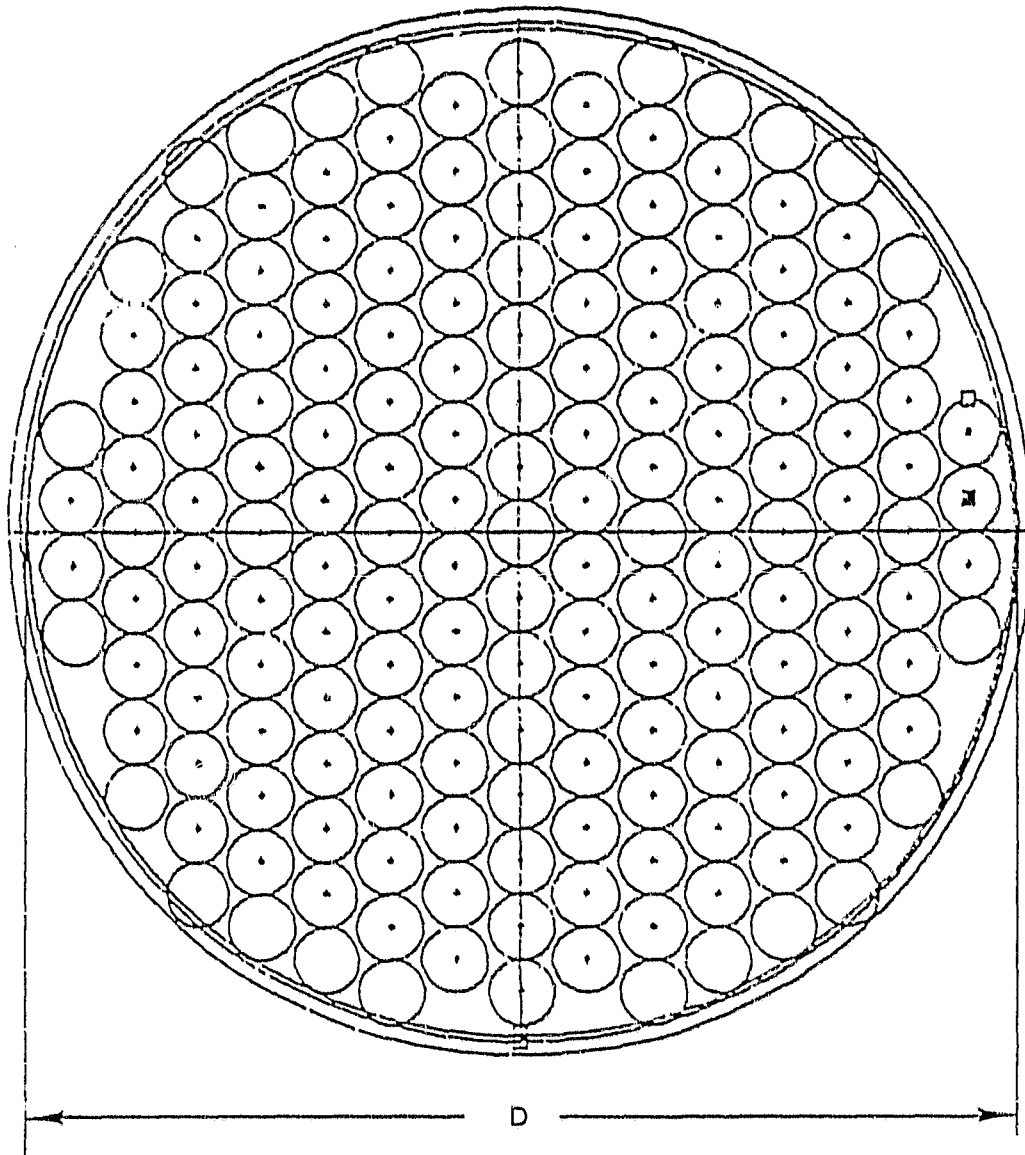
1450 82

Offset Near-Field Cassegrain Configurations

TYPICAL ARRAY CHOSEN FOR NEAR-FIELD CASSEGRAIN FEED

- Dominant TE_{11} mode conical horns.
- 177 elements.
- Amplitude weighting distribution proportional to $\cos(\theta/A)$.

ORIGINAL PAGE IS
OF POOR QUALITY



1454 82

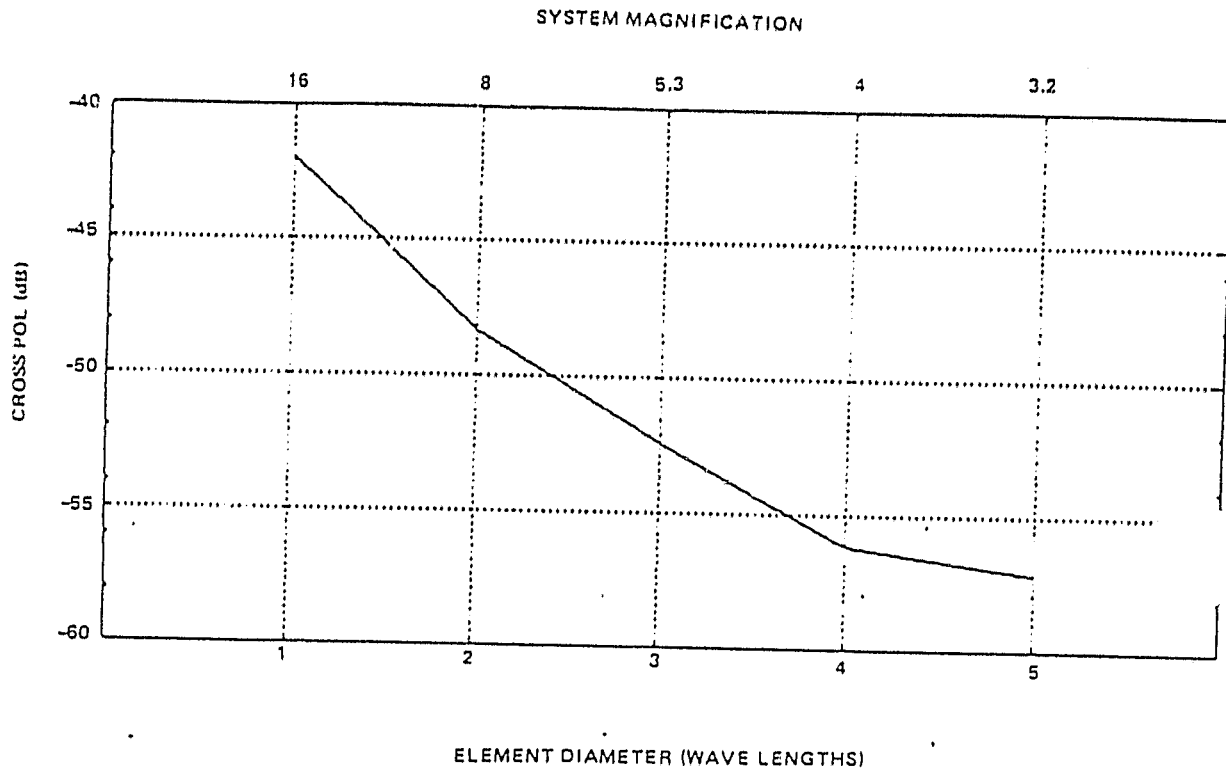
177 Phased Array Feed Elements Are Required
Based On The Far-Field Sector Scan Criteria

ORIGINAL PAGE IS
OF POOR QUALITY

PERFORMANCE OF NEAR-FIELD CASSEGRAIN

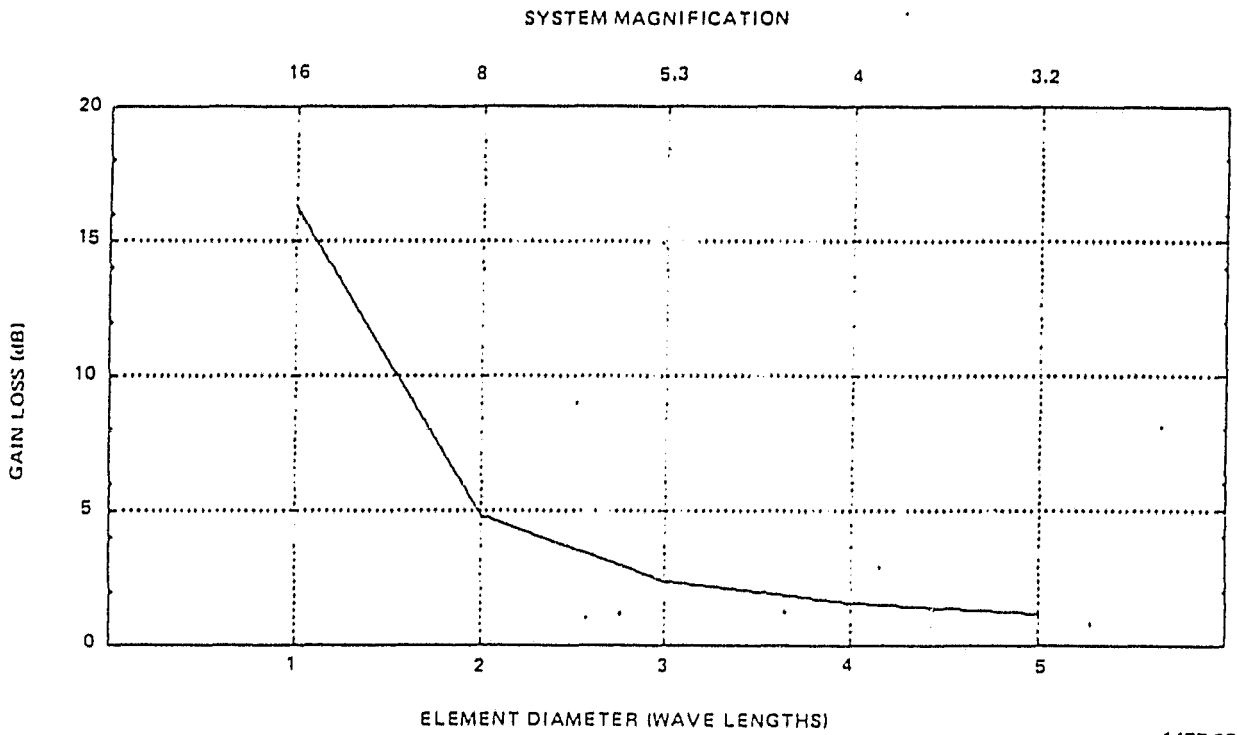
AS A FUNCTION OF MAGNIFICATION RATIO

- Cross polarization decreases with decreased system magnification.
- Gain loss decreases with decreased system magnification.
- There is an equivalent beam deviation factor for near-field systems.



Cross Polarization Levels Vs Element Diameter For An On-focus Beam.
Feed Array Contains 177 Dominant Mode Conical Horns with an
Amplitude Weighting Distribution Proportional to $\cos(\pi \rho / D)$

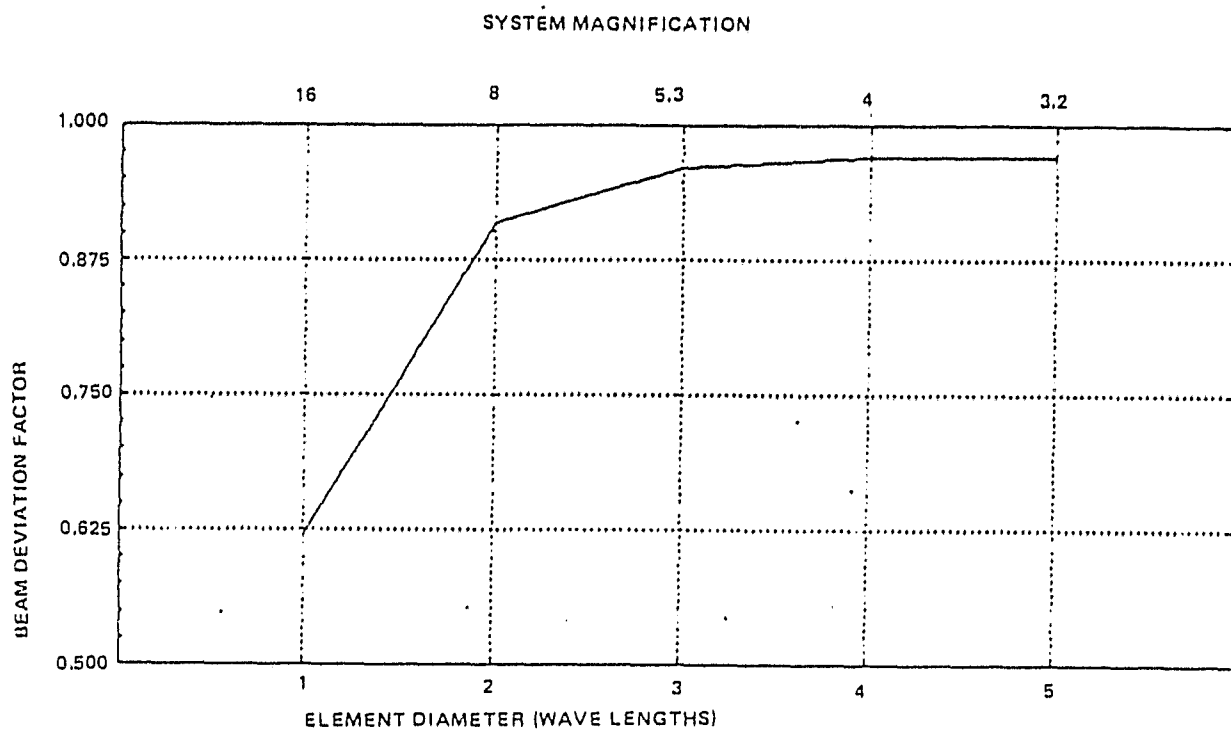
ORIGINAL PAGE IS
OF POOR QUALITY



1477 82

Gain Loss Vs Element Diameter for 2 1/2 Beamwidths Scan.
Feed Array Contains 177 Dominant Mode Conical Horns With An Amplitude
Weighting Distribution Proportional to $\cos(\pi \rho/D)$.

ORIGINAL PAGE IS
OF POOR QUALITY



1479 82

Beam Deviation Factor Vs Element Diameter for 2-1/2 Beamwidths Scan.
Feed Array Contains 177 Dominant Mode Conical Horns With An Amplitude
Weighting Distribution Proportional to $\cos(\pi \rho / D)$.

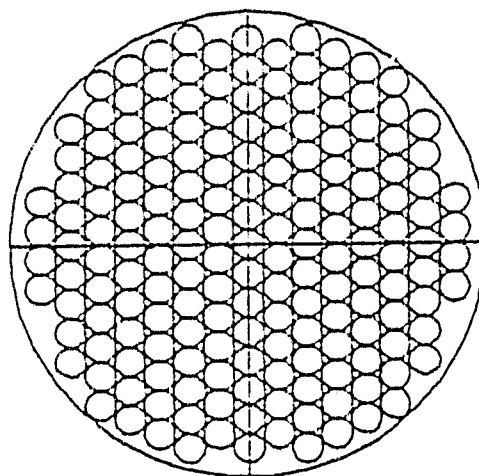
ORIGINAL PAGE IS
OF POOR QUALITY

MULTIPLE BEAM NEAR FIELD SYSTEM

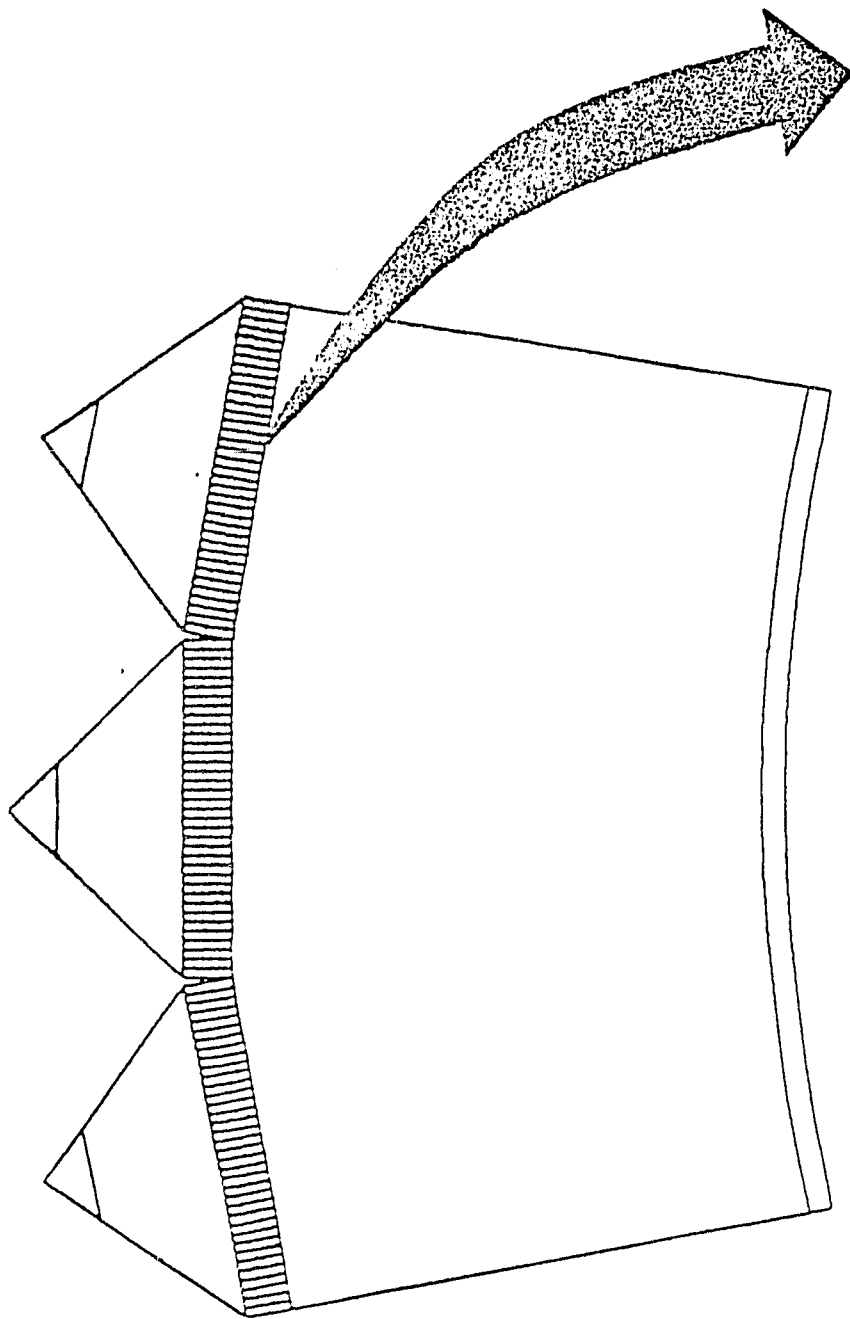
- Requires multiple array feeds for multiple beams.
- Can use OMT's to obtain simultaneous orthogonal linear polarizations.
- Can cover two of six CONUS zones with one dual polarization array.

THREE SECTOR FEED ARRAY LAYOUT

ORIGINAL PAGE IS
OF POOR QUALITY



FRONT VIEW



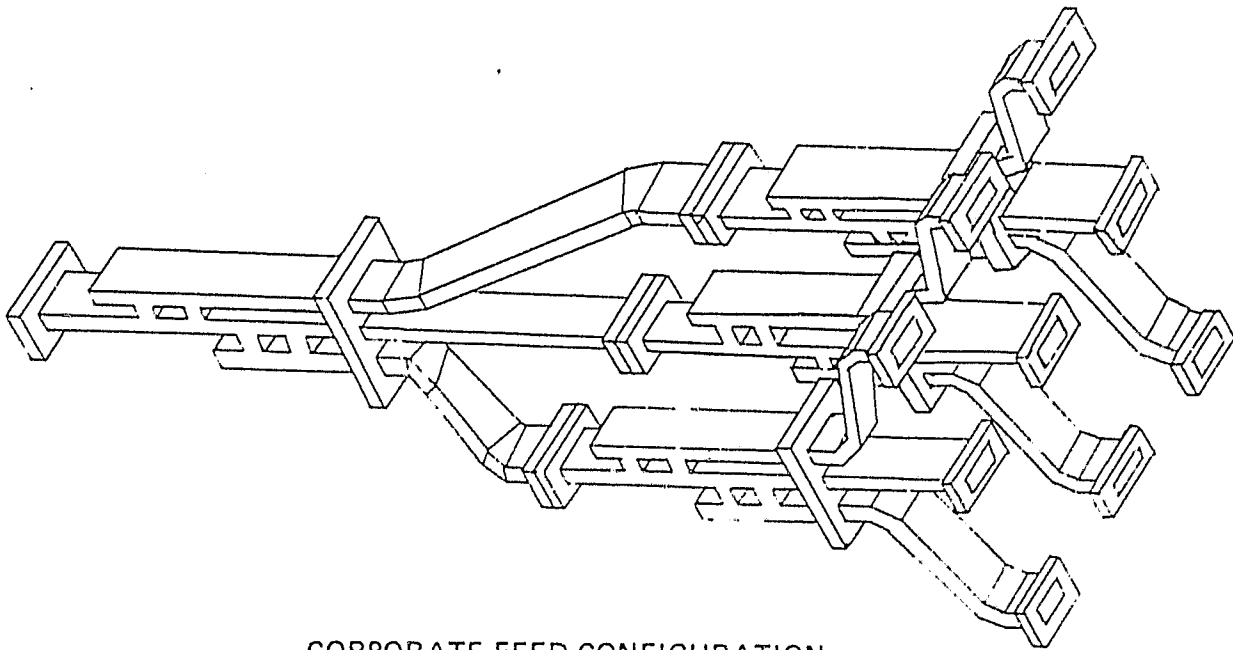
TOP VIEW

TRI-Focal Subreflector

1314 82

FEED SYSTEM DESIGN

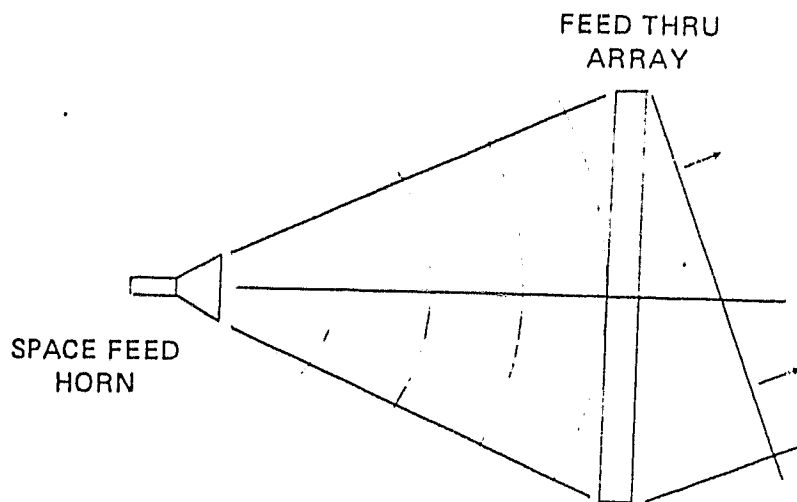
- CORPORATE FEED
 - USES POWER DIVIDERS, BENDS, TWISTS TO FORM "N" OUTPUTS FROM A SINGLE INPUT
 - POWER LOSSES OCCUR IN WAVEGUIDE COMPONENTS
 - PROVIDES EXACT POWER DIVISION BETWEEN FEEDS
 - SIMPLE TECHNIQUE
 - NO EXTRA RF RADIATION
 - SUBJECT TO PHASE VARIATIONS DUE TO THERMAL EFFECTS



CORPORATE FEED CONFIGURATION

FEED SYSTEM DESIGN (CONTINUED)

- SPACE FEED
 - USES FREE SPACE TO DIVIDE SIGNAL AMONG RADIATING ELEMENTS. IDEAL FOR ARRAYS OF LARGE NUMBER OF ELEMENTS.
 - SPILLOVER LOSS DUE TO ILLUMINATION NOT BEING CONFINED TO THE ANGLE SUBTENDED BY THE ARRAY
 - LESS WAVEGUIDE - LOWER COST AND WEIGHT
 - RESULTING AMPLITUDE TAPER CAN BE USEFUL



1545 82

SPACE FEED CONFIGURATION

SPACE VS CORPORATE FEED

FEED TYPE	MODULE TYPE	RF INPUT POWER PER ELEMENT	NUMBER OF ELEMENTS	TOTAL RF INPUT POWER*	DC INPUT POWER REQUIRED	TOTAL RF OUTPUT POWER	EIRP**	ARRAY EFFICIENCY
CORPORATE	VPS-VPA	10 mW	177	3.7 W	254.9 W	32.75 W	68.15 dBW	11.307%
SPACE	VPS-VPA	10 mW	177	4.5 W	254.9 W	32.75 W	68.15 dBW	11.083%
CORPORATE	VPS-CGA-VPA	0.125 mW	177	46.2 mW	260.7 W	32.75 W	68.15 dBW	12.535%
SPACE	VPS-CGA-VPA	0.125 mW	177	56.0 mW	260.7 W	32.75 W	68.15 dBW	12.541%

* INCLUDES FEED LOSSES

** INCLUDING 53 dB REFLECTOR GAIN

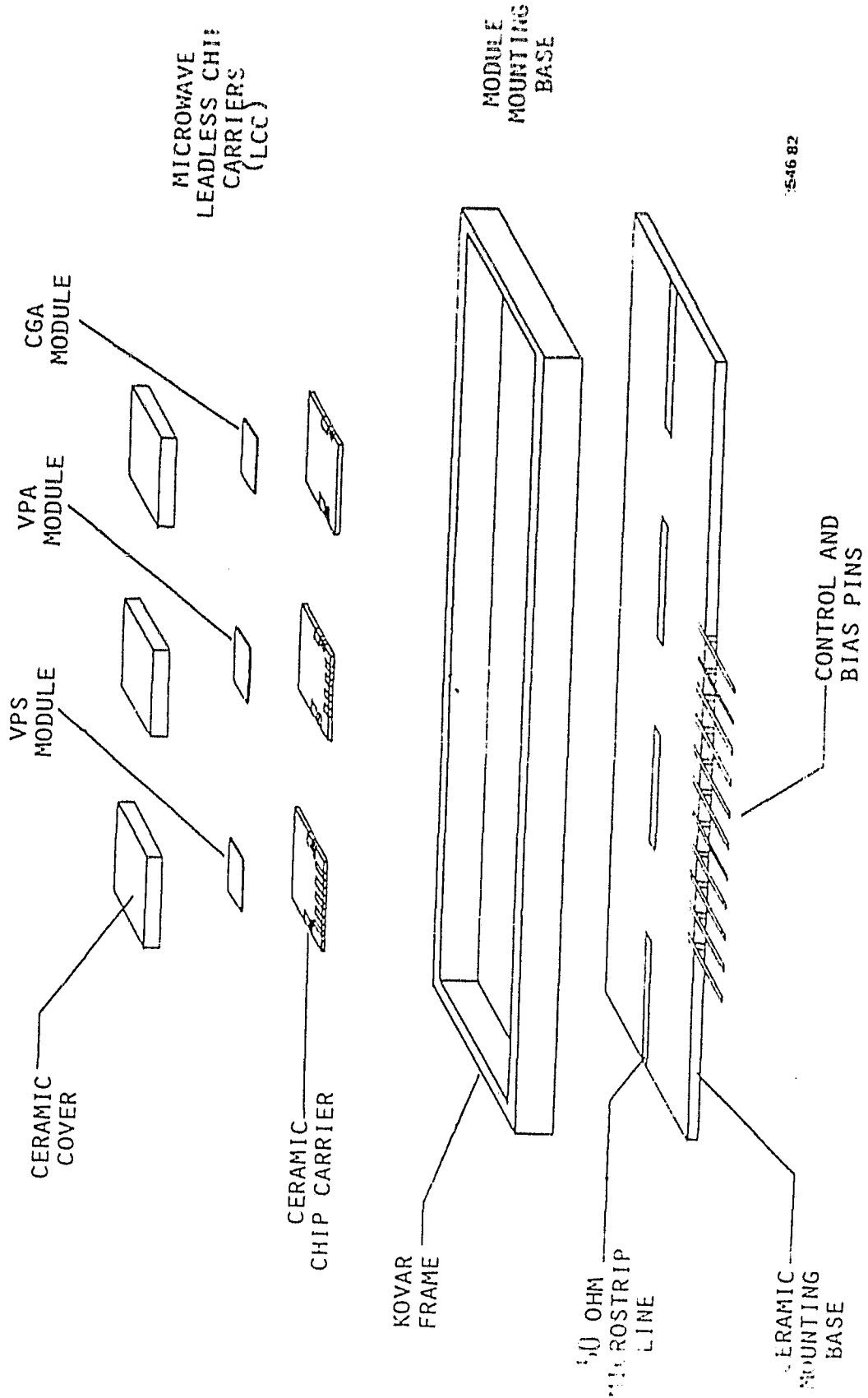
$$\text{ARRAY EFFICIENCY} = \frac{\text{RF OUTPUT} - \text{RF INPUT}}{\text{DC INPUT}}$$

ORIGINAL PAGE IS
OF POOR QUALITY

RECOMMENDED SSPA ELEMENT DESIGNS

- Use leadless chip carrier.
- Uses microstrip to interconnect the chip modules.
- Makes use of ridgeline transformer to convert from microstrip to waveguide (excellent performance measured at 30 GHz).

MONOLITHIC TRANSMIT MODULE MOUNTING CONFIGURATION

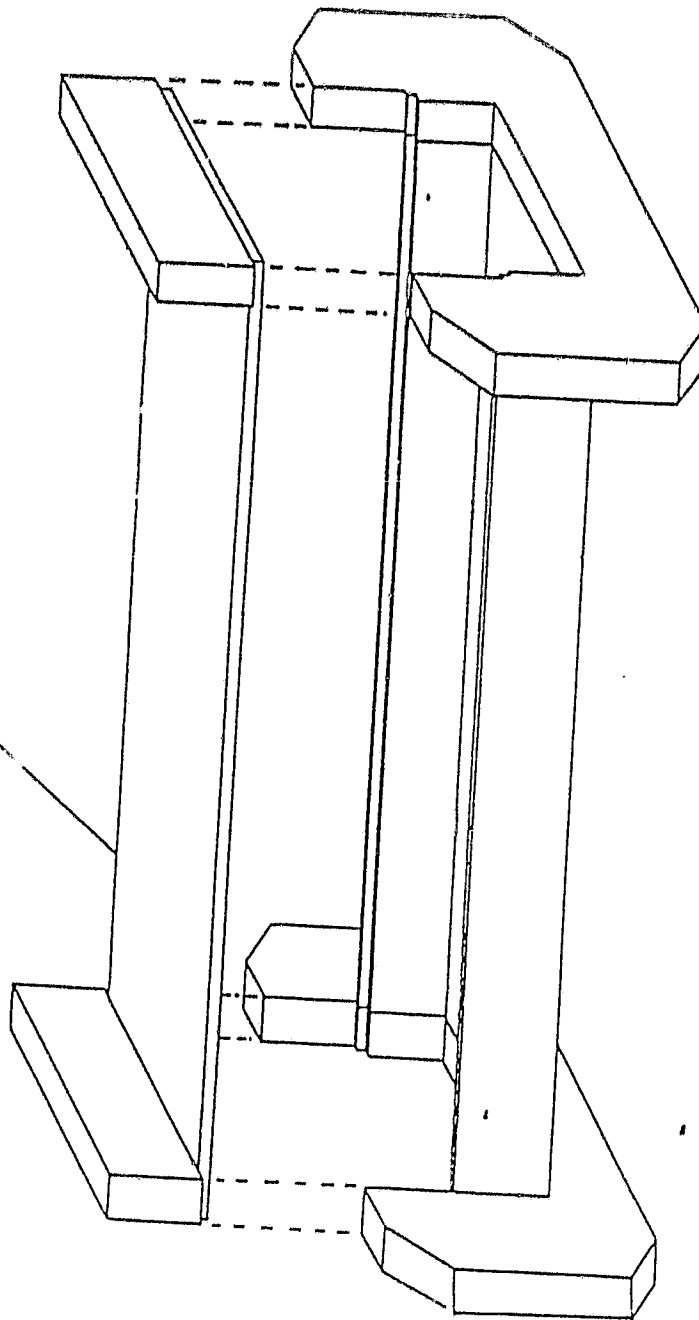


5-46 82

ORIGINAL PAGE IS
OF POOR QUALITY

MODULE SECTION

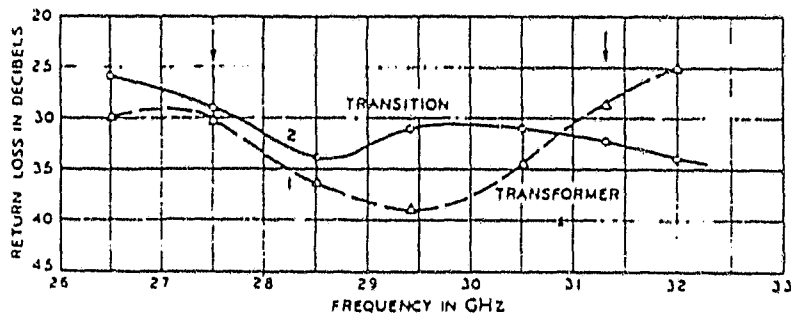
REMOVABLE COVER FOR
MOUNTING MONOLITHIC
TRANSMIT MODULE



1547 B2

WAVEGUIDE TO MICROSTRIP TRANSITION

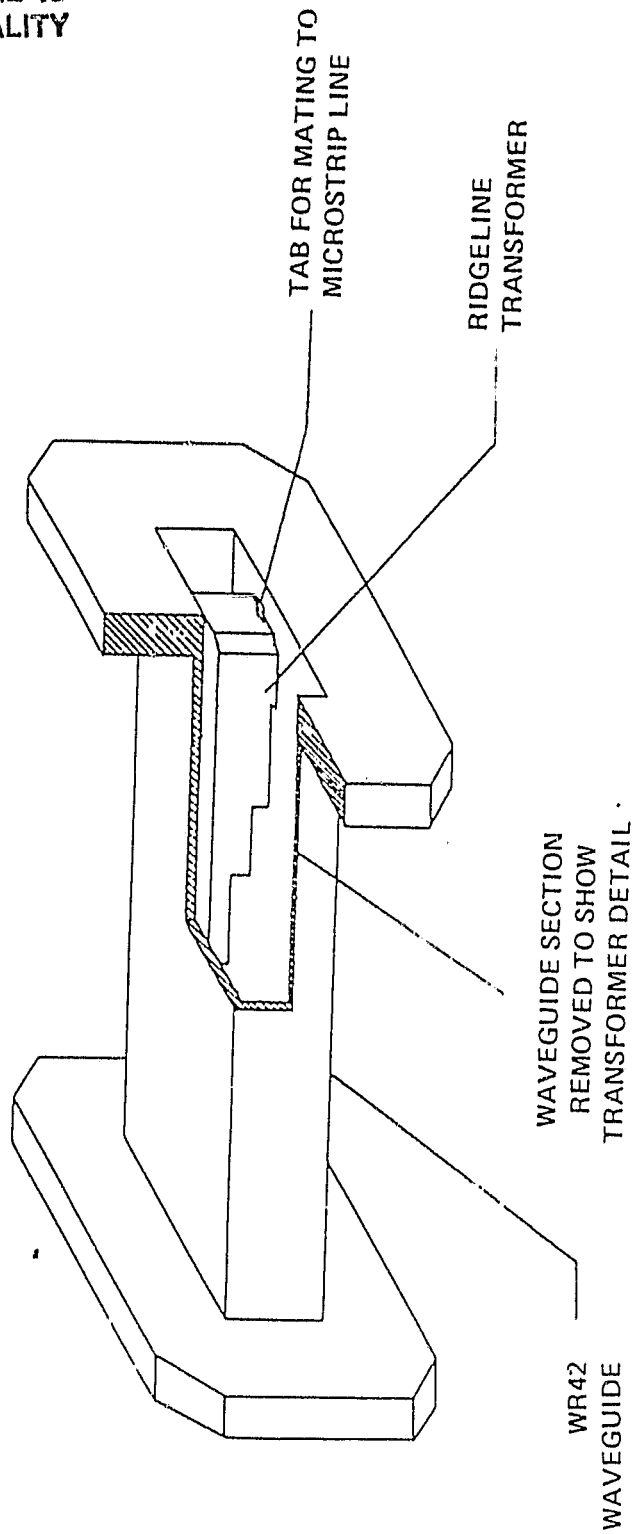
- DESIGN CHOICE: RIDGELINE TRANSFORMER
 - BROADBAND CAPABILITY
 - STRAIGHTFORWARD DESIGN
 - READILY ADAPTED TO UNSYMMETRICAL MICROSTRIP LINE
 - EASILY MACHINED AND ATTACHED TO WAVEGUIDE
- PERFORMANCE OF TRANSITION
 - SAMPLE TEST DATA FOR 27.5-31.3 GHz TRANSITION BUILT BY SCHNEIDER, ETAL



RETURN LOSS OF TRANSFORMER AND TRANSITION FROM
WAVEGUIDE TO MICROSTRIP FROM 26.5 GHz TO 32 GHz

ORIGINAL PAGE IS
OF POOR QUALITY

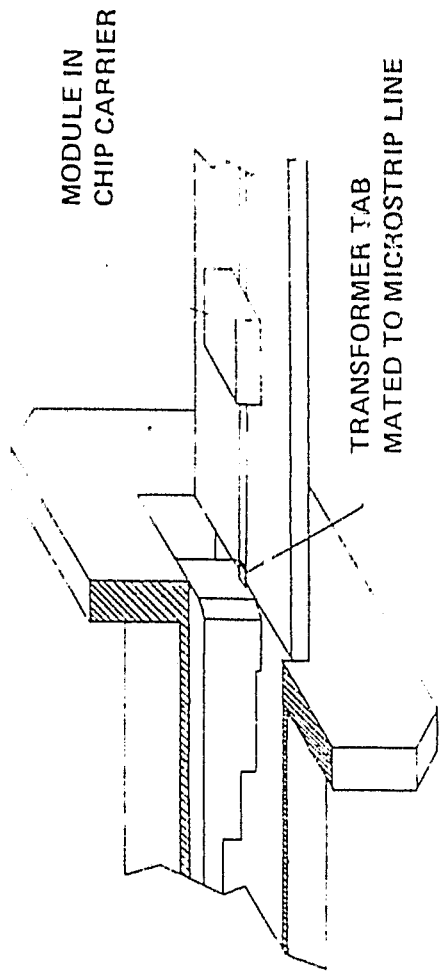
TRANSFORMER SECTION



1549 82

ORIGINAL PAGE IS
OF POOR QUALITY

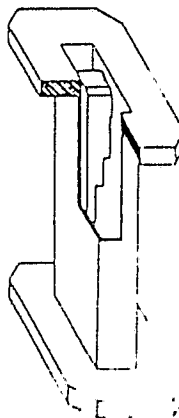
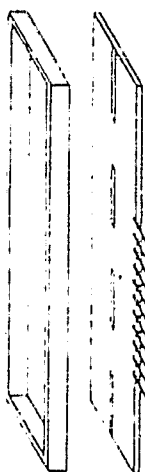
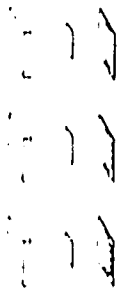
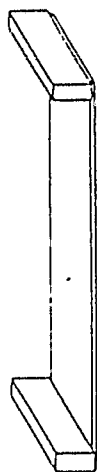
DETAIL OF TRANSFORMER - MICROSTRIP CONNECTION



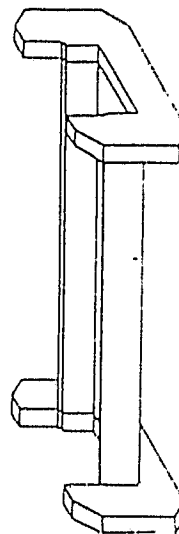
1347 82

ORIGINAL PAGE IS
OF POOR QUALITY

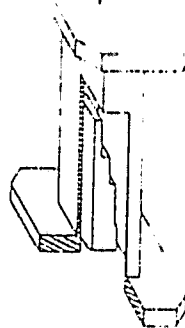
MONOLITHIC MODULE TRANSITION AND MOUNTING CONFIGURATION



TRANSFORMER
SECTION



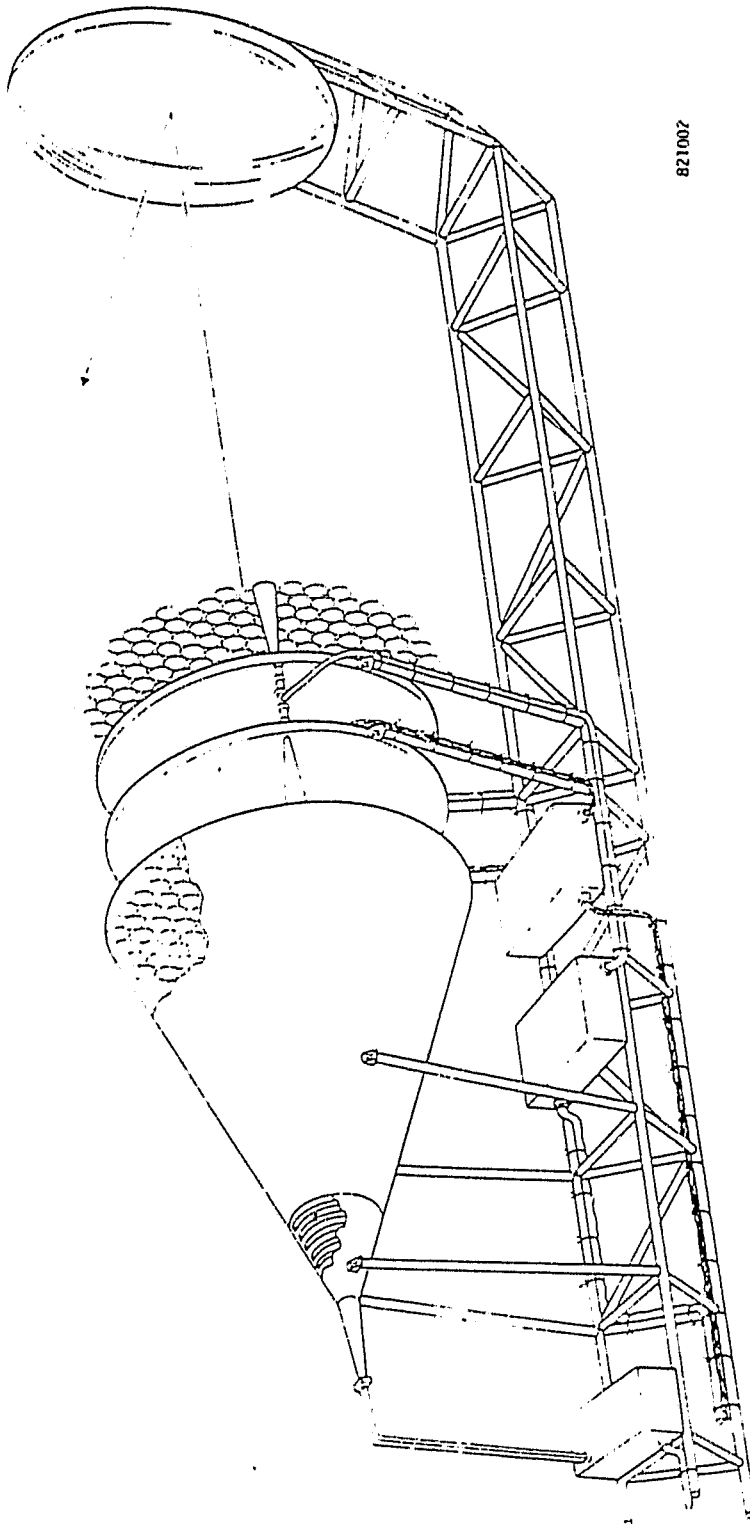
MODULE
SECTION



TRANSFORMER
SECTION

1348 82

ORIGINAL PAGE IS
OF POOR QUALITY

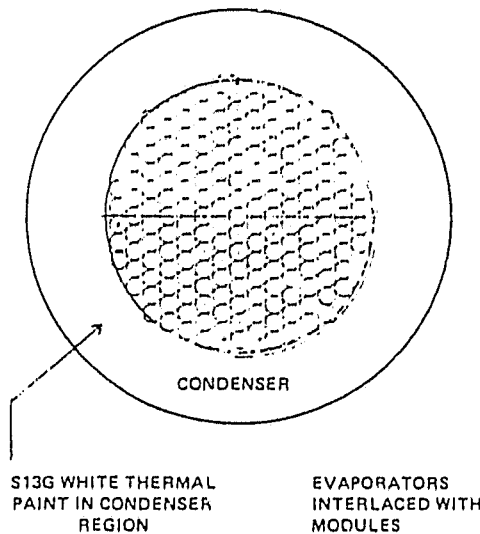


821007

Scanning Beam Space Fed Phased Array

ARRAY HEAT REMOVAL

- MUST REMOVE UP TO 500 WATTS HEAT DISSIPATION FROM THE CORE OF THE PHASED ARRAY
- INTEGRATE HEAT PIPES INTO A MOUNTING PLATE WHICH ATTACHES AT MODULE SECTION TO EACH ELEMENT
- 500 WATTS INPUT INTO 1.0 m DIAMETER EVAPORATOR AREA BY 177 WAVEGUIDE SECTIONS CONTAINING MODULES
- HEAT FLOWS Laterally BY HEAT PUMPING TO A 0.3 m WIDE BORDER COATED WITH S-13G PAINT; HEAT IS THEN REJECTED TO SPACE BY RADIATION



ESTIMATES FROM INDEPENDENT CONTRACTOR INDICATE THE STRUCTURE WILL DISSIPATE APPROXIMATELY 1200 WATTS WITH A MAXIMUM HEAT SINK TEMPERATURE OF 60°C

11. OFFSET NEAR-FIELD GREGORIAN

Imaging Reflector Configuration

In reference (2.2) Dragone & Gans pointed out several important properties of the Gregorian Imaging Reflector System.

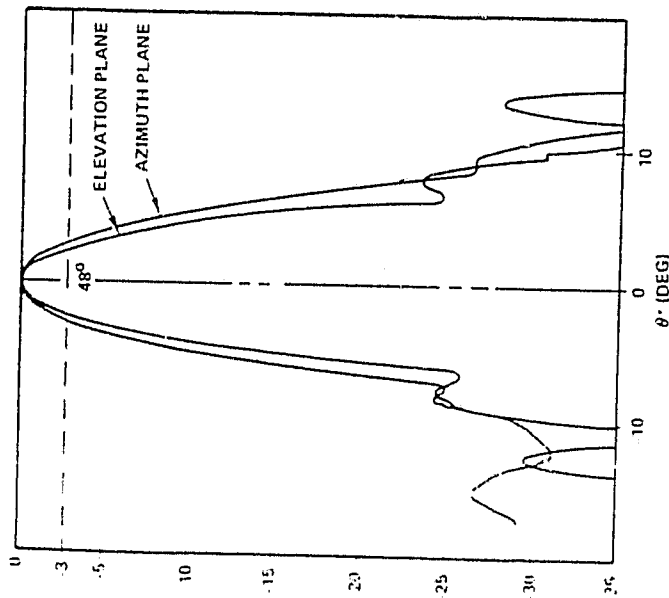
One important concept is that of conjugate elements, i.e., rays emanating from a point on a surface in an optical system are transformed to rays emanating from the conjugate point on a second surface. In a Gregorian optical configuration two conjugate planes can be determined. The array surface projection is the reference plane and the inverted image surface in the projected aperture of the main reflector is the conjugate plane.

A second important concept is the frequency independence of the transformation relating the array aperture to the main reflector projected aperture.

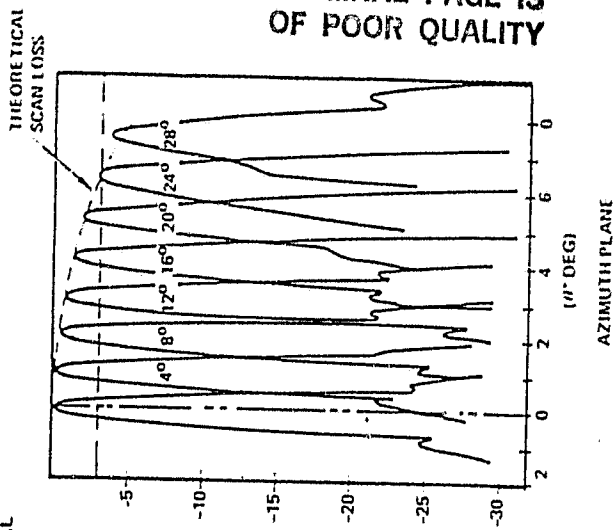
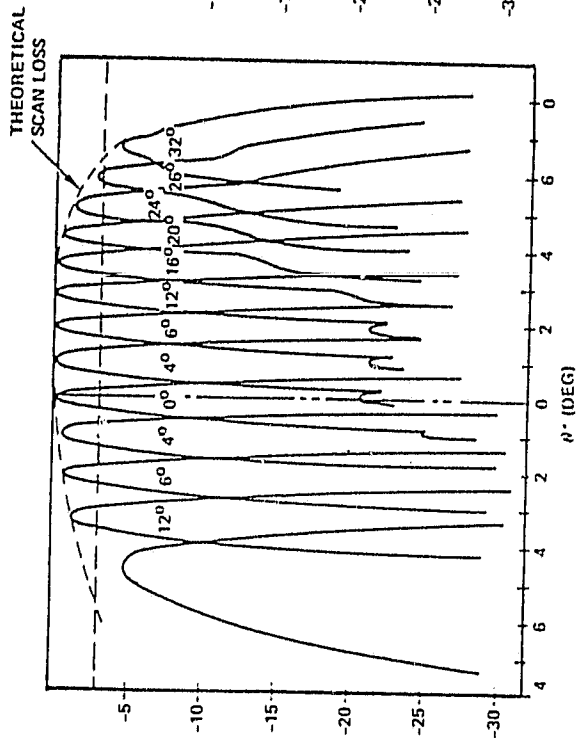
Reference (7.1) determined the performance of the Gregorian configuration by a plane wave expansion from a series of transformed plane waves. Dragone and Gans' entire analysis is based on the laws of Geometrical Optics.

OFFSET NEAR-FIELD GREGORIAN
FITZGERALD

MEASURED RESULTS



ON-AXIS PATTERNS
TWO PRINCIPLE PLANES

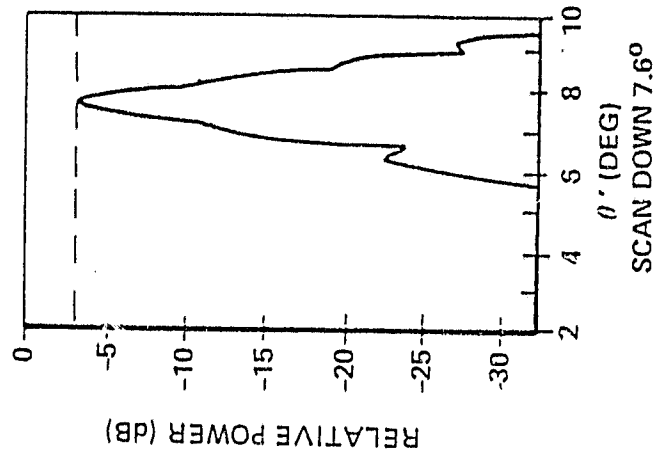
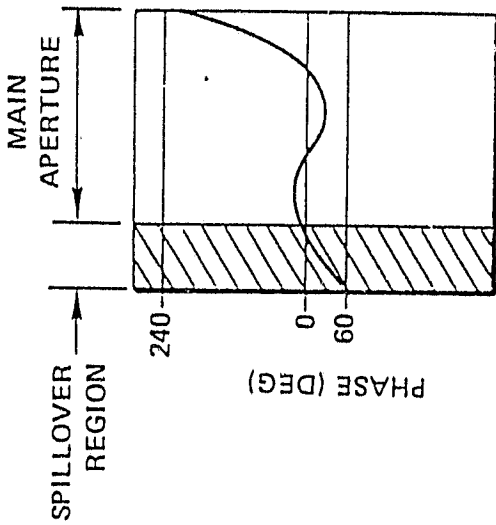
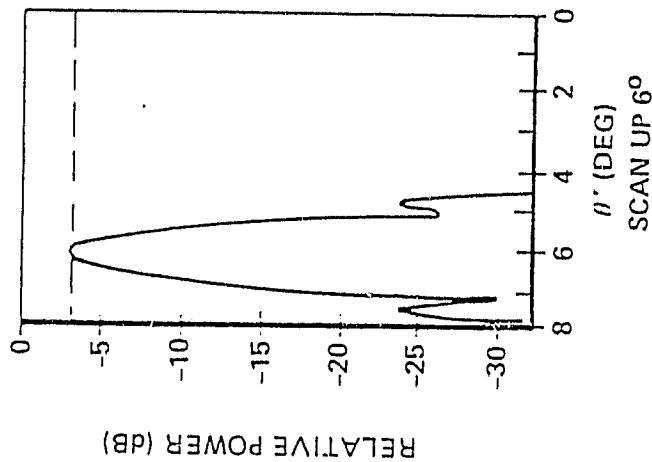
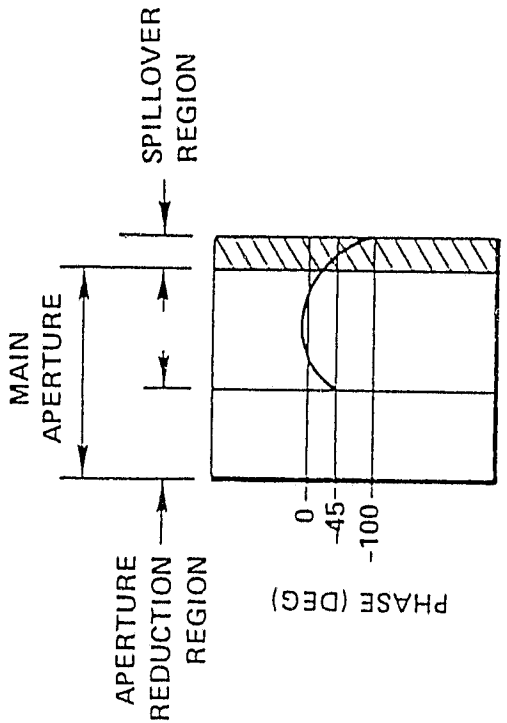


ORIGINAL PAGE IS
OF POOR QUALITY

APERTURE = 142 λ MAGNIFICATION = 4.0

820425

OFFSET NEAR-FIELD GREGORIAN
 APERTURE PHASE DISTRIBUTION AND ASSOCIATED PATTERNS



ORIGINAL PAGE IS
 OF POOR QUALITY

POLARIZATION

No information concerning the cross-polarization properties of any near-field system was found. However, much has been written about the polarization properties of on-axis beams in focused systems. Dijk, et.al. [12.2] compared the polarization efficiencies of 4 of the focused reflector systems that we have discussed:

- Symmetric front-fed paraboloid:
efficiency .999 to .939
 - for subtended angles from 60° to 160° or $f/D = .933$ to $.300$
 - Worse for lower f/D ratios

- Offset front-fed paraboloid:
efficiency .997 to .916
 - for subtended angles 40° to 100° (offset angle 30° and 60° , respectively)
 - Polarization efficiency is dependent on feed polarization

- Symmetric Cassegrain:
efficiency 1.0 to .996
 - for subtended angles from 60° to 160° $M = 2$
 - Worse for lower magnification (M) values

- Offset Cassegrain
efficiency .997 to .924
 - for subtended angles 40° to 100° (offset angle 30° and 60° , respectively)
 - Similar to the offset front-fed paraboloid; but, the results are less sensitive to polarization of the feed.

ORIGINAL PAGE IS
OF POOR QUALITY

POLARIZATION COMPENSATION

According to Rudge and Adata [2.4] depolarization in offset front-fed and offset Cassegrain antennas can be made to cancel by designing the primary feed to provide a conjugate match to the incoming fields. In contrast to a linearly polarized corrugated horn they suggest an approach where higher order asymmetric waveguide modes are used to provide the polarization correction. A similar effect might be obtained in an element cluster where some of the array elements were orthogonally polarized.

3. ARRAY FEEDS

ORIGINAL PAGE IS
OF POOR QUALITY.

ARRAY PROPERTIES

In addition to knowledge of the reflector optics it is important to discuss the properties of the array feeds. The electric-field from an array of elements can be expressed by a single fundamental equation. Many simplifications of the array equation are possible, but will not be discussed. An important consideration is that of array element complex weights, i.e, amplitude and phase. A general discussion is given; however, specifics can only be discussed in the context of a detailed design. This discussion concludes with examples of design considerations others have found to be important when dealing with array feeds in reflector systems.

EQUATION OF A 2-DIMENSIONAL ARRAY

- Applicable to both:
 1. A multiple fixed spot beam might consist of a cluster of elements used in a focused system with approximately 7 elements in the cluster.
 2. The scanning beam case is a near-field system consisting of at least 177 elements per beam.

- The electric field pattern of the array is given by:

$$\bar{E}(\bar{r}) = k \sum_i f_i(\theta, \phi) a_i \frac{e^{jk|\bar{r}-\bar{r}_i|}}{|\bar{r}-\bar{r}_i|}$$

where

- \bar{E} is the electric field vector
- \bar{r} the position vector from the origin to the observation point
- k a complex constant
- $f_i(\theta, \phi)$ element radiation pattern in the array environment as a function of the polar angles for the i^{th} element
- a_i the complex weight of the i^{th} element
- \bar{r}_i the position vector of the i^{th} element

- Element weight, a_i , is complex, i.e., amplitude and phase
 1. Multibeam clusters, a_i is fixed by the BFN. For dynamic beam control, a_i must be controlled in amplitude and phase.
 2. Scanning array, the a_i 's are modified in amplitude and phase to steer the beam.

EQUATION OF A 2-DIMENSIONAL ARRAY - contd.

3. Dynamic amplitude and phase control is usually reserved for adaptive antenna systems where all of the requirements are not known a priori. Antenna patterns are modified by the measurement of some parameter in a control loop that seeks to optimize that parameter. However, the optics configurations discussed earlier require both dynamic amplitude and phase control to correct for optics transform properties when the beam is repositioned.
4. Dynamic EIRP control, amplitude and phase control can be used when the need arises to change the effective radiated power from time to time.

● The position vector \bar{r}_j describes the location of the elements in the lattice. This lattice is very important to the control of grating lobes, which possess the properties of the main beam in the sampled aperture space. For large element spacing, these grating lobes appear in the "visible region" which means that there is propagation in the grating lobe direction.

● Element patterns $f_j(\theta, \phi)$

1. Finite array: each element has a slightly different pattern.
2. Array edge effects become important, vastly different element patterns near edge.
3. Typical array has elements with a $\cos \theta$ field pattern, some arrays use high gain elements where the pattern width is narrower, reason: limited scan and aperture filling.

GENERAL PROPERTIES OF ARRAY ELEMENT WEIGHTS

- Size of aperture determines beamwidth.
- Phase distribution determines scan angle and focal range.
- Amplitude and spatial tapers determine sidelobe characteristics.
- If all parameters are known a priori, then traditional synthesis methods are applicable.
- Synthesis methods:
 1. Fourier Transform Method
 2. Laplace Transform Method
 3. Woodward's Synthesis Method
 4. Optical Synthesis
 5. Iterative Methods
 6. Optimum Design Methods
 - a. Minimum Beamwidth
 - b. Taylor's Method
 - c. Dolph-Chebyshev
- Synthesis of 2-dimensional sources:
 1. Separable distribution, line source, uses methods mentioned above
 2. 2-Dimensional Fourier Transform
 3. Circular Source, Hankel Transform
- Fresnel Region Synthesis:
 1. Used if field distribution is specified in the Fresnel Region (radiating near-field).
 2. Integral equation of the Fresnel field is inverted to give integral equation for the source distribution.

C-2

GRATING LOBE CONTROLS AND MINIMUM CONTROLS

Considerations

- EIRP requirements met and exceeded for SSPA active array implementation when controlling grating lobes.
- Since wide scan angles are not envisioned, e.g., $\pm 2^\circ$ secondary scan with a magnification of 4 \rightarrow primary array must scan $\pm 8^\circ$.
- Cost, weight and mechanical tolerances of closely spaced arrays provides impetus for thinning the array feed.
- Partial choice of array lattice configuration based on observability of grating lobes in U - V space.
- Rectangular lattice configuration acceptable for narrow scan angles; Triangular lattice used for large scan angles and reduce coupling.

Array Controls

- Minimum number of controllers needed for LFUV phased array determined by:

$$\text{Max} \left\{ N/N_{\min} \right\} = 1, \text{ where } N \text{ is the number of phase shifters used;}$$

N_{\min} is the minimum number of control elements.

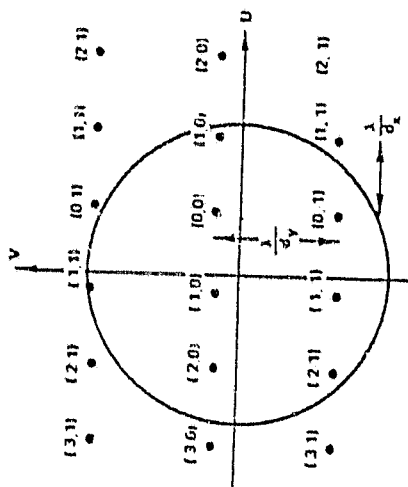
$$N_{\min} = \left[\frac{\sin \theta_{\max}^{(1)}}{\sin \left(\theta_3^{(1)} / 2 \right)} \right] \left[\frac{\sin \theta_{\max}^{(2)}}{\sin \left(\theta_3^{(2)} / 2 \right)} \right]$$

where $\theta_{\max}^{(1)}$, $\theta_{\max}^{(2)}$ are the maximum scan angle in the two planes at peak;

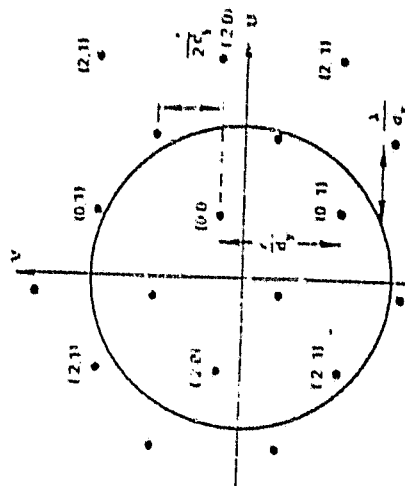
$\theta_3^{(1)}$, $\theta_3^{(2)}$ are the half-power beamwidths.

ORIGINAL PAGE IS
OF POOR QUALITY

Grating Lobes in U - V Space



GRATING LOBE LATTICE FOR RECTANGULAR GRID

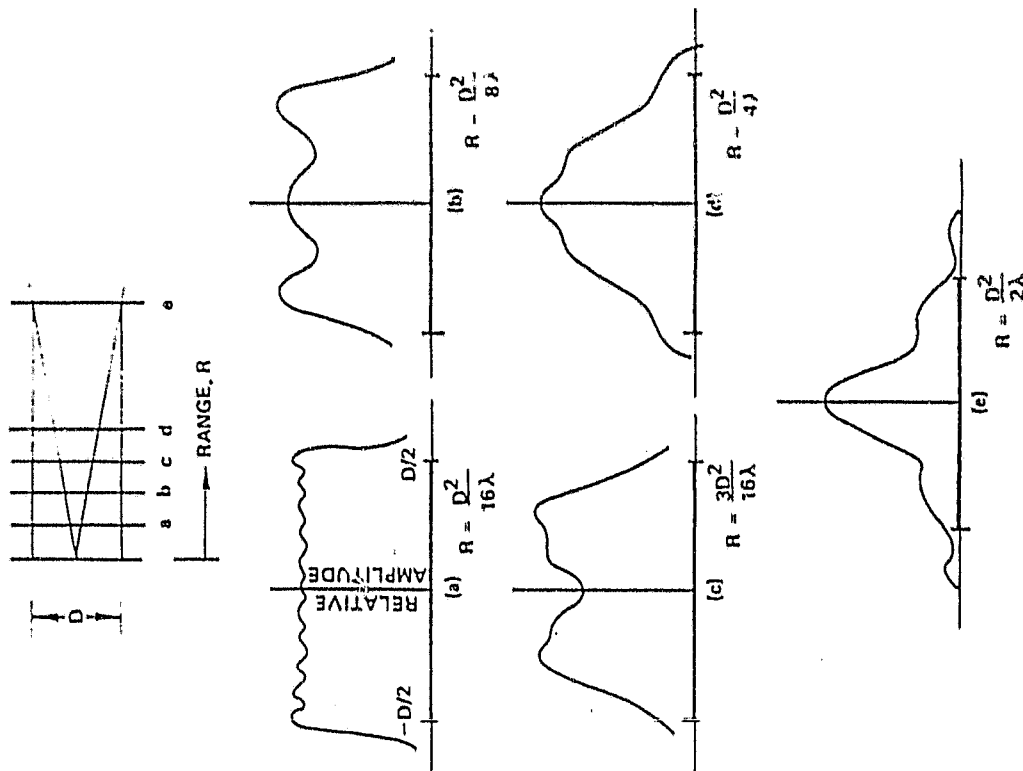


GRATING LOBE LATTICE FOR TRIANGULAR GRID

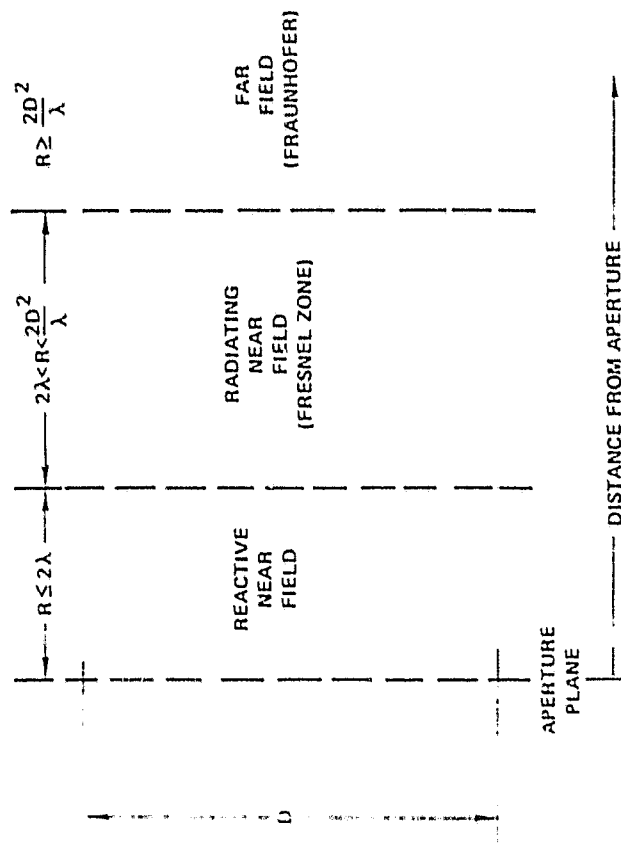
NEAR-FIELD OF AN ARRAY

- In this report we have discussed focused systems and their relationship to near-field systems.
- But, we have not set a criteria for what the near field range of an aperture is. This criteria is shown on the left in the following figure.
- Focused systems are designed such that the reflectors are placed in the far field of the primary aperture. The main beam of a primary aperture is usually well formed by the time the fields reach the reflector. However, in some configurations, i.e., configurations with high f/D ratios, the reflector is at the far field boundary or possibly in the Fresnel zone.
- Near field systems are configured in a way to place the subreflector in the radiating near field (Fresnel zone) of the primary aperture.
- Seen on the right (after Silver) is the relative field magnitude of a uniformly illuminated aperture at various ranges in the Fresnel zone. Field patterns in this region are very dependent on range. The main beam is not well formed until the far field boundary is reached.

FIELD PATTERNS IN THE RADIATING
NEAR FIELD OF AN APERTURE



FIELD REGIONS OF AN ANTENNA APERTURE



470490

OVERSIZED RADIATING ELEMENTS, WIDELY SPACED ARRAY ELEMENTS

Review of Amitay & Gans (2.2)

See Reudink D. O. & Y. S. Yeh

Bell Syst. Tech J. Volume 56 No. 8

Oct. 1977 pp. 1549 - 1560

Amitay & Gans used:

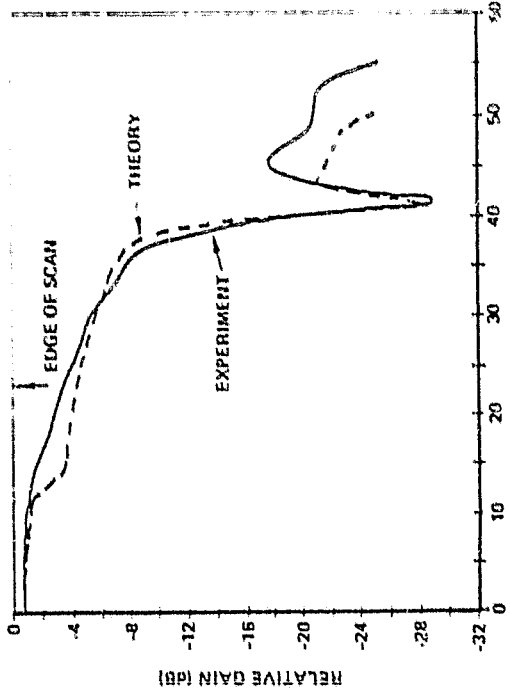
$$dx = 2.78, dy = 1.19$$

104 element array

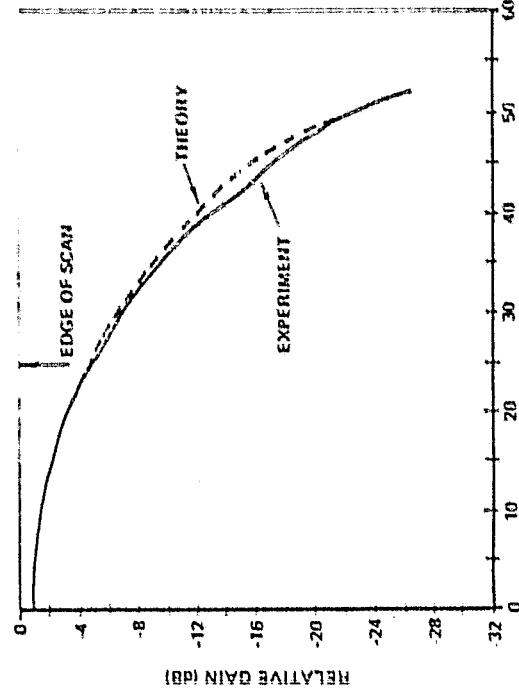
Studies blind spots in this oversized element array. Blind spots were discovered to be a result of a resonant TM_{12} waveguide mode at the aperture surface. They further discussed methods to modify the position of the blind spot such that the array could be useful as a feed for a LFOV antenna.

High gain elements, used with active element patterns, will control grating lobes past 50 deg. from boresight.

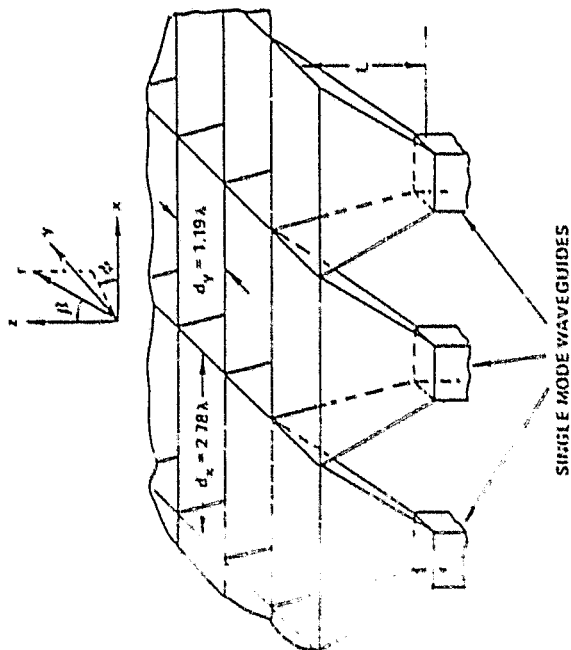
HIGH GAIN ARRAY ELEMENT PATTERNS



EXAMPLE OF AN ELEMENT PATTERN
BLIND SPOT RESULTING FROM THE
TM₁₂ RESONANT WAVEGUIDE MODE



ELEMENT PATTERN OF A MATCHED
HIGH GAIN ARRAY ELEMENT



PORTION OF A 104 ELEMENT ARRAY FEED
FOR AN IMAGING REFLECTOR SYSTEM,
HIGH-GAIN ELEMENTS WITH LARGE
ELEMENT SPACINGS

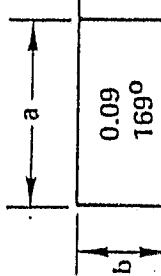
ACTIVE ELEMENT REFLECTION COEFFICIENT

It is important in array design to consider the reflection coefficient that will be observed at each array element when the array is fully excited. There are many techniques available for both infinite and finite array active reflection coefficient analysis [12.1]. For large arrays such as those encountered in near-field systems, infinite array approximations can be used successfully to design element matching for scan angles as high as 30 degrees. The behavior of internal elements of a large array are nearly identical and only the outer elements require special treatment.

But, in small arrays such as the cluster array proposed for use in a focused multibeam antenna, the active reflection coefficient cannot be predicted by infinite array techniques. One method available to analyze finite arrays is an integral equation formulation (moment method). Results were published by Fenn, Thiele, and Munk [3.4] using open-ended rectangular waveguide radiators. The magnitude and phase of Γ predicted for a 25 element array fed at broadside is shown on the following page. Note that the worst case reflection coefficient corresponds to a VSWR of 2.6:1 while the corner elements have a VSWR of 1.2:1. It was discovered that when the array is scanned in the H-plane, $|\Gamma|$ was generally reduced, where as E-plane scans tended to increase $|\Gamma|$.

ORIGINAL PAGE IS
OF POOR QUALITY

COMPUTED ACTIVE ELEMENT REFLECTION COEFFICIENTS
5X5 ARRAY OF OPEN-ENDED WAVEGUIDE ELEMENTS



0.09 169°	0.18 167°	0.16 176°	0.18 167°	0.09 169°
0.31 151°	0.39 150°	0.35 157°	0.39 150°	0.31 151°
0.37 134°	0.44 134°	0.38 141°	0.44 134°	0.37 134°
0.31 151°	0.39 150°	0.35 157°	0.39 150°	0.31 151°
0.09 169°	0.18 167°	0.16 176°	0.18 167°	0.09 169°

BROADSIDE RADIATION $a = 0.57\lambda$ $b = 0.25\lambda$

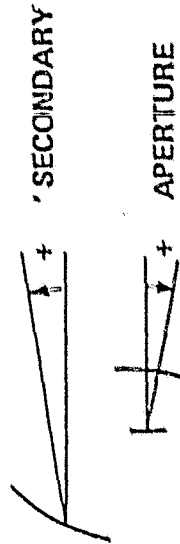
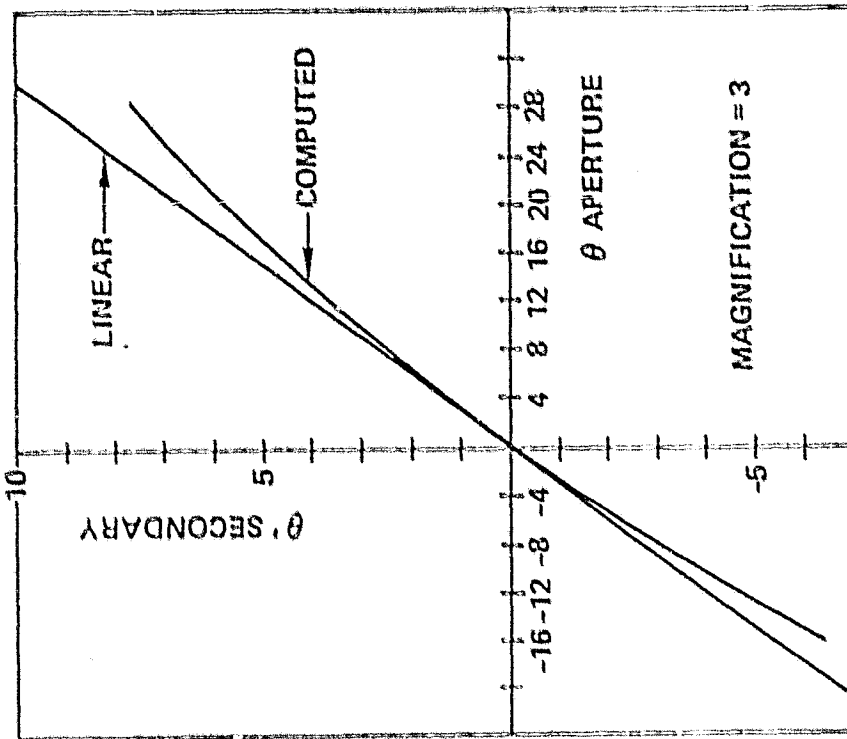
820465

SCAN LIMITS OF A NEAR-FIELD ARRAY

Here, the aperture-to-secondary scan transfer properties of the Gregorian configuration studied in Ref. [1.3] are compared with a linear beam steering approximation based on the magnification ratio (D/d). It is seen that in the positive θ' direction that the array understeers the beam, i.e., an increase in aperture scan does not produce a proportional increase in the secondary beam scan. In this case, a beam scan of $\theta' = +7^\circ$ makes it necessary to increase the scan capabilities of the feed array by 20% from the linear approximation. The condition is reversed in the $-\theta'$ direction; here the secondary beam is oversteered. This example uses computed data from a configuration with a magnification of 3. As shown in this study for magnification ratios on the order of 10 to 15, even greater non-linear scan transfer characteristics are produced.

ORIGINAL PAGE IS
OF POOR QUALITY

NEAR-FIELD SCANNING SYSTEM
APERTURE TO SECONDARY SCAN ANGLE TRANSFORM



820466

NEAR-FIELD OFFSET GREGORIAN

ORIGINAL PAGE IS
OF POOR QUALITY

4. EHF SOLID STATE AND PASSIVE COMPONENTS

TECHNOLOGY OF RF AMPS AND PHASE SHIFTERS

This section will address the current status and growth prospects of technologies required of phased array elements having integral monolithic transmit or receive control devices. The literature search concentrated on monolithic modules and phased array elements operating above 18 GHz.

Monolithic Modules

In general, a lot of work, both theoretical and developmental has been done in the area. As early as 1965 diode switches were available to 24 GHz, and to 40 GHz by 1967. Diodes (BARITT, IMPATT, TRAPATT) have been used extensively for reflection type amplifiers and phase shifters. Dual-gate GaAs MESFET's show the most promise for Variable Gain and Variable Phase amplifiers in the 20-30 GHz Band. Power combining from several FET's is necessary to achieve appreciable output power.

Engineers from Hughes Corp. and Texas Instruments both indicated that variable power amplifier module fabrication is feasible with current technology. Texas Instruments is currently fabricating a four-stage monolithic amplifier module for the Advanced Communications Technology Satellite (ACTS). The chip size will be approximately 100 x 200 mils. The module uses dual-gate FET's for gain control and should have performance similar to NASA's design goals. It will be fabricated on a GaAs chip which would then be mounted in a leadless chip carrier and connected to the desired interface.

ORIGINAL PAGE IS
OF POOR QUALITY

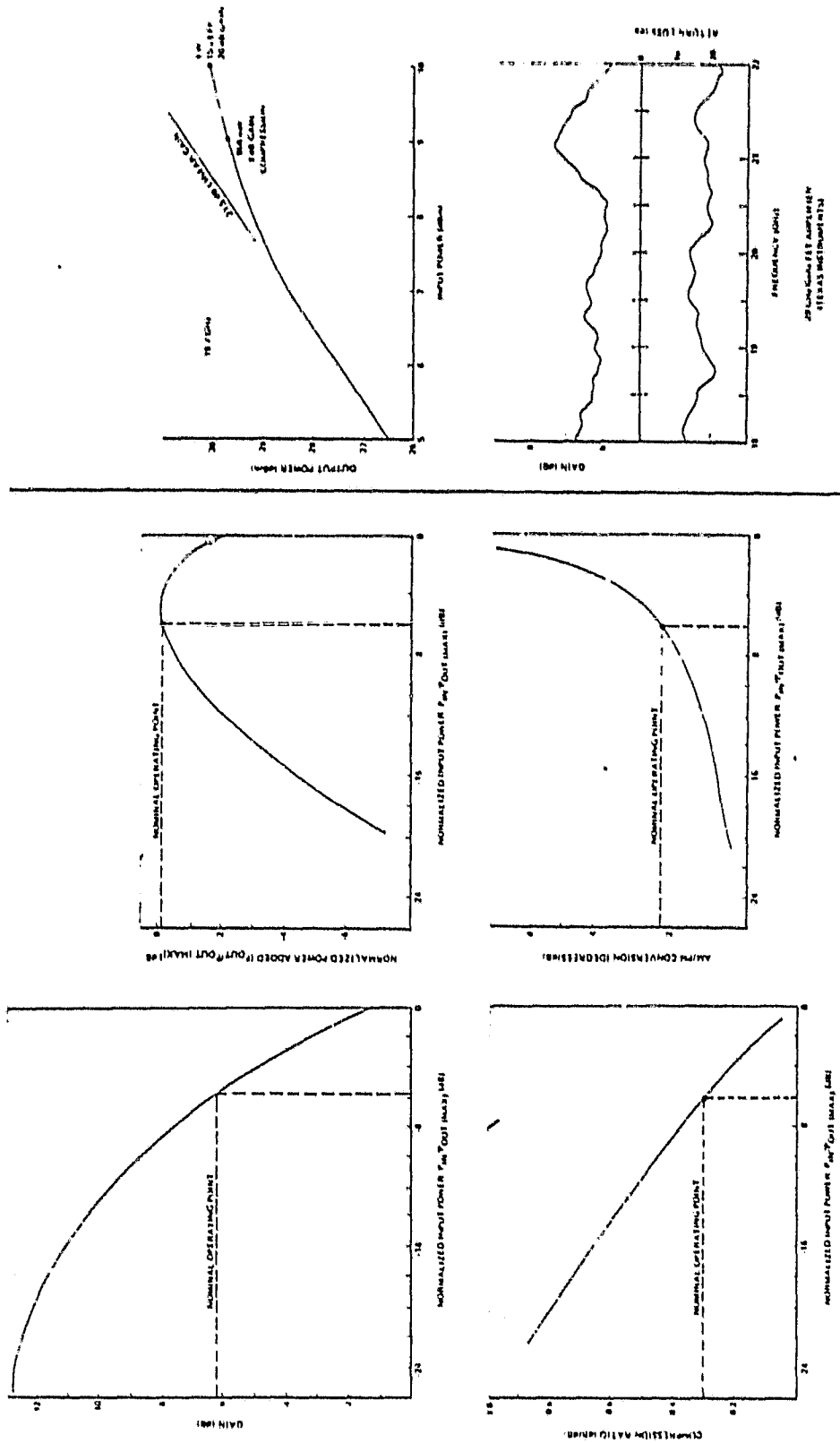
RF LINEAR AMPLIFIER CONSIDERATIONS

Since an active array is under consideration in this study the scope of investigation must go beyond the techniques of an antenna designer of reflector antennas and beyond the scope of a designer of phased arrays. The technology of the design must now include the concepts of the RF linear power amplifier designer such as AM/PM conversion, dynamic range, linearity, response time and harmonics.

- Typical values of EHF components include:
 - AM/PM Conversion: 2 degrees/dB
 - Linearity: $\pm 15^\circ$
 - Stability: $\pm 5^\circ$
 ± 0.3 dB
 - Third-Order IM: -23 dBc

- Effects on Multiple Beam Generation
 - SSPA array RF amplifier non-linearities can produce 3rd order spacial intermodulation.
 - Affect the antenna pattern by producing spacial gitter and lobing phenomenon.

EHF SOLID STATE POWER AMPLIFIER CHARACTERISTICS



230482

28 GHz SOLID STATE AMPLIFIER
FOR COMMUNICATIONS (MCT)

ARRAY PHASE CALIBRATION

An important consideration in an active element array is phase synchronization of the RF signal at the array face. The ideal case at broadside would be constant planar phase front. Many factors will perturb this ideal situation. Some of these are by design i.e. linear phase steering and beam shaping but many will be undesirable effects. These undesirable effects include:

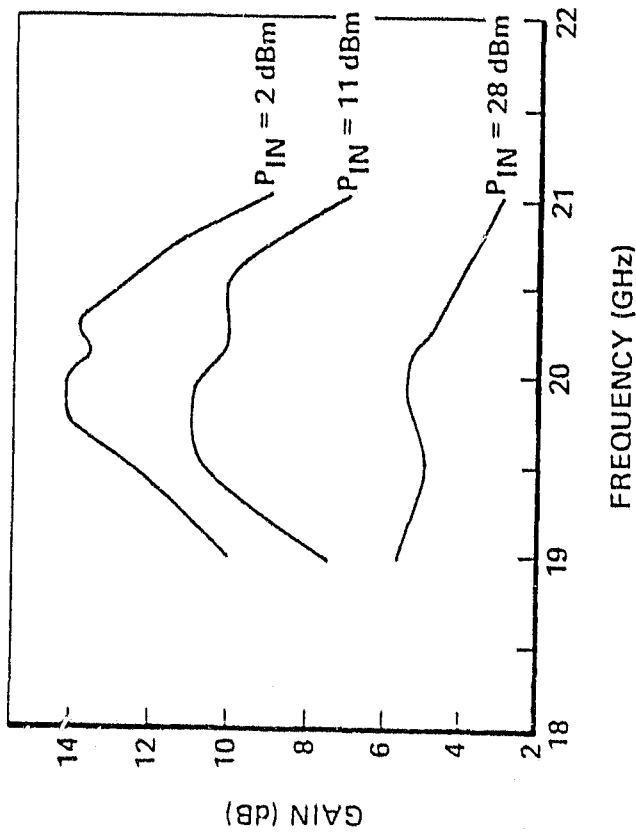
- SSPA insertion loss variations from element to element.
- Differential phase variations from element to element as a function of frequency.
- Phase shifter quantization effects.

One suggested remedy is given by (5.1) as an interpolation locking technique.

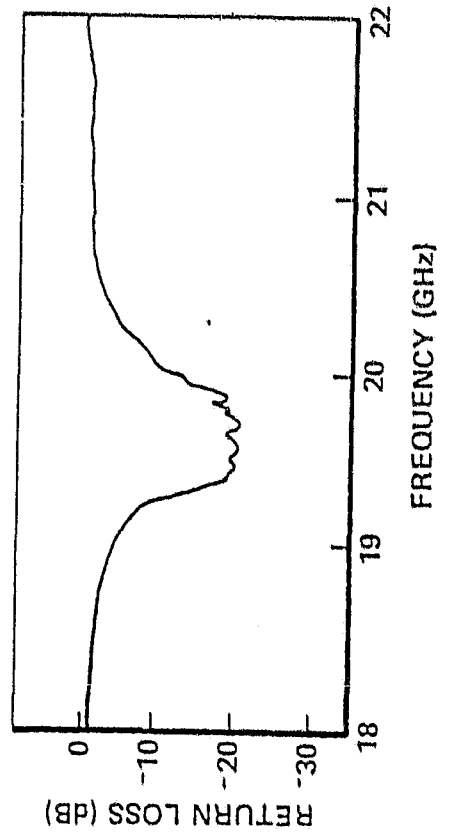
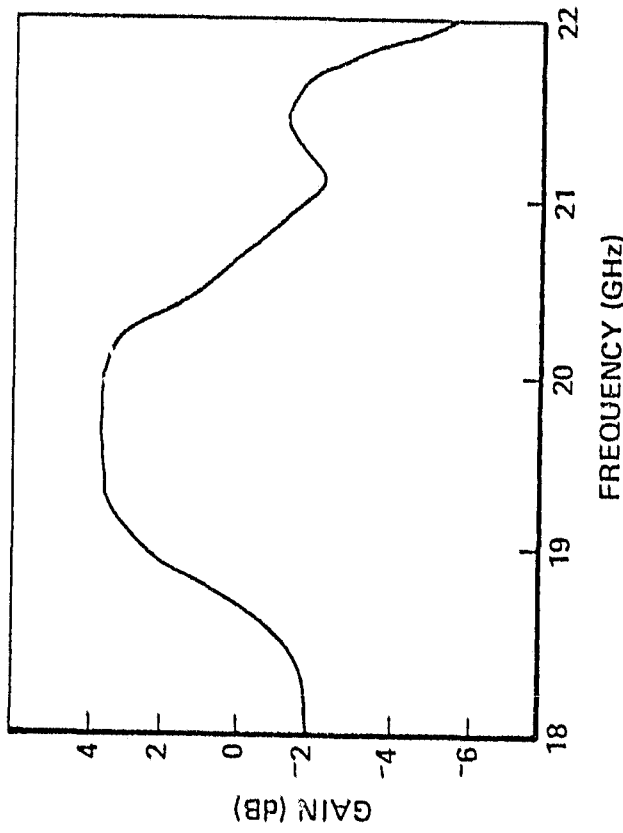
MEASURED FREQUENCY RESPONSE
TYPICAL SOLID STATE POWER AMPLIFIERS

Ga As IMPATT AMPLIFIER
LNR, IWC

MAXIMUM POWER OUT = 1.75W, η = 10-15%



Ga As FET AMPLIFIER
MIT LINCOLN LABORATORY
MAXIMUM POWER OUT = 0.5W, η = 15% TYP



ORIGINAL PAGE IS
OF POOR QUALITY

ORIGINAL PAGE IS
OF POOR QUALITY

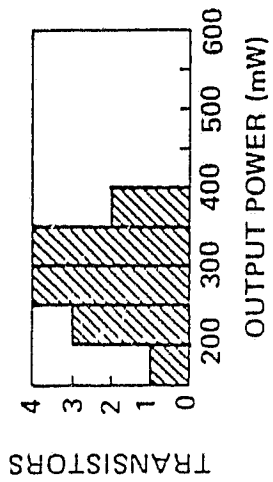
GaAs FETS, UNIT-TO-UNIT VARIATIONS

- The FETS can be biased and tuned for either:
 - a) optimum efficiency
 - or b) optimum output power
- The same set of 14 solid state amplifiers were measured at 20 GHz and at 21 GHz.
- The power output of randomly selected SSPA's in an active aperture could vary widely. For example, at 21 GHz and optimum efficiency the power output from the highest to the lowest differs by more than 3 dB. Array design is difficult with random variations of this magnitude.
- The standard deviation of output power is smaller when the amplifiers are biased and tuned for optimum efficiency.
- Note that efficiencies ranging from 20 to 25% are obtainable. But, the power output is typically lower by 150 mW. Because of the thermal problems encountered in active apertures of this type, optimum efficiency is preferred.

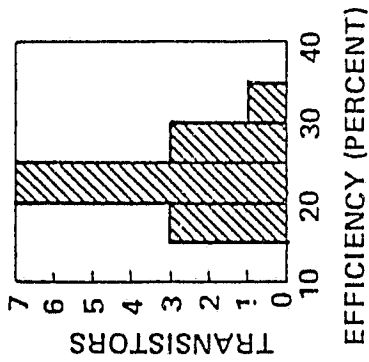
Ga As FET UNIT-TO-UNIT VARIATIONS

MIT LINCOLN LABORATORIES

20 GHz

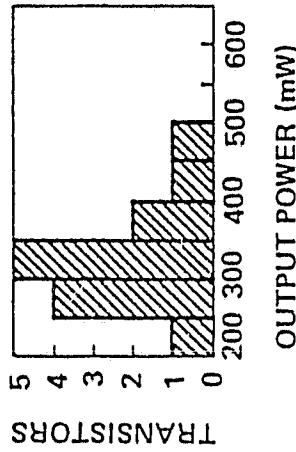


OPTIMUM EFFICIENCY

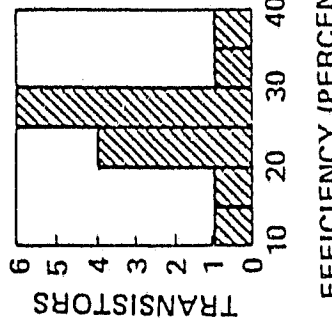


EFFICIENCY (PERCENT)

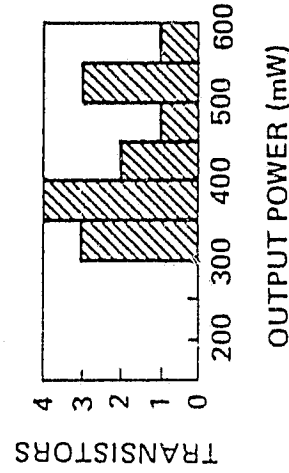
21 GHz



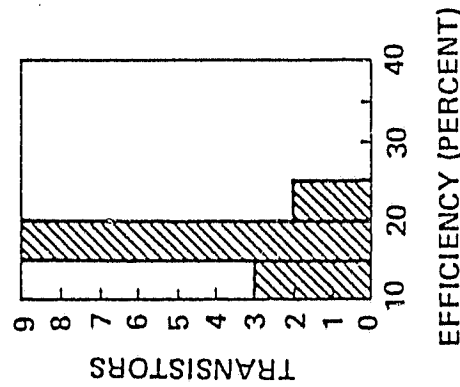
OPTIMUM EFFICIENCY



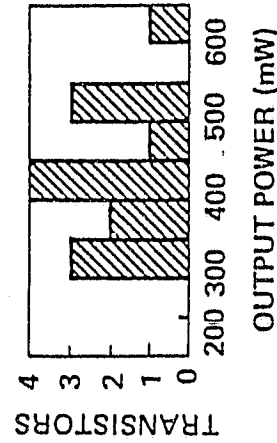
EFFICIENCY (PERCENT)



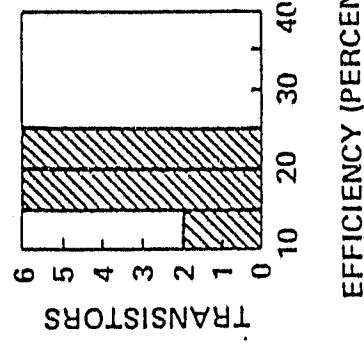
OPTIMUM POWER



EFFICIENCY (PERCENT)



OPTIMUM POWER



EFFICIENCY (PERCENT)

ORIGINAL PAGE IS OF POOR QUALITY

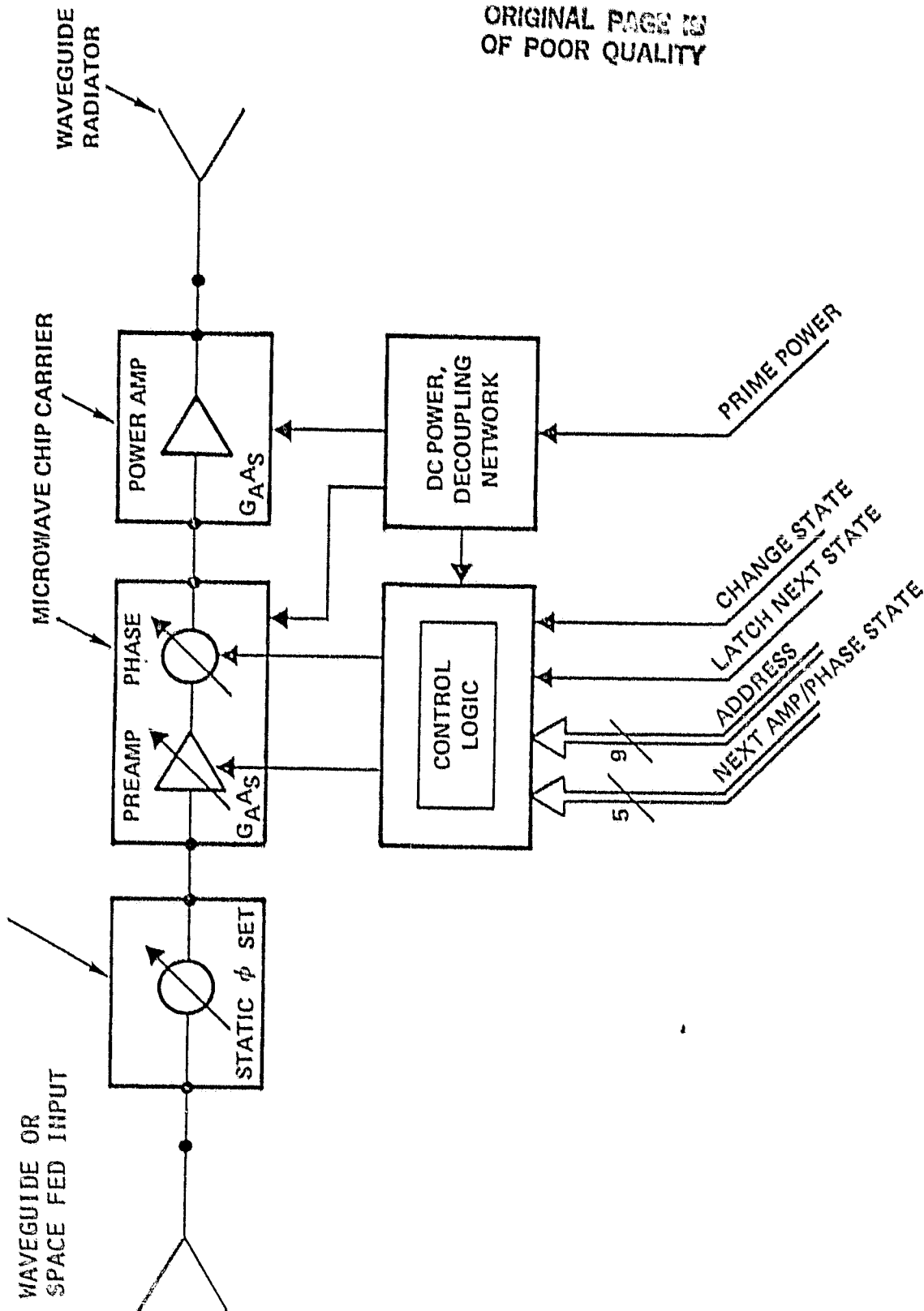
SSPA/RADIATING ELEMENT DESIGN

Shown here is a block diagram of a solid state power amplifier integrated into a radiating element.

- Final Stage - It is recommended that the final amplifier stage be set at its optimum efficiency, and should not have any dynamic control of amplitude nor phase. It was found in the literature that fixed, low-gain (5 to 10 dB) SSPA's are generally more efficient. Since heat dissipation in the array is a severe limiting factor, efficient operation is extremely important. In addition, some fixed gain amplifier designs are now available; thus, the reliability history will be more well known. The remaining portion of the SSPA element gain would be supplied by a preamp module. This module would operate at modest power output levels (50 to 150 mW) and have dynamic amplitude and/or phase control.
- Rapid Scanning - Since rapid beam steering is required each element would be equipped with the ability to store the next amplitude and phase state. Individual elements would be loaded sequentially via an address and data bus structure. This structure would reduce the total number of control lines and reduce layout complexity for large arrays. A single control would command the phase shifters and variable gain amps to change state. Beam updating could be done quite rapidly; but, the power supply must be designed to handle the power surge.

ORIGINAL PAGE IS
OF POOR QUALITY

820432



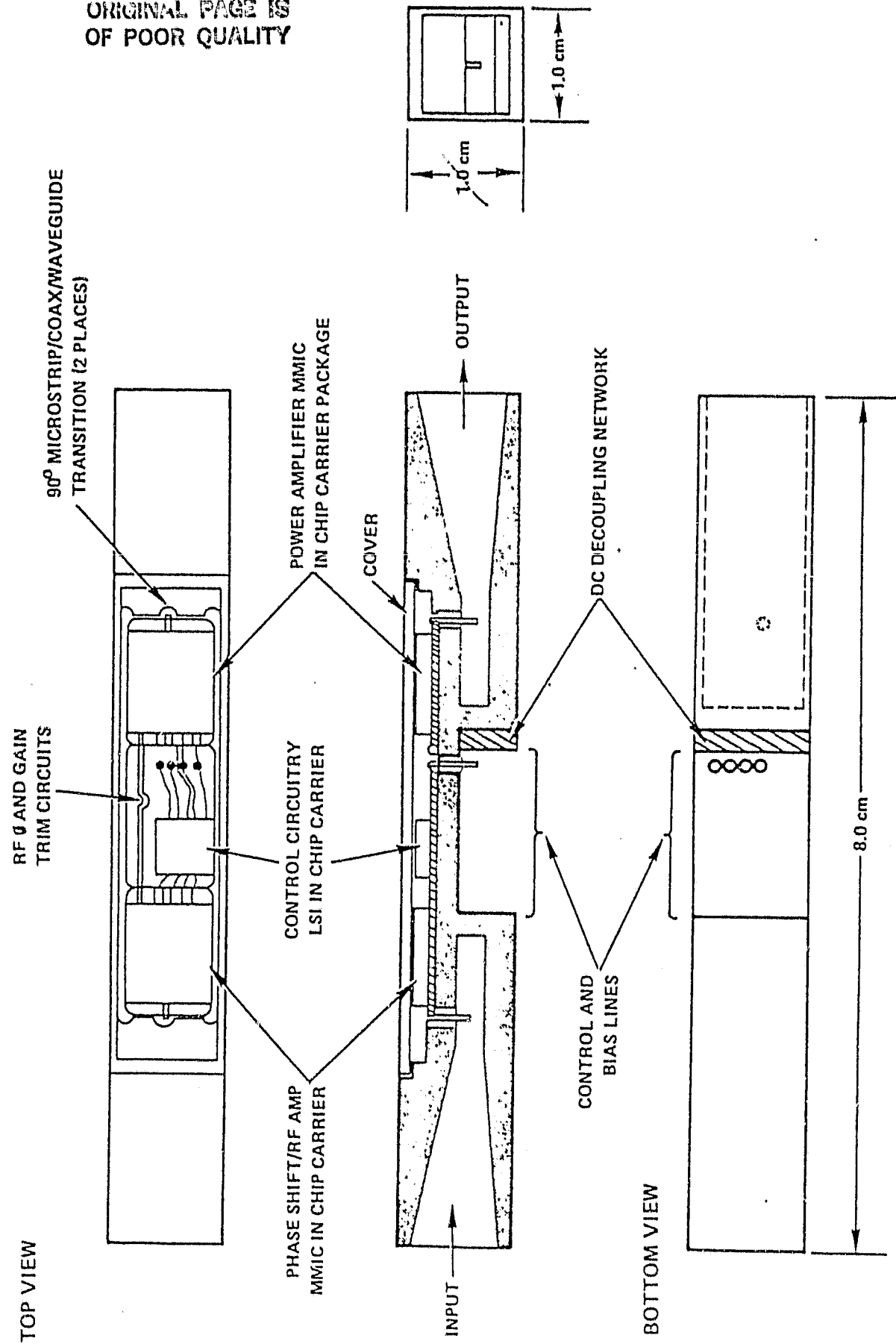
BLOCK DIAGRAM OF ARRAY ACTIVE ELEMENT

SSPA/RADIATING ELEMENT DESIGN

- Static Phase Set - Each element will need a precise static phase setting device to establish a coherent wave front at the aperture. One method would be to use various lengths of dielectric slabs to cover a portion of a microstrip line.
- Chip Carrier Construction - Prior to placement into the radiating element, SSPA's would be packaged in hermetically sealed, leadless chip carriers. The chip carriers are typically made of berillium copper. They would be afixed to the element with silver epoxy for thermal and RF continuity. Wire bonds would be used between chip carriers and coupling devices.

The configuration shown here is for a space-fed active aperture with rectangular receive elements. Other radiating apertures could be selected, such as: square apertures, small pyrimidal horns, conical horns, and rectangular to circular transitions.

ORIGINAL PAGE IS
OF POOR QUALITY



ORIGINAL PAGE IS
OF POOR QUALITY

ARRAY ELEMENTS

There are a wide variety of elements which could be used with a monolithic module in a Phased Array at 20 GHz. These elements are briefly discussed below in order of applicability to the project.

Some successful experimentation has been done at Harris in the EHF Band on dielectric rod antenna elements. A dielectric rod element is an extension to an open-ended waveguide radiator which provides additional beam shaping and impedance matching design parameters.

Microstrip array elements offer an extremely easy interface with monolithic modules including the possibility of simultaneous fabrication and connection. There is a moderate amount of analytical tools available and the array would be rather simple to construct. However, printed-circuit microstrip patch has low bandwidth and only moderate aperture efficiency and polarization purity. A similar technique, the printed-circuit notch antenna, offers a wide bandwidth and is easily matched to free space as well as to the fed line.

Dipole or printed circuit dipole elements have moderate bandwidth, polarization purity, and aperture efficiency. However, fabrication of dipoles for broadband EHF operation is difficult. Cavity backed slots have parameters similar to those of open-ended waveguide. They might be considered if array depth becomes a driving factor. Waveguide slot arrays are popular, but are not applicable to the use of a single monolithic module per element.

Open-ended rectangular waveguide is a commonly used element, and would be convenient for initial studies. It has a wide bandwidth, with moderate aperture efficiency, and high polarization purity. It is easily combined with monolithic modules, and provides for a relatively simple array structure with either a triangular or rectangular lattice. Blind spots which are often associated with waveguide arrays can be avoided due to the small scan angle requirements of the system. There is a large amount of analysis available for waveguide arrays.

ORIGINALS
OF POOR QUALITY

ARRAY ELEMENTS - Contd.

In some instances a small pyramidal horn may be needed, especially if a large aperture area must be filled with a few elements. It has the same general characteristics as the waveguide above. If a high packing density is needed, the element spacing may be smaller than the size of normal waveguide. In this case, ridged waveguide would be used. It has the same parameters as regular waveguide, except for a lower cut-off frequency and wider bandwidth for a given size.

Another alternative is open-ended circular waveguide. It allows for polarization diversity, elimination of some array resonance problems, and lends to dense hexagonal packing. A small conical horn would be used if a large aperture of circular elements is desired and is recommended here.

SSPA TO WAVEGUIDE RADIATOR TRANSITIONS

- Two examples of an SSPA transition to a rectangular waveguide radiator are shown in the following figure.
- The element on the left shows the use of a stepped waveguide transition.

This type of transition is typically used for matching IMPATT diode cavities to rectangular guide.

The loop coupling shown here for the GaAs FET is impractical at EHF frequencies because of the tight tolerances required; but, the coaxial feed through does provide environmental protection for the SSPA.

- A second transition is shown on the right.

Measured data for this transition is shown at the end of this section.

The SSPA chip can be mounted to a heat sink (not shown) that extends half way into the waveguide from behind the SSPA.

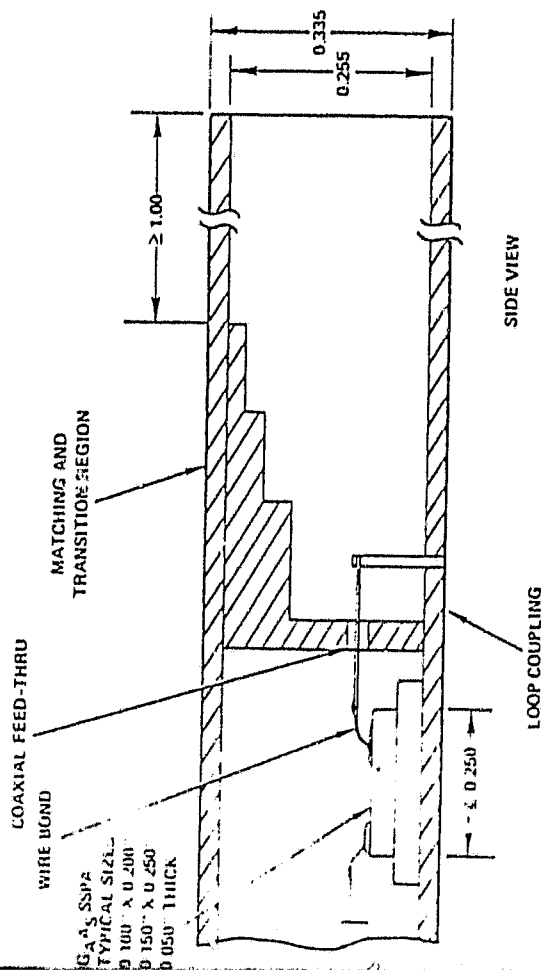
The heat sink and support for the SSPA as well as the element itself could be machined from a single piece of metal. This provides an excellent thermal path to a cooling plate.

- Another alternative is the use of a broadband stepped ridgeline transformer shown on the following page.

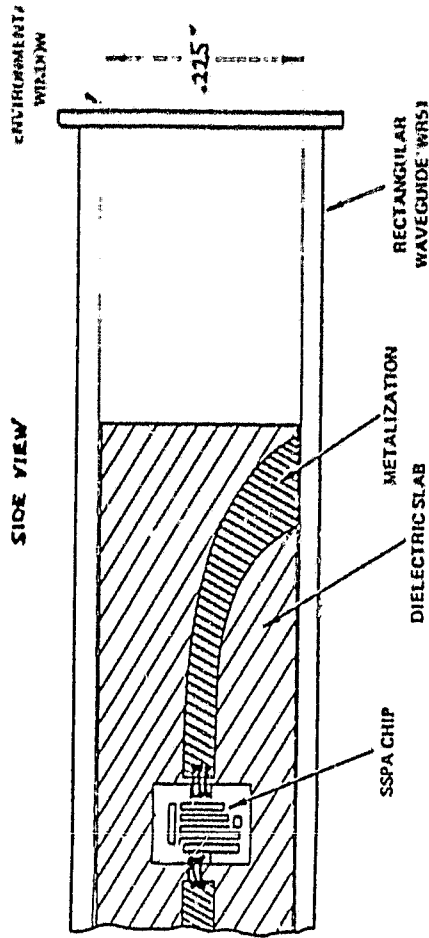
Measured data for this type transition indicates good bandwidth characteristics. The following pages illustrate how the MMIC modules can be integrated into microstrip line and rectangular waveguides.

ORIGINAL PAGE IS
OF POOR QUALITY

SSPA TO WAVEGUIDE RADIATOR TRANSITIONS



DIMENSIONS IN INCHES

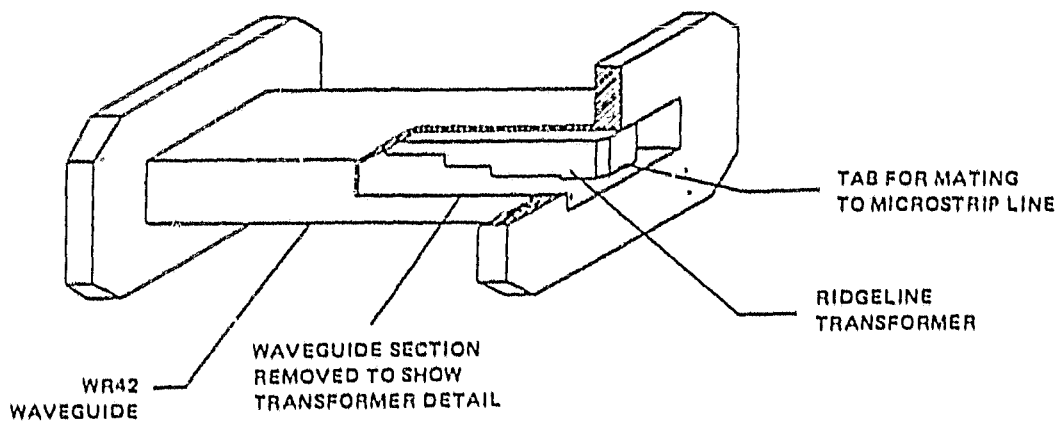


639457

ORIGINAL PAGE IS
OF POOR QUALITY.



(a)



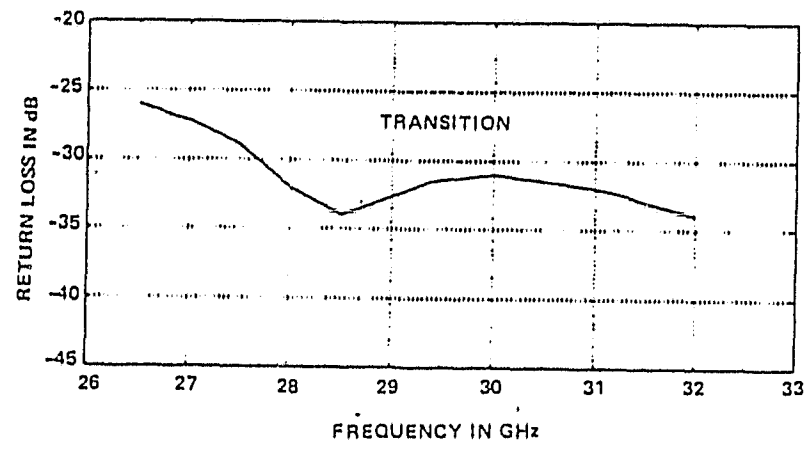
(b)

1498 82

Waveguide to Microstrip Transition:

- (a) Ridgeline Transformer
- (b) Completed transition - wall sectioned to show detail

ORIGINAL PLOT
OF POOR QUALITY



1494 82

Return Loss of Microstrip-to-Waveguide
Transition from 26.5 to 32 GHz

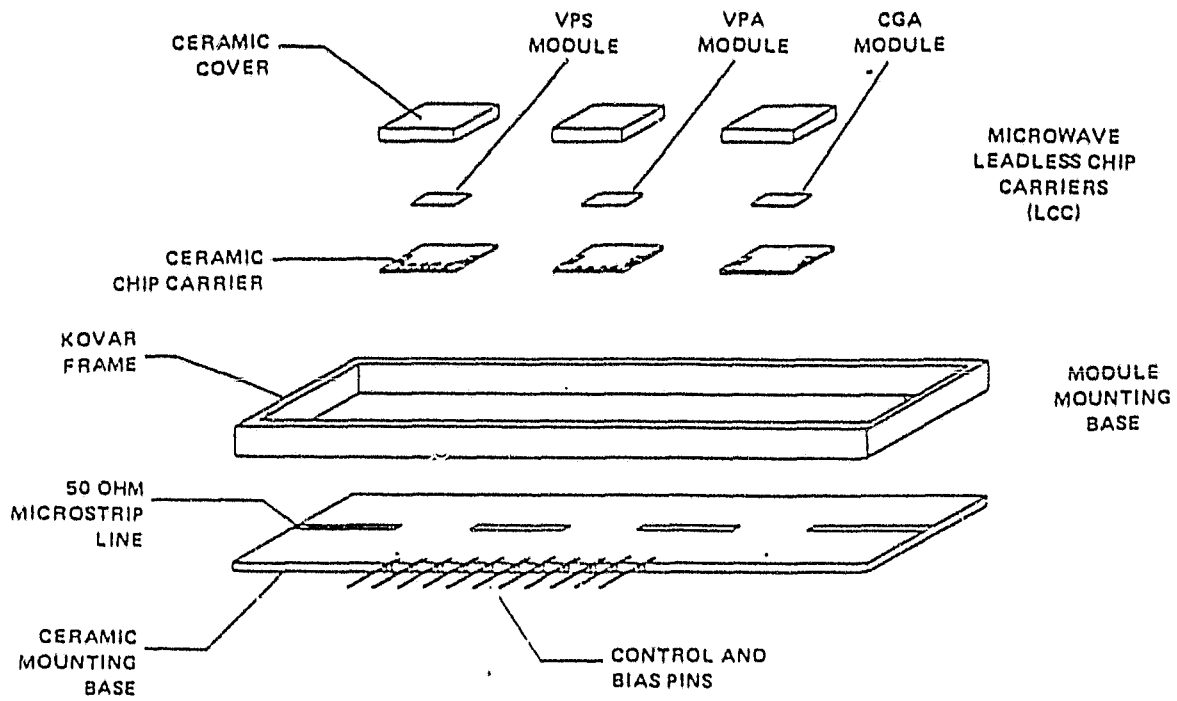
ORIGINAL PAGE IS
OF POOR QUALITY

SSPA ELEMENTS/CIRCULAR RADIATOR INTERFACE

- Rectangular SSPA Package
 - Uses the same transitioning design as shown in the previous illustrations.
 - Input is either microstrip line or rectangular waveguide transition.
 - Rectangular to circular waveguide transition utilized to match modes in the circular radiator.

- SSPA in Circular Waveguide Pipe
 - SSPA region must be isolated from input/output transitions.
 - Microstrip modes are matched in a rectangular package in the SSPA region.
 - Flaired slot transitions match circular waveguide input/output modes.

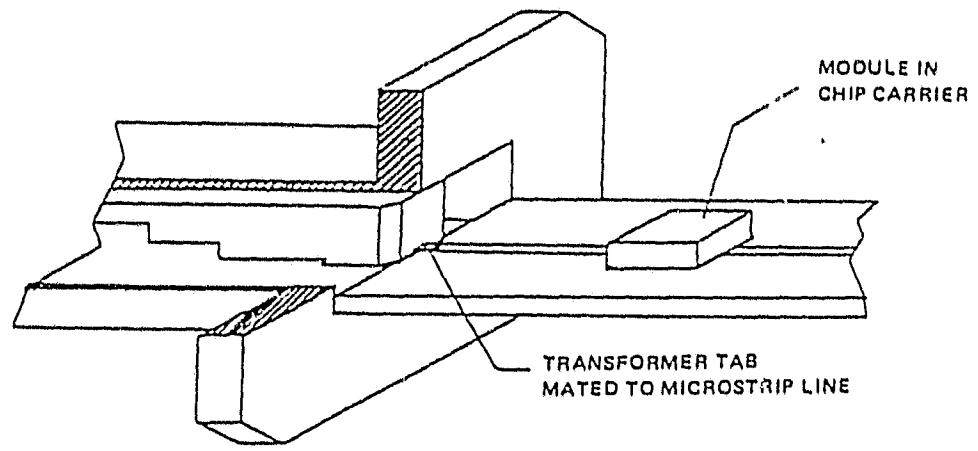
ORIGINAL PAGE IS
OF POOR QUALITY



1493 82

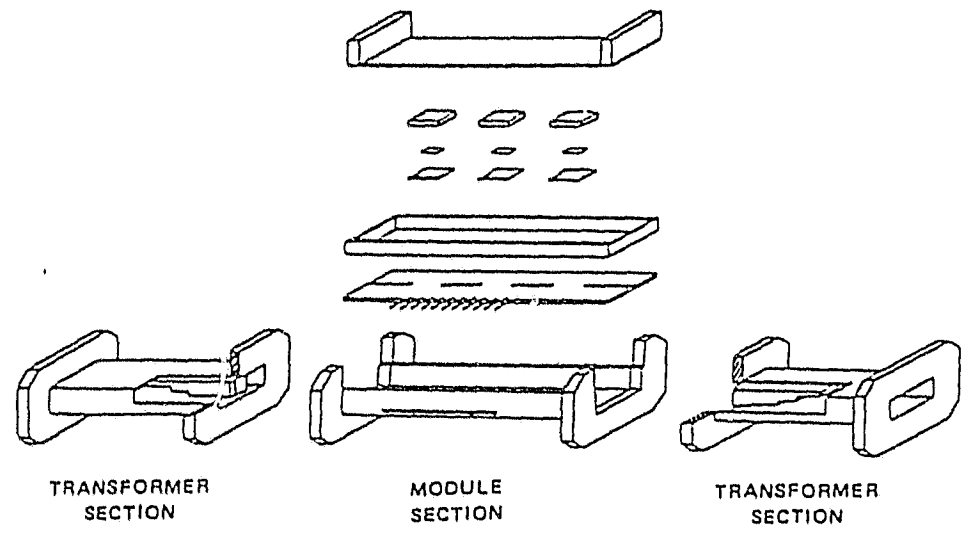
Monolithic Transmit Module Mounting Configuration

ORIGINAL PAGE IS
OF POOR QUALITY



1496 82

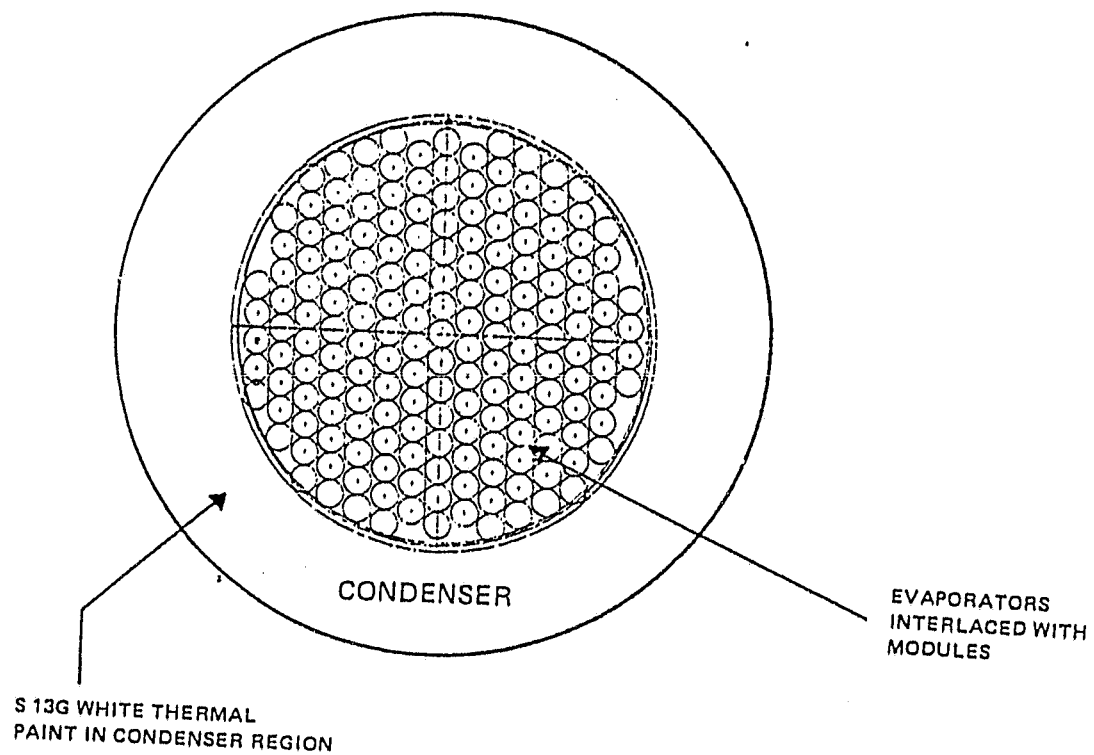
Detail of Transformer - Microstrip Connection



1497 82

Monolithic Module Transition and Mounting Configuration

ORIGINAL PAGE IS
OF POOR QUALITY.



ORIGINAL PAGE IS
OF POOR QUALITY

pg. -125-

SCANNING BEAM EIRP DC POWER REQUIREMENTS

Conventional Spacecraft Communication Satellite systems utilize TWTA's to produce power levels commensurate with the required coverage EIRP. The required EIRP for the scanning beam case is 67 dBW with 53 dB assumed for the antenna. An RF output power of 25 W is required. A comparison of TWTA's having an efficiency of 25% and the specified efficiency of 15% for the SSPA's is presented. The DC power dissipated by the TWT is 195 watts and for the SSPA's is 158 watts. It should be pointed out in this comparison that the logic power loss has not been considered and would be higher for the SSPA's due to the larger number of devices required.

POWER COMPARISON TWT/BFN VS MONOLITHIC MODULE ARRAY

	<u>TWT/BFN</u>	<u>MONOLITHIC TRANSMIT MODULE</u>
RF OUTPUT POWER	25 W	25 W
BFN LOSS*	3 dB	-
POWER AMPLIFIER OUTPUT	50 W	25 W
EFFICIENCY	25% (TWT only)	15%
AMPLIFIER LOSS	150 W	142 W
H.V. SUPPLY EFF.	91%	(L.V.) 91%
H.V. SUPPLY LOSS	20 W	(L.V.) 16 W
BFN SWITCHING POWER*	25 W	-
TOTAL POWER REQUIRED	195 W	158 W

* BFN SYSTEM ASSUMED: 63 VPD's in 6 stages, 5 dB/Stage loss, 200 μ J switching energy per VPD, BFN reconfigured every 500 m sec.

ORIGINAL PAGE IS
OF POOR QUALITY

ACTIVE ARRAY HEAT DISSIPATION

An active array like the one studied by Motorola produces significant heat (~ 380 Watts in this case). Assuming that the method of heat dissipation is via conduction through a structure possessing moderate thermal mass to a thermal radiator(s), significant thermal gradients are prevalent which will distort the array. Distortions resulting from the thermal differences of this magnitude can be compensated for as long as the thermal environments are predictable. Thermistor sensor devices can be utilized in practice to monitor the array thermal condition so that the appropriate phase shifts may be trimmed providing the needed compensation.

An example of a new type of thermal radiator is shown on the following page. A honeycomb heat pipe plate is utilized where the individual waveguides pass through the plate and are mechanically attached at their center section, the region of heat dissipation. Heat is conducted into the plate and evaporates a working fluid such as methanol. By capillary action, vapor is radially transported through wicks to the plate edge where condensation takes place. Heat is then rejected to space via the plate edge region which acts as a space radiator. There is very little build up of temperature from the plate center to the edge which is ideal for the SSPA's.

EHF COMPONENTS

At EHF frequencies the performance of the RF components becomes increasingly critical. Shown below on the left is the measured insertion and return loss of a back-to-back waveguide to microstrip transition. This configuration is important for the utilization of the SSPA modules in waveguide radiators. Other measured data was available for a 20 GHz microstrip 3 dB hybrid. A VSWR of 1.5:1 was maintained over 4 GHz with an insertion loss averaging .7 dB. Comparing this with readily available stripline 3 dB hybrids at X band one finds typical VSWR's of 1.35:1, isolation greater than 18 dB, and insertion loss less than .4 dB. Predicted performance at 21 GHz for 2-way and 4-way in-phase stripline power dividers is shown here:

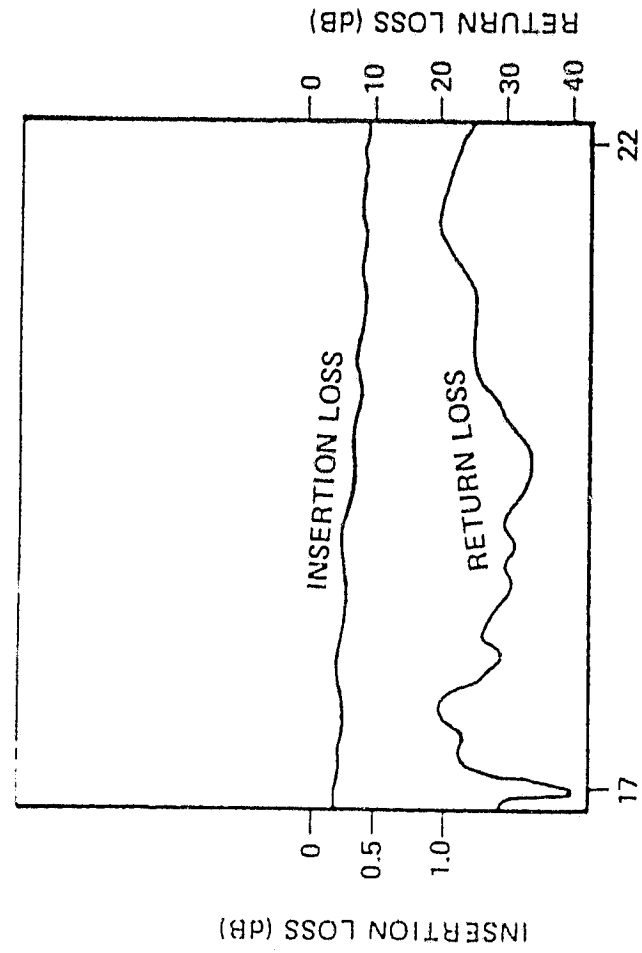
	<u>VSWR</u>	<u>INSERTION LOSS</u>	<u>ISOLATION</u>	<u>AMP BAL</u>	<u>PHASE BAL</u>	<u>BW</u>
2-Way	2.0:1	0.9 dB	14 dB	±.3 dB	±6°	36%
4-Way	2.0:1	2.0 dB	14 dB	±.4 dB	±12°	36%

For coaxial connections the 3 mm coaxial connectors are the most suitable. These connectors can operate up to 38 GHz free of higher order modes. The maximum VSWR expected in the 20 GHz band is 1.27:1 while the maximum insertion loss expected is 0.18 dB. The 3 mm connectors are compatible with .085 semi-rigid coaxial cable. A typical 6 inch cable assembly operated at 20 GHz can be expected to have a maximum VSWR of 1.6:1 and a maximum insertion loss of 0.83 dB. In contrast, the theoretical insertion loss of a 6 inch length of WR42 aluminum waveguide is .12 dB; however, waveguide tolerances of ±.001 inches are required.

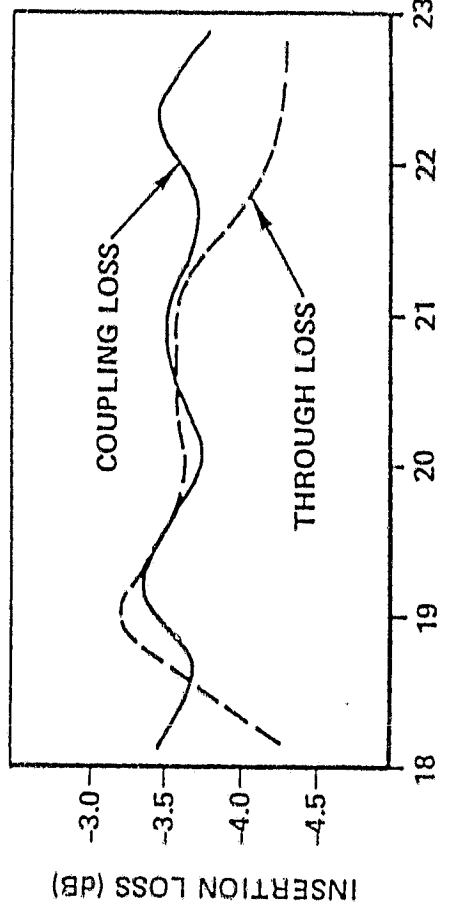
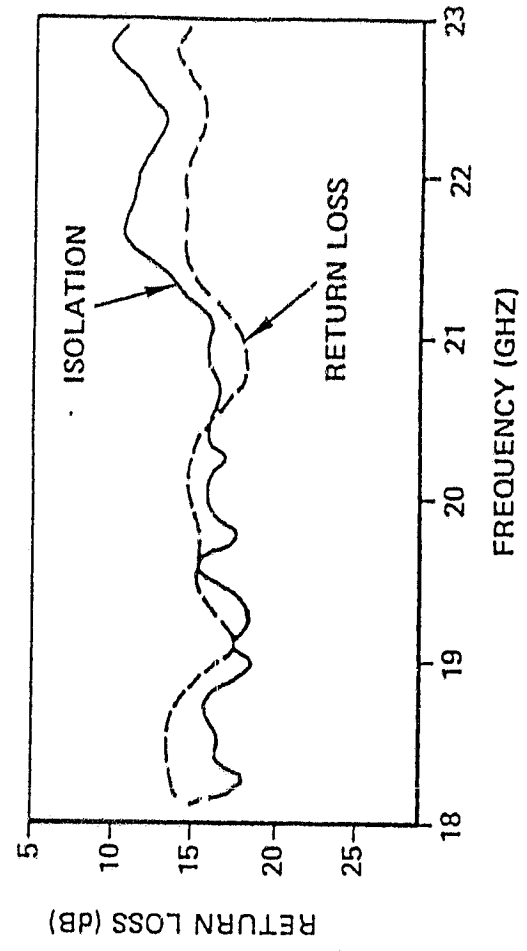
ORIGINAL PAGE IS
OF POOR QUALITY

20 GHZ COMPONENTS

MEASURE
BACK-TO-BACK
WAVEGUIDE TO MICROSTRIP
TRANSITION
(TEXAS INSTRUMENTS)



MEASURED 3 dB MICROSTRIP HYBRID
ON QUARTZ SUBSTRATE
(TEXAS INSTRUMENTS)



5. SUMMARY

NEEDED TECHNOLOGY

Technology developments needed for multiple reflector system with array feeds include:

- A study of specific optics designs with array feeds and with array compensation techniques. (addressed in this contract)
- Solid State phased array technology (addressed in this contract)
- Multiple beam forming networks for active arrays
- Further investigation of mounting configuration of SSPA modules into a complete antenna system
- Additional studies on the distribution of bias and control lines to the individual SSPA modules
- Optimize amplitude and phase quantization; needs versus hardware capability
- Studies of advanced cooler designs

BIBLIOGRAPHY

- 1.1 Rahmat-Samii, Y., V. Galindo-Israel, "Scan Performance of Dual Reflector Antennas for Satellite Communications", Radio Science, Volume 16, No. 6, p.p. 1093-1099, Nov.-Dec., 1981.
- 1.2 Fitzgerald, W. D., "Limited Electronic Scanning with a Near-Field Cassegrainian System", ESD-TR-71-271, Tech. Report 484, Lincoln Laboratory, 24 Sept. 1971, AD-735661.
- 1.3 Fitzgerald, W. D., "Limited Electronic Scanning with an Offset-Fed Near-Field Gregorian System", ESD-TR-71-272, Tech. Report 486, Lincoln Laboratory, 24 Sept. 1971, AD-736029.
- 1.4 Mailloux, R. J., "Limited Scan Arrays-Parts 1 and 2", Practical Phased-Array Systems, Microwave Journal, Dedham, MA, 1975.
- 2.1 Dragone, C., M. J. Gans, "Imaging Reflector Arrangements to Form a Scanning Beam Using a Small Array", Bell Syst. Tech. J., Volume 58, No. 2, Feb., 1979.
- 2.2 Amitay, N., M. J. Gans, "Design of Rectangular Horn Arrays with Oversized Aperture Elements", IEEE Trans. AP, Volume AP-29, No. 6, Nov., 1981.
- 2.3 Lee, S. W., P. Cramer, Jr., K. Woo, Y. Rahmat-Samii, "Diffraction by an Arbitrary Subreflector: GTD Solution", IEEE Trans. Ant. and Prop., Volume AP-27, No. 3, May, 1979.
- 2.4 Rudge, A. W., Adata, "Offset-Parabolic-Reflector Antennas: A Review", Proc. of IEEE, Volume 66, No. 12, Dec., 1978.
- 3.1 Nan San Wong, R. Tang, E. E. Barber, "A Multielement High Power Monopulse Feed with Low Sidelobes and High Aperture Efficiency", IEEE Trans. Antennas and Propagation, Volume AP-22, No. 3, May, 1974.
- 3.2 Mrstik, A. V., P. G. Smith, "Scanning Capabilities of Large Parabolic Cylinder Reflector Antennas with Phased-Array Feeds", IEEE Trans. Antennas and Propagation, Volume AP-29, No. 3, May, 1981.
- 3.3 Oliner, A. A., G. H. Knittel, "Phased Array Antennas", Artech House, 1972.
- 3.4 Fenn, A.J., G. A. Thiele, B. A. Munk, "Moment Method Calculation of Reflection Coefficient for Waveguide Elements in a Finite Planar Phased Antenna Array", Ohio State University Tech. Report 784372-7, Sept., 1978, Contract N00014-76-C-0573.

BIBLIOGRAPHY - Contd.

- 4.1 Adata, N. A., "Diffraction Effects in Dual Offset Cassegrain Antenna", IEEE AP-Symp., 1978, p.p. 235-238.
- 4.2 Mitra, R., F. Hyjazie, "A Method for Synthesizing Offset, Dual Reflector Antennas", IEEE AP-Symp., 1978 p.p. 239-242.
- 4.3 Galindo-Israel, V., R. Mitra, "Aperture Amplitude and Phase Control of Offset Dual Reflectors", IEEE AP-Symp., 1978, p.p. 243-246.
- 4.4 Krichevsky, V., D. F. DiFonzo, "Optimum Feed Locus for Beam Scanning in the Symmetry Plane of Offset Cassegrain Antennas", COMSAT Tech. Review, Volume 11, No. 1, Spring 1981, p.p. 131-156.
- 5.1 Forrest, J. R., A. A. de Sallen, J. Austin, J. G. Schoenenberger, "Design Considerations for Phased Array Modules", RADC-TR-80-354, Final Technical Report, Rome Air Development Center.
- 5.2 Holt, D. J., "Devices and Techniques for all Solid State Radars", Eascon '76 Record, Sept., 1976.
- 5.3 Foldes, P., "Recent Advances in Multibeam Antennas", 11th European Microwave Conference, 1981, p.p. 59-72.
- 5.4 Hua Quen Tserng, "Advances in Microwave GaAs Power FET Device and Circuit Technologies", 11th European Microwave Conference, 1981, p.p. 48-58.
- 6.1 Frediani, D. J., "Technology Assessment for Future MILSATCOM Systems: The EHF Bands", Lincoln Laboratory Project Report DCA-5, 12 April 1979.
- 6.2 Stockton, R., M. M. Balint, "15 GHz Microstrip Array Development", Final Technical Report, RADC-TR-80-403, February, 1981.
- 6.3 Mailloux, R. J., et. al., "Grating Lobe Control in Limited Scan Arrays", IEEE Trans AP-27, No. 1, January, 1979, p.p. 79-85.
- 6.4 Salkins, B. E., D. Jones, "Communications Satellite Active Aperture Study", Final Report, AFWAL-TR-81-1074, April 1981.
- 7.1 Reudink, D. O., Y. S. Yeh, "A Scanning Spot-Beam Satellite System", Bell System Tech. J., Volume 56, No. 8, October, 1977, p.p. 1549-1560.
- 7.2 Woo, Kenneth, P. Cramer, Jr., "Limited Scan Near-Field Cassegrain Antenna", IEEE AP-Symp., p.p. 323-325.
- 7.3 Patton, W.T., "Limited Scan Arrays", "Phased Array Antennas", Olinear and Knittel, Artech House, 1972.

BIBLIOGRAPHY - Contd.ORIGINAL PAGE IS
OF POOR QUALITY

- 7.4 Rudge, A. W., M. J. Withers, "New Technique for Beam Steering with Fixed Parabolic Reflectors", Proc. IEE, Volume 118, No. 7, July, 1971, p.p. 857.
- 8.1 Rudge, A. W., "Multiple-Beam Antennas", "Offset Reflectors with Offset Feeds", IEEE Trans, Antennas and Propagation, Volume AP-23, p.p. 317-322, May, 1975.
- 8.2 Hannan, P. W., "Microwave Antenna Derived from the Cassegrain Telescope", IRE Trans. Antennas Propagation, Volume AP-9, p.p. 140-153, March, 1961.
- 8.3 Assaly, R. N., L. J. Ricardi, "A Theoretical Study of a Multi-Element Scanning Feed System for a Parabolic Cylinder", IEEE Trans. Antennas and Propagation, Volume AP-14, No. 5, September, 1966.
- 8.4 Stark, L., "Comparison of Array Element Types", "Phased Array Antennas", Artech House, Edition Oliner and Knittel, 1972.
- 9.1 "30/20 GHz Spacecraft Multi-Beam Antenna System Review No. 1", NASA LeRC, NAS 3-22498, November, 1980, Ford Aerospace.
- 9.2 Semplak, R. A., "100-GHz Measurements on a Multiple-Beam Offset Antenna", Bell System Tech. J., Volume 56, No. 3, March, 1977.
- 9.3 Akagawa, M., D. F. DiFonzo, "Beam Scanning Characteristics of Offset Gregorian Antennas", IEEE International Symp. on Antennas and Propagation, p.p. 262-264, 1979.
- 9.4 Hogg, D. C., R. A. Semplak, "An Experimental Study of Near-Field Cassegrain Antennas", Bell Syst. Tech. J., Volume 43, p.p. 2677-2704, November, 1964.
- 10.1 Ta-Shing Chu, R. J. Turrin, "Depolarization Properties of Offset Reflector Antennas", IEEE Trans. Antennas and Propagation, Volume AP-21, p.p. 339-345, May, 1973.
- 10.2 B. MACA. Thomas, "Cross-Polarization Characteristics of Axially Symmetric Reflectors", Electron. Letters, Volume 12, p.p. 218-219, April 29, 1976.
- 10.3 Salkins, B. E., D. Jones, "Communications Satellite Active Aperture Study", Final Report, AFWAL-TR-81-1074, April, 1981.
- 10.4 Rusch, W. V. T., "Scattering from a Hyperboloidal Reflector in a Cassegrain Feed System", IEEE Trans. Antennas Propagation, Volume AP-11, p.p. 414-421, July, 1963.

BIBLIOGRAPHY - Contd.

- 11.1 Winter, C., "Phase Scanning Experiments with Two-Reflector Antenna Systems", Proc. IEEE, Volume 56, No. 11, p.p. 1984-1999, Nov., 1968.
- 11.2 Dragone, C., D. C. Hogg, "The Radiation Pattern and Impedance of Offset and Symmetrical Near-Field Cassegrain and Gregorian Antennas", IEEE Trans. Antennas and Propagation, Volume AP-22, p.p. 472-475, May, 1974.
- 11.3 Morgan, S. P., "Some Examples of Generalized Cassegrain and Gregorian Antennas", IEEE Trans, Antennas and Propagation, p.p. 685-691, November, 1964.
- 11.4 Rudge, A. W., D. E. N. Davies, "Electronically Controllable Primary Feed for Profile-Error Compensation of Large Parabolic Reflectors", Proc. IEE, Volume 117, No. 2, February, 1970, p.p. 351-358.
- 12.1 Amitay, N., C. P. Wu, V. Galindo, "Methods of Phased Array Analysis", Phased Array Antennas, Oliner and Knittel, Artech House, 1972.
- 12.2 Dijk, J., C. T. W. Van Diepenbeek, E. J. Mannders, L. F. G. Thurlings, "The Polarization Losses of Offset Paraboloid Antennas", IEEE Trans. Antennas Propagation, Volume AP-22, p.p. 513-520, July, 1974.